University of Alberta

The Physical and Geochemical Characterization of Oxygen-Depleted Breathing Wells in Central Alberta

by

Sarah Rebecca Hill 

A thesis submitted to the Faculty of Graduate Studies and Research in partial fulfillment of the requirements for the degree of Master of Science

Department of Earth and Atmospheric Sciences

Edmonton, Alberta
Fall 2004

Your file Votre référence
ISBN: 0-612-95765-9
Our file Notre référence
ISBN: 0-612-95765-9

DEDICATION

This thesis in dedicated to the memory of
Susan and Douglas Staudinger
and
Maurice Lewis

ACKNOWLEDGEMENTS

The completion of this thesis would not have been possible without the help and cooperation of a great number of people. First and foremost, I would like to thank my supervisor, Dr. Carl Mendoza, for his guidance, patience and support throughout my graduate and undergraduate degrees at the University of Alberta.

I am deeply indebted to Dr. Cathy Ryan and Kimberly McLeish at the University of Calgary for their valued cooperation and assistance throughout the project. Thanks also to Roger Clissold for his contributions at the start of the study, and for the use of his company's resources.

I would like to thank the owners of the breathing water wells monitored during this study. Sincere gratitude is extended to Harvey and Lois Staudinger who sacrificed more than could ever have been asked for this study of breathing wells. Thanks also to the Ammeter, Nicholson and Sheer families, for the allowed access to their properties and wells.

A special thanks is extended to Maurice Lewis for initiating the interest in this project, although whose untimely death deprived me of particularly valuable council. I would like to think his wife, Diane Lewis, for her support, assistance, and encouragement throughout this project.

Financial support for the MSc. was provided in part by the Department of Earth and Atmospheric Sciences, the Canadian Ground Water Association, and from NSERC grants to Dr. Carl Mendoza. Field research was supported by a grant from the Geological Society of America and the Prairie Farm Rehabilitation Administration.

Thanks to my fellow graduate students and friends who helped me out along the way. Thanks to Brian Smerdon, Adrienne Price, Heather von Hauff, Trevor Butterfield, Gavin Jensen, Daniele Palombi, Maya Bhatia, Zabrina Gibbons, Dustin Shauer, Jessica Liggett and the infamous Michelle Pallier. Special thanks to Brian and Adrienne, whose encouragement and words of wisdom were always welcomed, whether they dealt with hydrogeology or not.

My final acknowledgements and sincere gratitude go to my family who were understanding and supportive throughout the entire process. They did more for me than can be expressed here on paper to help bring this thesis to completion.

TABLE OF CONTENTS

CHAPTER 1: INTRODUCTION 1

CHAPTER 2: LOCATING and SELECTING BREATHING WATER WELLS 8

2.1 Locating Breathing Water Wells 8

2.1.1 Locating Breathing Water Wells 8

2.1.2 Questionnaire 9

2.1.3 Personal Communication 11

2.2 Site Selection 11

CHAPTER 3: FIELD and LABORATORY METHODS 12

3.1 The Staudinger Well 12

3.1.1 Meteorological Data Collection 12

3.1.2 Gas and Air Monitoring 12

3.1.3 Water Quality Sampling 15

3.1.4 Water Levels 18

3.1.5 Dissolved Gas 18

3.2 Additional Breathing Water Wells 19

3.3 Health and Safety 20

3.4 Monitoring Schedule 20

3.5 Supporting Methods 21

3.5.1 Shallow Well Water Quality Sampling 21

3.5.2 *Water Elevations for Regional Groundwater Distribution* 22

CHAPTER 4: RESULTS and DISCUSSION of the STAUDINGER WELL 23

4.1 Site Description 23

4.1.1 Location and Completion Details 23

4.1.2 Geography and Climate 25

4.1.3 Geology 25

4.1.4 Hydrogeology 27

4.2 Oxygen Concentrations and Barometric Pressure 30

4.2.1 Eight Month Trends 30

4.2.2 Two Week Trends 32
4.2.3 Individual Trends 37
4.3 Carbon Dioxide and Methane 38
4.4 Volumetric Flow Rate 40
4.5 Groundwater 41
4.5.1 Shallow Water Chemistry 41
4.5.2 Staudinger Well Water Quality 42
4.6 Down-hole Measurements 45
4.6.1 Total Dissolved Gas Pressure 45
4.6.2 Passive Gas Samplers 47
4.7 Interpretation and Discussion 49
4.7.1 Geochemical Characterization 49
4.7.2 Possible Mechanisms 51
4.7.3 Mass-Balance Model 58
4.8 Summary 69

CHAPTER 5: COMPARISON and DISCUSSION of OTHER BREATHING WELLS 71
5.1 Site Description 71
5.1.1 Ammeter Well 71
5.1.2 Onoway Well 72
5.1.3 Delburne Well 74
5.2 Gas and Meteorological Sensor Observations 76
5.3 Groundwater 80
5.4 Comparison to the Staudinger Well 84
5.5 Summary 86

CHAPTER 6: CONCLUSIONS 88

REFERENCES 91

APPENDIX A: COLLECTED DATA FILES 98

APPENDIX B: ISOTOPES 99
B.1 Methods 99
B.1.1 Sampling 99
B.1.2 Laboratory Analysis 100

B.1.3 Vacuum Extraction.....101
B.2 Oxygen and Hydrogen Isotope Compositions 101
B.2.1 Staudinger Well Results 101
B.2.2 Staudinger Well: Interpretation and Discussion 103
B.3 Additional Wells.....106
B.4 Conclusions.....108
B.5 References 108

APPENDIX C: TEMPERATURE DEPENDENCE of OXYGEN SENSOR .....
.....110

APPENDIX D: GAS PRODUCTION by DENITRIFICATION.....115

LIST OF FIGURES

Figure 1.1: *Schematic of a Breathing well* 2

Figure 2.1: Breathing Well Distribution in Alberta 10

Figure 3.1: The Airmadillo.....13

Figure 3.2: Flow-through Sampling Cell.....16

Figure 4.1: Location of Monitored Breathing Water Wells Near Sylvan Lake.....24

Figure 4.2: Completion Details of the Staudinger Well 26

Figure 4.3: Hydraulic Head Distribution in the Paskapoo Formation.....28

Figure 4.4: Eight Month Distribution of Oxygen and Barometric Pressure31

Figure 4.5: Two Week Distribution of Oxygen and Barometric Pressure .33

Figure 4.6: Daily Rates of Change in Oxygen and Barometric Pressure .36

Figure 4.7: Daily Rates of Change for Three Individual Cycles.....37

Figure 4.8: Distribution of Carbon Dioxide and Barometric Pressure.....39

Figure 4.9: Volumetric Flow Rate and Oxygen Concentration Distribution 40

Figure 4.10: Total Dissolved Gas Pressure and Barometric Pressure Distribution 47

Figure 4.11: Redox Distribution in the Staudinger Well 50

Figure 4.12: Conceptual Design of the Mass-Balance Model 59

Figure 4.13: Modelled and Observed Oxygen Concentrations for the Large-Scale Pressure Cycle 64

Figure 4.14: Modelled and Observed Carbon Dioxide Concentrations for the Large-Scale Pressure Cycle 64

Figure 4.15: Modelled and Observed Oxygen Concentrations of the Intermediate and Small-Scale Pressure Cycles.....67

Figure 5.1: Completion Details of the Ammeter Well 72

Figure 5.2: Completion Details of the Onoway Well.....73

Figure 5.3: Completion Details of the Delburne Well 75

Figure 5.4: Two Week Distribution of Oxygen and Barometric Pressure for the Three Additional Wells.....77

Figure 5.5: Volumetric Flow Rate and Oxygen Concentration Distribution Through the Ammeter Well.....79

Figure 5.6: Piper Diagram for the Four Monitored Breathing Water Wells... 82

Figure B.1: $\delta^{18}O$-δD Plot for Staudinger and Shallow Well Groundwater 102

Figure B.2: Barometric Pressure Influence on the Isotopic Composition of Groundwater.....104

Figure B.3: Non-Equilibrium Evaporation Processes Across a Water Table 105

Figure B.4: Stable Isotopic Composition of the Four Monitored Breathing Wells.....107

Figure C.1: Oxygen and Temperature Distribution (Laboratory Tests)...111

Figure C.2: Corrected and Raw Oxygen Concentrations at Onoway 112

Figure C.3: Corrected and Raw Oxygen Concentrations at the Ammeter and Delburne Wells 113

LIST OF TABLES

Table 3.1: Breathing Water Wells Instrumentation Schedule 21

Table 4.1: Chemical Composition of the Staudinger and Shallow Well Groundwater.....43

Table 4.2: Dissolved Gas Concentrations 48

Table 4.3: Aqueous and Gas Concentration of N_2 and CO_2.....56

Table 4.4: Mass-Balance Model Input Parameters 63

Table 5.1: Maximum and Minimum Observations of Barometric Pressure, O2 and CO2 concentrations.....76

Table 5.2: Comparison of the Correlation Coefficients Between Monitored Breathing Wells 78

Table 5.3: Chemical Composition of all Sampled Water Wells.....83

Table B.1: Isotopic Composition of the Sampled Water wells.....102

Table D.1: Maximum and Minimum Mass Flux of Nitrogen Gas.....117

CHAPTER 1: INTRODUCTION

A breathing water well is a man-made phenomenon defined in the *Glossary of Geology* (Bates and Jackson, 1987) as:

> [a] well, generally a water well, that, in response to changes in atmospheric pressure, alternately takes in and emits a strong current of air, often with an alternating sucking and blowing sound. It penetrates, but is uncased in at least part of a thick zone of aeration that is porous and permeable enough to exchange air freely with the well but otherwise is poorly connected with the atmosphere because of the presence of tight soil or other low-permeability material above the unsaturated material.

Figure 1.1 is a schematic of the mechanics and construction of breathing water wells. Expanding on the above definition, breathing wells require the three following conditions:

1. The well must be completed in a partially saturated aquifer. Such cases occur when certain physical parameters, such as recharge rates, storativity, and well usage, do not permit the aquifer to be fully saturated. The partial saturation of the aquifer can occur naturally or be human induced.

2. A confining unit must overly the partially saturated aquifer. This unit has a lower hydraulic conductivity than the aquifer. Consequently, the unit does not easily transmit either water or gas. The confining unit prevents the partially saturated aquifer from being in direct contact with the atmosphere, other than through the well itself. In some areas, these wells are completed beneath perched groundwater systems.

The perched water is unconfined and separated from the underlying main body of groundwater by the confining unit and the deeper aquifer's unsaturated zone (Figure 1.1).

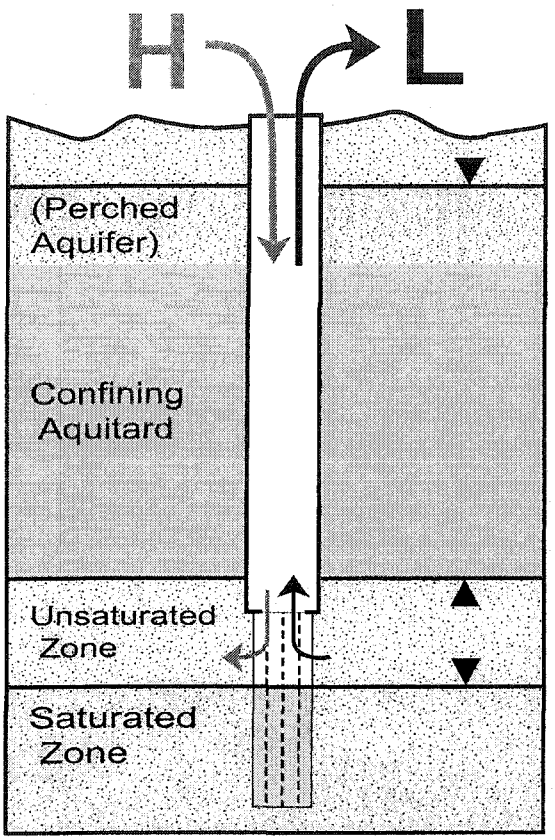

Figure 1.1: Schematic of a breathing well. A rise in atmospheric pressure (H) causes ambient air to be driven into the unsaturated zone of the aquifer. When barometric pressure falls (L), air within the unsaturated zone is drawn into the well and exhaled to the atmosphere. Some breathing wells are completed beneath a perched groundwater system where the shallow groundwater is separated from deeper regional groundwater by the confining aquitard and the unsaturated zone of the partially saturated aquifer.

3. A portion of the unsaturated zone must be in direct contact with an open zone of the well. An open section of the borehole must extend above the water level, so that it straddles both the saturated and unsaturated zones of the aquifer, thus allowing soil gas to be freely exchanged between the subsurface and the atmosphere.

A well that meets all three conditions will be able to exchange gases effectively between the surface and the subsurface through the well.

Fluctuations in atmospheric pressure create vertical pressure gradients between the atmosphere and the subsurface, driving gases either into, or out

of, the well. When barometric pressure rises, air is transferred from the high-pressure surface to the relatively lower pressure subsurface, forcing atmospheric gases through the well and into the unsaturated zone. When barometric pressure falls, a pressure gradient is created in the opposite direction; gases in the unsaturated zone are drawn into the well and exhaled to the surface.

Numerous researchers (Thorstenson and Pollock, 1989; Massmann and Farrier, 1992; Auer et al., 1996; Elberling et al., 1998; Rossabi and Falta, 2002) have discussed the theories and behaviours related to the mechanics of breathing wells. Massmann and Farrier (1992) examined the physical effects of atmospheric pressure variations on gas transport in the vadose zone. They conclude that ambient air can migrate into the subsurface several metres radially during a barometric pressure cycle, significantly affecting gas-monitoring results. Building on this work, Elberling et al. (1998) modelled the transport of oxygen in a confined unsaturated zone. They looked at the importance of the amplitude and length of surface pressure variations on the transport of oxygen into the subsurface. They observed that oxygen migration into the subsurface creates a reaction zone where, for example, oxidation of pyrite can proceed. The area within the subsurface that is influenced by these changes is related to the length and amplitude of the pressure cycles: larger and longer barometric pressure cycles produce a greater radius of influence in the subsurface.

During high barometric pressure periods, breathing wells intake oxygen-rich atmospheric air. This oxygen may be utilized or dispersed in the subsurface so that concentrations are depleted when the well exhales to the surface, often at levels lower than the critical concentration needed to sustain human life. Thorstenson and Pollock (1989) describe the mathematical and physical

concepts involved in the transport of gas through an unsaturated zone. They conclude that the behaviour of steady-state gas transport can only be analysed through multi-component analysis. If one component is removed, other gas components will take its place to maintain pressure equilibrium. Likewise, if one component is added, the relative concentrations of the other gases will decrease.

Breathing wells are often identified by the strong currents of air, or the loud blowing and sucking sounds they produce. However, this identification can not be used to identify all breathing wells. Some are silent and/or transmit slow-moving air. Other breathing wells are identified because they freeze during periods of sub-zero temperature. That is, ambient air from the surface can be cold enough to freeze the water in the well. To prevent such freezing, many wells were constructed in well pits, which are much like basements. They are constructed so that the floor of the pit is below the frost line of the area. The well casing is then cut off above the floor of the pit. The pressure tank, pump lines and outlets are also conveniently located in these pits. Air circulation within well pits is often poor. They can become confined-space hazards if a breathing well is completed in the pit and oxygen-deficient air is emitted from the well during exhaling events. Alberta's *Environmental Protection and Enhancement Act* (Province of Alberta, 1993) outlawed the construction of well pits because of their potential for aquifer contamination and their confined-space safety hazards. Despite this regulation, pre-existing well pits are still common on farms across the prairies.

Oxygen-deficient exhaling events associated with breathing water wells have been the cause of a number of tragic accidents on farms across North America (Lewis, 1999). In 1922, two men died in a hand dug water well on a farm east of Red Deer. One source (Creelman, 1967) explains that the men

were attempting to deepen an existing well. The first man, Alex Clutton, had begun to climb down the well to begin digging for the day, when he seemingly let go of the ladder and fell 20 metres to the bottom of the well. Alex Johnson, who witnessed the fall, quickly ran to tell his wife and to obtain rope. Believing that Clutton had only slipped on the ladder, Johnson attempted to lower himself down the well to save Clutton. When Johnson reached the same depth, he too let go of the ladder and fell to his death. At the time, their deaths were blamed on a "black damp gas", which may have entered the well over night, or gas poisoning, much like that experienced in coal mines (Creelman, 1967). A similar tragedy occurred in the 1970's when a couple died in their well pit just east of the village of Delburne, Alberta. This well was confirmed as a breathing water well, but there is no documentation as to what gases were present in the pit at the time of their deaths (Lewis, 1999).

A more recent tragedy occurred in July 1999. Two teenagers died of asphyxiation in a well pit on a farm near Sylvan Lake, Alberta (Cooper, 1999; Lewis, 1999; Staudinger, 2002). The daughter, Susan Staudinger, had gone down into the pit to collect some vegetables for dinner when she passed out. Her father, Harvey Staudinger, found his daughter lying on the floor of the pit. Not realizing the danger, he attempted to enter the pit to revive her. He too lost consciousness. Susan's brother, Douglas, also attempted a rescue, but did not succeed. All three were taken to hospital; Harvey was discharged the next day, but Susan and Douglas both passed away shortly after. Authorities first attributed the cause of their deaths to the production of carbon dioxide from rotting vegetables (Cooper, 1999), but later found that the vegetables in the pit were not rotten. It was also observed that the near-by weather station (Red Deer) had recorded continuously decreasing atmospheric pressure in the three days prior to the incident (Hydrogeological Consultants Ltd., 2000).

Laboratory analysis of the air in the Staudinger's well pit a month following the deaths revealed that carbon dioxide concentrations were near 0.6%, compared to atmospheric concentrations of 0.035%. Oxygen concentrations were extremely low (8.7%), and nitrogen concentrations were unusually high (90.7%) (Hydrogeological Consultants Ltd., 2000). Further investigations (including water levels, barometric pressure, temperature and oxygen concentration measurements) the following summer indicated that the aquifer was indeed partially saturated and that the well released oxygen-deficient air during low barometric pressure periods (Hydrogeological Consultants Ltd., 2000).

The Staudinger tragedy is the motivation behind this study. Not only are Harvey and his wife Lois very passionate about determining the reason behind their childrens' deaths, and how their well was linked to the accident, but members of the professional groundwater community also recognize the need to determine the causes and extent of such wells. The full distribution of breathing water wells has not yet been identified, and many individuals who deal with such wells are still unaware of the associated risks and safety issues. These reasons help outline the thesis objectives.

The first objective of this study is to identify breathing water wells in Alberta, and other parts of North America. The intention is to provide an idea of the distribution of these wells, so as to increase the awareness and education within communities, and to hopefully prevent any further loss of life.

The second objective is to determine the physical relationship between barometric pressure fluctuations and breathing water wells. That is, to understand how changes in barometric pressure influence the gas concentrations emitted from these wells. To fulfill this objective, four wells

were monitored to compare and contrast their behaviours and characteristics. Driller's logs and previous hydrogeological studies were examined, and field monitoring procedures and laboratory analyses were performed.

The third objective is to determine the cause of oxygen-deficient air being exhaled from these wells. This goal was achieved by investigating water and gas chemistry within the subsurface, and determining the processes that lead to the alteration of the air composition.

The following chapter discusses the methods involved in locating breathing water wells and presents their identified distribution across Alberta and North America. The chapter also introduces the four wells selected for monitoring, the main study well being the Staudinger well, and three additional wells. Field and laboratory methods are discussed in Chapter 3. Chapter 4 presents the results from analyses conducted on the Staudinger well and discusses the physical processes and chemical reactions that lead to the observed behaviour. Chapter 5 compares and contrasts the behaviour of three additional breathing water wells to the Staudinger well, and discusses whether the same mechanisms are applicable to the individual sites. Conclusions and research implications are presented in Chapter 6.

CHAPTER 2: LOCATING and SELECTING BREATHING WATER WELLS

The first objective of this study was to locate breathing water wells and provide an idea of their distribution across Alberta and other areas of North America. This chapter discusses the methods used to locate breathing water wells and the steps leading up to the selection of the wells monitored as part of this research.

2.1 Locating Breathing Water Wells

The first task of the project was to locate breathing water wells, with particular interest in those located in central Alberta. Three methods were used: driller well logs, a questionnaire, and personal discussions with drillers.

2.1.1 Driller Well Logs

Driller water well logs were analyzed to find potential breathing water wells in Alberta. Electronic versions of well logs are available on a western Canadian database (The Groundwater Centre, 2004). Using this database, a query was conducted to determine how many wells in Alberta have the potential to breathe. The criterion was that the top of the completion interval must extend above the reported non-pumping water level. More than 12,000 wells across Alberta meet this requirement (Hydrogeological Consultants, 2000).

Once a water well has been constructed, it is difficult to verify if the three conditions for a breathing well (presented in Chapter 1) exist without an accurate, complete and well-documented well log. Unfortunately, much of the information in water well drilling reports can be inaccurate, incomplete or unsatisfactory (Tóth, 1966); therefore, it is often difficult to correctly determine

whether a well will breathe by classifying it solely by its driller's log and measured water levels. Field verification is required.

2.1.2 Questionnaire

The late Maurice Lewis, former executive officer for the Canadian Ground Water Association, conducted investigations as to the distribution of breathing water wells. He compiled a table of correspondents who had informed him whether they had knowledge of, or had encountered, breathing water wells in their regions. To supplement Maurice's investigations, a questionnaire was published in the June 2002 issue of *Ground Water Canada,* a quarterly publication distributed across Canada and parts of the United States. The questionnaire was also available on-line. The purpose of the questionnaire was to obtain feedback from the drillers, to determine where breathing water wells exist in Canada. Responses were received from drillers across the country. The results are tabulated in Appendix A. The information gathered by Maurice is also included in the table; unfortunately many of the local (Central Alberta) calls he received were not documented.

Results from the questionnaire show that breathing wells are not uncommon and are found across North America. Breathing wells were reported in parts of Oregon, South Carolina, Ohio, and Missouri. In Canada, breathing wells were reported in Alberta, Saskatchewan, British Columbia, and southern Ontario. Respondents from the eastern provinces (Nova Scotia, New Brunswick and Newfoundland) did not know of any breathing wells in their regions. Breathing wells are completed in a wide variety of geological settings, varying from sedimentary bedrock in Alberta, to limestone aquifers in Ontario, and basalts in western U.S.A.

The distribution of the reported and monitored breathing water wells in Alberta is shown in Figure 2.1. Many breathing water wells are located in the region around the villages of Delburne and Lousanna, and more are located in the

region around Sylvan Lake. The main drawback of the questionnaire is that it was voluntary. Although no wells were reported in some regions, the potential for breathing wells in these areas is still probable.

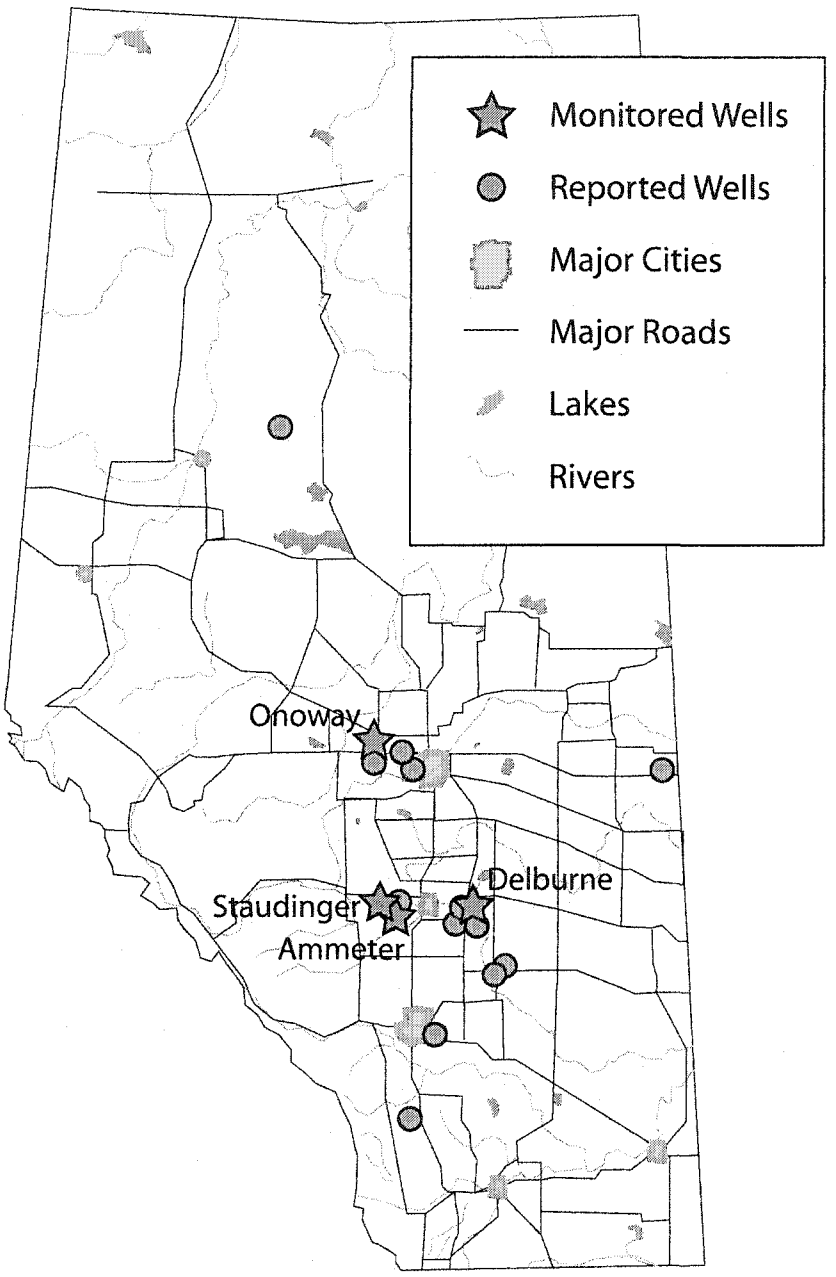

Figure 2.1: Reported and monitored breathing well distribution in Alberta.

2.2.3 Personal Communication

Local water well drillers (Central Alberta) were contacted to enquire whether breathing wells exist in their regions. Well drillers were either interviewed over the phone or in person.

2.2 Site Selection

Four breathing water wells in Central Alberta were selected for monitoring (Figure 2.1). The primary study well was the Staudinger well where the two teenagers died in 1999. It was intensively studied to continue the investigations following the accident, and to collaborate with McLeish (in prep.). Three other wells were monitored to validate the findings from the Staudinger well, and to confirm that the behaviour is similar at different sites. The Ammeter well was chosen because of its close proximity to the Staudinger well (i.e., 1600 m to the east), and because of its similar physical features, such as geology and completion in a well pit. The second additional well is located near Onoway. This well was identified through personal communication with the local water well driller. The third additional well, located near Delburne, was identified through the questionnaire and was later confirmed as a breathing well in personal communications with the driller. Well logs were analyzed prior to field verification to confirm that the three criteria exist for each of these wells.

CHAPTER 3: FIELD and LABORATORY METHODS

This chapter presents the field and laboratory methods used to analyze the four monitored breathing wells. The techniques used at the Staudinger well are presented first, followed by the variations employed at the other monitored well locations. A monitoring schedule is also included.

3.1 The Staudinger Well

The Staudinger well was the most intensively studied of the four monitored breathing wells. It was monitored for a longer period of time (two 4-month periods) and with additional equipment. The following outlines the equipment and methods used to monitor the Staudinger well.

3.1.1 Meteorological Data Collection

Barometric pressure was recorded continuously using a Vaisala PTB101 pressure sensor and recorded on a Campbell Scientific CR10X datalogger. The sensor was mounted on the wall of the datalogger enclosure. Ambient air temperature was measured using a Campbell Scientific 107-L temperature probe. The temperature probe was housed in a RM Young radiation shield, designed to block any direct or reflected solar radiation, yet still permit the free passage of air.

3.1.2 Gas and Air Monitoring

An air flow-through chamber was constructed to monitor the concentration of gases moving into and out of this well. The gas and airflow sensors were mounted to the walls of the chamber, fondly named "the Airmadillo" (Figure 3.1). The body of the Airmadillo was constructed from 1.52 m x 20.3 cm (5' x 8") square furnace duct, encased in a custom-made wood shell to mount sensors and protect the equipment during transport. Square-to-round

adapters were attached to each end of the furnace duct, tapering down to 3.81 cm (1½"). An adapter was used to connect the furnace duct to an air tube (2.54 cm), which fed to the top of the well seal. Silicon was used to seal the area between the tube and the well seal to prevent leakage of air. The other end of the Airmadillo was left to vent to the pit for the first two months of the initial monitoring period and for the entire second 4-month monitoring period in 2003. The Airmadillo was vented out to the atmosphere for the latter two months of initial monitoring period in 2002.

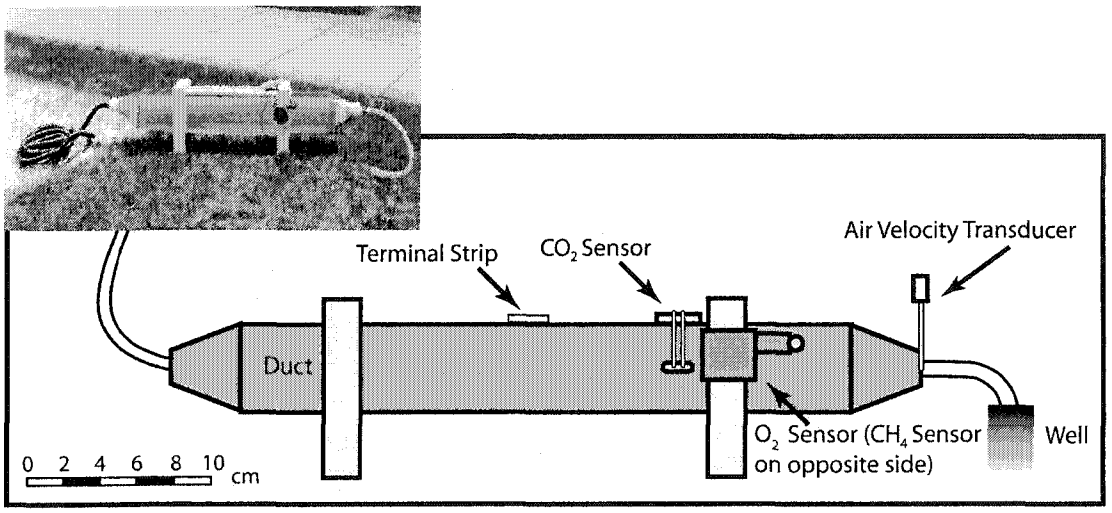

Figure 3.1: The Airmadillo showing sensor locations

Oxygen concentrations were measured using a QTS-1300 oxygen sensor (Quatrosense Environmental Ltd. (QEL), 2002a). This sensor allows air to pass through a flow limiting diffusion barrier and then into a self-contained cell where the oxygen reacts within the electrolyte, creating an electrical current between two electrodes. The standard measurement range of the sensor is 4 - 20 mA, equivalent to 0 to 25% O_2 v/v. The lower limit of the sensor (zero) is 4.00 mA +/- 0.1 mA (+/- 0.2%).

A QTS-1710 combustible transmitter (QEL, 2002b), used to detect methane gas, was attached directly opposite the oxygen sensor. If a combustible gas is introduced to the sensor, it will react with the platinum coating on one of

two pellister beads in the unit, causing oxidation, raising the temperature, and thus increasing the resistance between the two beads. The relative difference in resistance is proportional to the concentration of the gas. The standard measurement range of the sensor is 4 - 20 mA, equivalent to 0 to 5% CH_4 v/v. The lower limit of the sensor (zero) is 4.00 mA +/- 0.1 mA (+/- 0.03%).

A CTS M-20 carbon dioxide sensor (QEL, 2002c) was used to measure carbon dioxide concentrations. This sensor operates by allowing air to pass into the sensor's air column by diffusion. A time-cycling tungsten light source periodically emits infrared energy through the air column. Any carbon dioxide within the air column adsorbs this energy at a specific wavelength. A thermopile element at the opposite end of the air column senses the remaining infrared energy, producing a voltage signal. Energy measurements during the "off" cycle of the lamp provide an absolute reference to compensate for changing environmental conditions (i.e. temperature). The difference in the thermopile output between the "off" and the "on" cycles is proportional to the concentration of carbon dioxide (QEL, 2002c). The standard measurement range of the sensor is 4 - 20 mA, equivalent to 0 to 0.3% CO_2 v/v. The lower limit of the sensor (zero) is 4.00 mA +/- 0.4 mA (0 % CO_2 v/v +/- 0.0075%).

The three gas sensors attached to the Airmadillo were calibrated in the laboratory prior to installation using known ambient background concentrations of 20.9%, 0% and 0.035% for oxygen, methane and carbon dioxide respectively. Manual oxygen measurements, with corresponding checks for adequate sensor calibration, were also completed in the field using a hand held sensor: a BW Defender multi-gas detector (BW Technologies Ltd., 2002). The Defender monitors four gas concentrations simultaneously and continuously. It measures oxygen, combustibles, carbon monoxide and hydrogen sulphide.

An OMEGA FMA-900 (OMEGA Engineering Inc., 2000) air velocity transducer was installed for the second 4-month monitoring period of the Staudinger well. The sensor was mounted in the square-to-round adaptor on the Airmadillo (Figure 3.1). The standard measurement range of the sensor is 4 - 20 mA, equivalent to 0.05 to 0.5 m/s. The lower limit of the sensor (zero) is 4.00 mA +/- 0.4 mA (0.0125 m/s).

All of the sensors mounted on the Airmadillo were wired to a terminal strip attached to the top of the wood shell. These wires were fed through the old well casing in the roof of the pit and connected to a CR10X datalogger. Measurements were recorded every 15 minutes. The datalogger program and a schematic of the datalogger and terminal strips wiring are located in Appendix A.

3.1.3 Water Quality Sampling

Water samples were collected for geochemical, bacteria and stable isotope analyses. Water was pumped using the permanent submersible pump in the well. A direct pump hydrant was fed out of the well pit, through the old casing in the roof, and attached to a flow-through sampling cell. A flow-through sampling cell is used to ensure that aquifer water, not stagnant well water, is sampled, and to minimize atmospheric contact with the water. The flow-through sampling cell was constructed with a 1 litre Rubbermaid container (Figure 3.2). Poly-vinyl tubing was used to connect the sampling cell to the pump hydrant and to allow water to exit the cell. Water sampling commenced after pH, temperature, electrical conductivity (EC), and dissolved oxygen (DO) had stabilized. These parameters were measured using an Oakton pH 300 (Oakton Instruments, 2002a) and an Oakton DO 300 meter (Oakton Instruments, 2002b). On average, these parameters stabilized within 15 minutes of the submersible pump being turned on. Other measured field parameters included alkalinity (using a Hach titration kit (Hach Company,

1997)), and dissolved and total iron (using a CHEMmets kit (CHEMetrics, Inc., n.d.)).

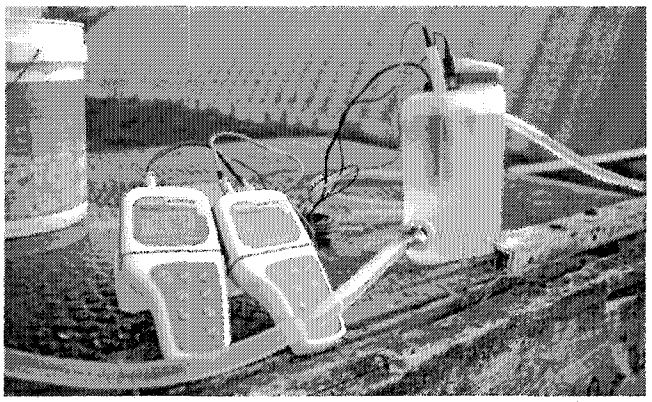

Figure 3.2: Flow-through sampling cell and Oakton meters.

After field parameters stabilized, two 500 mL water samples were collected into high-density polyethylene Nalgene bottles. The Nalgene bottles were rinsed three times with pumped water prior to collection. One bottle was filled with water filtered through a polyethersulfone (PES) membrane with a 0.45 micron pore size filter. Two 20 mL scintillation vials were filled with filtered water for NO_2^-+NO_3^- and NO_2^- analysis, and two vials were filled with non-filtered water to analyze for NH_4^+ and Total Nitrogen (TN). Samples were placed on ice during transport and then frozen until analyzed.

Water samples were analyzed in the Limnology laboratory at the University of Alberta, using standard methods set out by the American Public Health Association (Clesceri et al., 1998; Burgess, 2002). Cation concentrations were determined using an atomic absorption spectrometer (Perkin Elmer Model 3300), and anion concentrations were analyzed by ion chromatography (Dionex Model DX600). Analysis of nitrate plus nitrite was analyzed using flow injection analysis (FIA) colorimetric method.

Dissolved oxygen and temperature profiles were performed in December 2002, using an OxyGuard D041M18 dissolved oxygen and temperature probe

(OxyGuard, n.d.). The down-hole probe was lowered at discrete one metre intervals from the water table (25 metres below ground surface (mbgs)) to the depth of the pump (approximately 32.5 mbgs). The measurement range of the probe for dissolved oxygen is 0 to 20 mg/L, with sensitivity of +/- 1% of the full scale. The range of the probe for temperature is -5 to 45°C, with a sensitivity of +/- 0.2°C.

3.1.3.1 Biological Activity

Biological Activity Reaction Tests (BART) were used to determine the activity and presence of particular bacteria in the sampled groundwater. A positive test requires that a minimum number of desired bacteria be present in the sample to cause an observed reaction. The time lag to that observation is an approximation of the population size. The longer the time lag, the smaller the population of the targeted bacteria. Thus, responses are qualitative.

Four different tests were used: Denitrifying bacteria (DN-BART), Iron-related bacteria (IRB-BART), Nitrifying bacteria (N-BART), and Sulfate-reducing bacteria (SRB-BART). The sampling and testing procedures are outlined in Cullimore (1999).

A positive observation, indicating the presence of a particular class of bacteria, varies for each BART. A positive test in a DN (denitrifying) tester requires the formation of foam to collect on over 50% of the area under, and around, the ball (Cullimore, 1999). There are a range of possible iron related bacteria (IRB) reactions and reaction patterns, representing a range of dominant bacteria, outlined in Cullimore (1999). There are three reaction patterns that are positive for sulphate reducing bacteria (SRB), consisting of blackening of the base of the tester, the blackening around the ball or a combination of both. The time lag sequence to observe these reactions proceeds the same as IRB. The test for nitrifying bacteria is interpreted by the amount of pink-red coloration generated, and the location of the colour

after a 5 day lag time (Cullimore, 1999). In this thesis, bacteria reactions are expressed as: no reaction (n/a), background concentrations (bck.), moderately aggressive (m.a.), or aggressive (a.).

3.1.3.2 Isotopes

Groundwater samples were obtained for the analyses of the stable oxygen and hydrogen isotopes. A description of the field and laboratory methods, the data, and interpretation are all discussed in Appendix B.

3.1.4 Water Levels

A Solinst LT Levelogger M10 was lowered 29.6 mbgs. The Levelogger recorded both the temperature and pressure head measurements of the water every 15 minutes. The output data from the Levelogger does not correct for barometric pressure changes. These corrections were made in the laboratory after both the barometric pressure and the Levelogger data were downloaded. The resolution of the sensor is 0.2 cm. Manual water level measurements were made at each visit to verify the Levelogger outputs.

3.1.5 Dissolved Gas

3.1.5.1 Total Dissolved Gas Probe

A Common Sensing SM1 Total Dissolved Gas Pressure (TDGP) probe was lowered 29.5 mbgs. The general design and operating principles of TDGP probes are outlined in Manning et al. (2003). The probe does not distinguish between dissolved gas constituents. The standard measurement range of the sensor is 0 to 203 kPa with a sensitivity of 0.27 kPa.

3.1.5.2 Passive Gas Samplers

Passive diffusion samplers detect a time-averaged in-situ gas concentration (Powell and Puls, 1993). Three passive gas samplers, designed at the University of Calgary (McLeish, in prep), were installed in the Staudinger well. One was placed above the water level, at 22.5 mbgs, to measure the average

composition of the air in the unsaturated zone. The two other samplers were submerged at a depth of 29.3 mbgs, directly above one another (for quality control), to measure the dissolved gas concentration at depth. The samplers were left in the well for a period of one month to allow the dissolved gases in the water (or gases in the air) to reach equilibrium with the gases in the sample chamber. The samplers were removed and analyzed for the different gas components on a gas chromatograph (Hewlet Packard 5890) at the University of Calgary.

3.2 Additional Breathing Water Wells

The field methods carried out at the additional well sites were similar to those conducted at the Staudinger well, but not as intensive. The meteorological and Airmadillo sensors were set up at all of the sites. When the Airmadillo was positioned on the ground surface, the oxygen sensor demonstrated a strong dependence on diurnal temperature fluctuations. Laboratory tests, performed in February 2002, showed a distinct relationship between the temperature of the sensor and its concentration output. During subsequent field monitoring, the temperature probe was housed directly in the oxygen sensor casing to record the temperature of the sensor itself. These temperatures were used to correct the raw data measurements. These dependencies and correction methods are discussed in Appendix C

Unavailability of the down-hole equipment prevented the TDGP probe and the passive gas samplers from being installed at the additional wells. The Levelogger was installed at the Onoway well at a depth of 45 mbgs, but not at the Delburne or the Ammeter wells. Manual water level measurements were taken at all sites prior to water quality sampling. Sampling of the Onoway well was conducted on a bi-weekly basis, whereas the Delburne and Ammeter wells were sampled once. Samples were obtained from the first possible water outlet from the well (i.e., before the pressure tank) instead of a direct

pump line. Otherwise, the water sampling protocol for the additional wells was the same as that performed at the Staudinger well.

3.3 Health and Safety

The true function of the Defender is to monitor hazardous gases. Gas measurements of the air in well pits were made prior to entry. When oxygen concentrations were detected lower than 19.7%, an industrial vacuum cleaner was used to replace the air in the pit with fresh ambient air until oxygen concentrations rose to safe levels. The Defender accompanied anyone working in the pits to ensure that the conditions remained safe. During exhaling periods, the vacuum cleaner was turned on for the entire duration that work was performed within the pit in order to provide adequate ventilation. A second person was always required to be on-site while someone was in the pit.

3.4 Monitoring Schedule

The Staudinger well was the most intensively studied well of the four monitored breathing wells. Installation of monitoring equipment and data collection commenced in June 2002, and ended in September 2002 (summer period). A second monitoring period spanned February to May 2003 (winter/spring period). The three other wells were monitored for only four weeks each. A summarized schedule for the instrumentation and operations conducted at all four sites is presented in Table 3.1.

Table 3.1: Schedule for instrumentation of breathing water wells.

Year	Month	Instrumentation	Barometric Pressure	Air Temperature	O_2, CO_2 and CH_4 Concentrations	Air velocity	Pressure Transducer (Levelogger)	TDGP* and Passive Gas Samplers*	Water Sampling (# times well sampled)
2002	June	Installation of equipment at **Staudinger** well - summer monitoring period	√	√	√	√	√	√	7
	September	Remove Airmadillo and Meteorological sensors and install at **Onoway** well	√	√	√	√	√		2
	October	Remove equipment from Onoway							
	December	DO and temperature profile of Staudinger well							
2003	February	Re-install Airmadillo and Meteorological sensors at **Staudinger** well - winter/spring monitoring period	√	√	√	√	√	√	1
	May	Remove all equipment from Staudinger and install Airmadillo and Meteorological sensors at **Delburne** well	√	√	√	√			1
	June	Remove equipment from Delburne and install at **Ammeter** well	√	√	√	√			1
	July	Remove equipment from Ammeter well							

* (McLeish, in prep.)

3.5 Supporting Methods

Additional off-site methods were employed to complement the data collected from the Staudinger well.

3.5.1 Shallow Well Water Quality Sampling

A shallow groundwater well was sampled in July 2003 to compare the water chemistry between the shallow groundwater in the area (water level = 2.8 mbgs) and the deeper aquifer groundwater in which the Staudinger well is completed. The closest shallow water well is located approximately 1200 m west of the Staudinger well. The well is abandoned and there is no well log available. The approximate depth of the well is 8.9 m, determined using a

weighted tape. The well was purged using a WaTerra pump and tubing until approximately three well volumes were removed, and the standard field parameters had stabilized. The water sampling protocol of the shallow water well was the same as that conducted for the Staudinger well.

3.5.2 Water Elevations for Regional Groundwater Distribution

Water levels in selected water wells southwest of the town of Sylvan Lake were measured to characterize the groundwater flow regime in the area around the Staudinger well. Landowners were contacted by phone and asked if land access and water level measurements were authorized. Water levels were obtained from 15 wells completed in the Paskapoo formation, and from three wells completed in the shallow drift deposits. Measurements were manually acquired over the course of two days in June 2003.

CHAPTER 4: RESULTS and DISCUSSION of the STAUDINGER WELL

The breathing water well located on the Staudinger farm was the primary well in this investigation. Observations and results were used to investigate the physical relationships between barometric pressure and gas compositions in the subsurface, and to determine the cause of the oxygen depletion in the unsaturated zone of the partially saturated aquifer. This Chapter presents:

- A brief description of the completion details of the Staudinger well, and the local geology and hydrogeology for the region.
- The field and laboratory results obtained from the Staudinger well
- An explanation of the physical and chemical reasons for the depletion of oxygen within the exhaled air.

4.1 Site Description

4.1.1 Location and Completion Details

The Staudinger well is located south of Sylvan Lake, Alberta, on the eastern edge of the Rocky Mountain House area (Figure 4.1). The well is located in the northwest corner of Section 12, Township 38, Range 2, west of the 5th Meridian. It is located at UTM 11 U 0694091 east and 5793424 north (longitude 114°09'21.7" west and 52°15'32.3" north) at an elevation of 988 metres above sea level (masl).

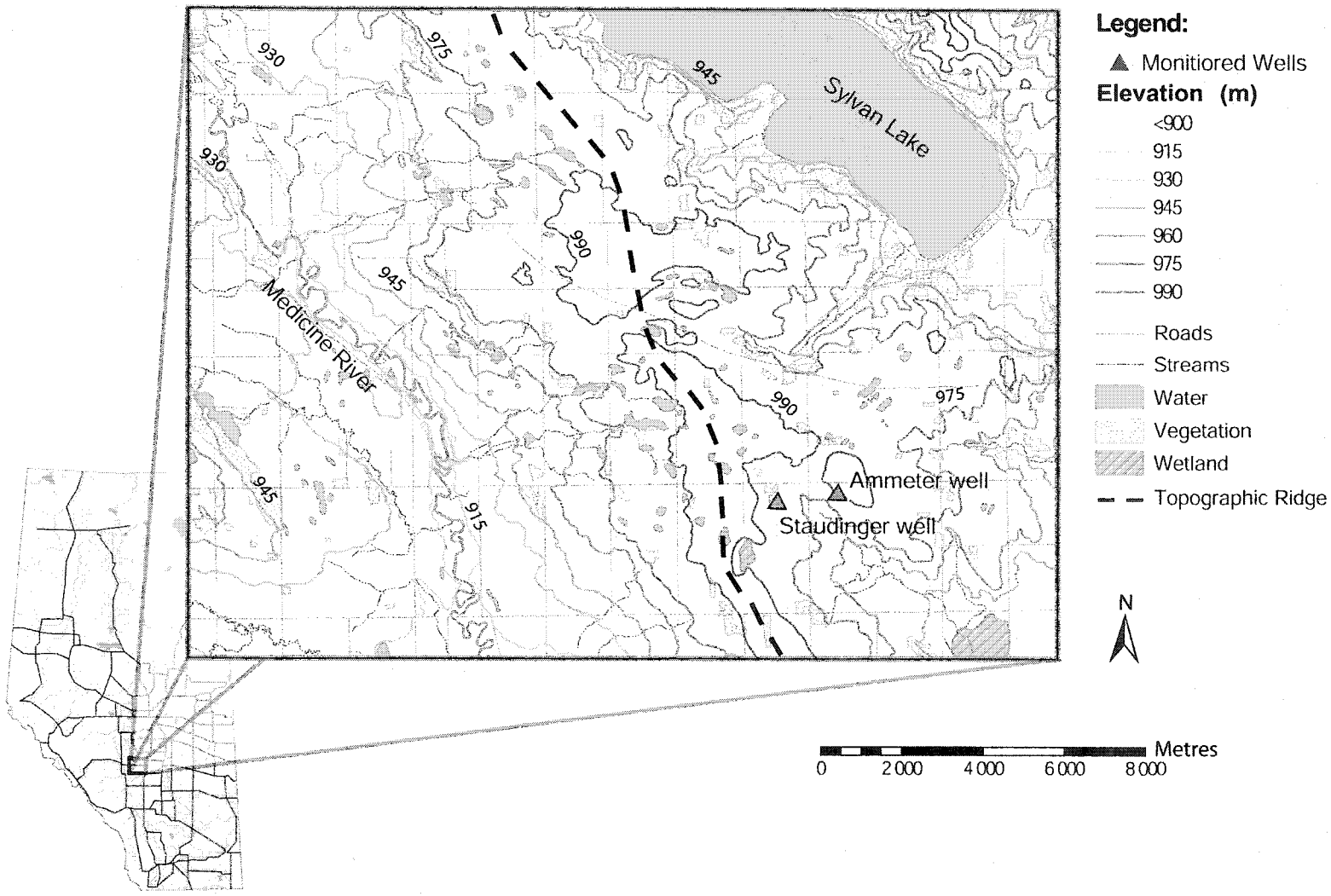

Figure 4.1: Location of monitored breathing water wells, south of Sylvan Lake Alberta. Reproduced with the permission of Natural Resources Canada (2002a,b).

The Staudinger well is completed to 48.2 metres below ground surface (mbgs), or 939.8 masl (Figure 4.2). The 15.2 cm (6") diameter surface casing extends to 13.4 mbgs. The well is located in a 2.5 m deep concrete pit, with its entrance through the floor of an overlying barn. The average water level over the course of this study was 963.5 +/- 0.5 masl. The distance between the bottom of the confining aquitard and the water level provides an unsaturated thickness of 8.7 m in the aquifer.

4.1.2 Geography and Climate

The Sylvan Lake area is primarily used for agriculture. Over half of the land is cultivated for mixed farming and livestock, but some land is influenced by oil and gas production (Gabert, 1975). The climate is strongly influenced by the Rocky Mountains to the west. According to the Köppen classification, the area lies in the Dfc climatic zone (Trewartha, 1980), which is characterized by a humid continental climate, with brief cool summers and bitterly cold winters. Average annual precipitation is approximately 550 mm (Environment Canada, 2000). Most precipitation falls as rain during the summer months. Average annual potential evapotranspiration, approximately 600 mm (Environment Canada, 2000), exceeds annual precipitation, thus limiting the amount of groundwater recharge. Most groundwater recharge occurs in March and April during spring melt and ground thaw (Gabert, 1975).

4.1.3 Geology

The landscape of the region is relatively flat with slightly rolling to hilly topography (Tokarsky, 1971). A local topographic ridge, running northwest to southeast (Figure 4.1), is located to the west of the Staudinger well. The three relevant hydrostratigraphic units of this study include a sandstone

aquifer and a confining shale aquitard, both in the Paskapoo Formation, and the surficial Quaternary deposits.

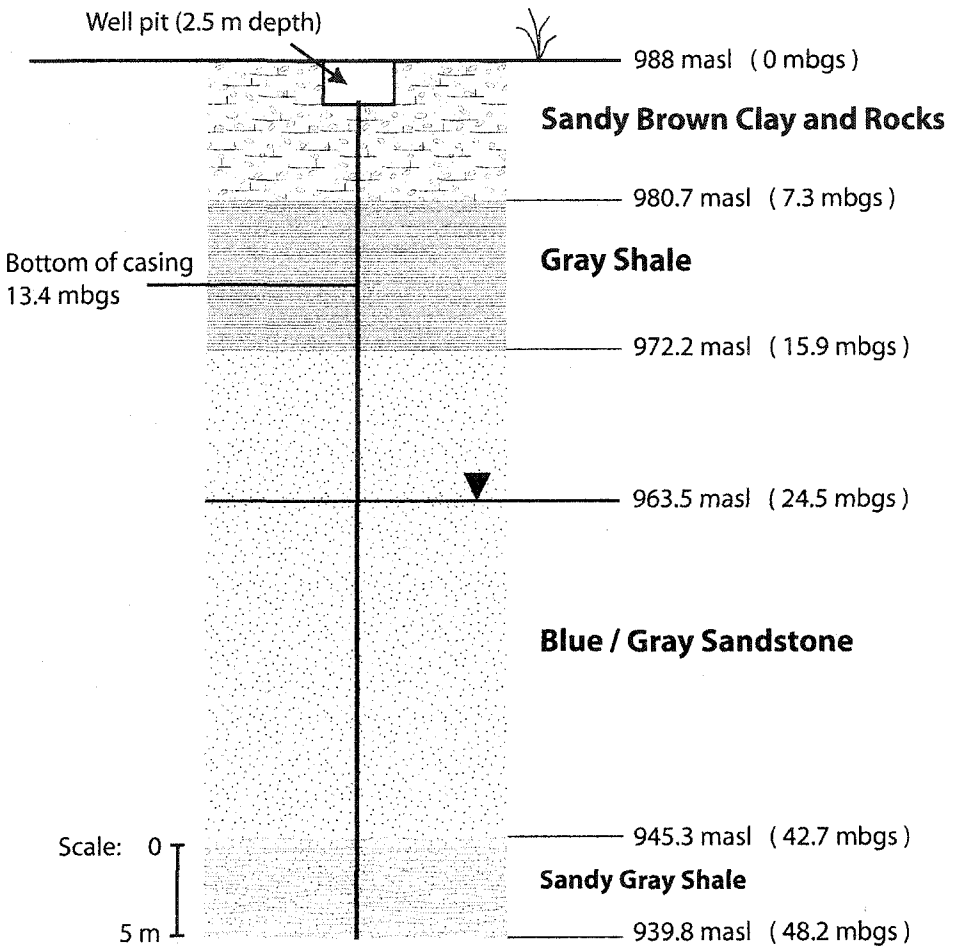

Figure 4.2: Completion details of the Staudinger well (generalized from driller's log)

The Paskapoo is a freshwater sedimentary deposit, Tertiary in age, containing the uppermost bedrock deposits in the region. It was deposited on a low, sinking surface and represents a combination of fluvial and shallow lake conditions (Tóth, 1966; Carrigy, 1970). The Paskapoo consists of alternating shale-siltstone bentonitic beds and sandstone units. The sandstones consist of predominantly quartz and plagioclase minerals (Carrigy, 1970), with grain sizes varying from very fine to medium (Tóth,

1966; Gabert, 1975). Volcanic ash, iron oxide and coal deposits are dispersed throughout the unit (Tokarsky, 1971). It is not certain how thick the Paskapoo formation is beneath the Staudinger well; however, it is estimated that this hydrostratigraphic unit is up to 200 m thick south of Sylvan Lake (Gabert, 1975).

The Staudinger well is located in an upland area of the Paskapoo Formation, an area that resisted most pre-Pleistocene erosion (Carrigy, 1970). This local topographic high exists because the sandstones are capped with a shale-siltstone layer, also part of the Paskapoo Formation (Gabert, 1975). This shale layer, which has a high montmorillonite content, is 9 m thick at the Staudinger location and acts as a confining aquitard.

The upper boundary of the shale aquitard is an erosional surface, overlain by Quaternary (drift) deposits. Thickness is variable, but these deposits are generally less than 10 m thick in the immediate vicinity of the well. They are classified as ground moraine deposits, deposited by the Laurentide ice sheet as it retreated to the north (Gabert, 1975). They are non-sorted and non-stratified, consisting of sandy brown clays, gravel, rocks or till. The quaternary deposits are rich in quartz, dolomite, plagioclase and calcite (Wallick, 1981).

4.1.4 Hydrogeology

Most active groundwater flow in the area occurs in local and intermediate flow systems at depths up to 180 m; the remainder of the flow occurs in high permeability sandstone layers at greater depths (Gabert, 1975). A water table map was created to visualize the distribution of hydraulic head in the Paskapoo aquifer surrounding the Staudinger well (Figure 4.3). The hydraulic head distribution was plotted using Surfer7, a contouring and surface-mapping program (Golden Software Inc, 1999). This map was then

overlain onto a digital area map of Sylvan Lake using ArcMap 8.1 (ESRI, 2001). The map area is 17.5 km by 11.5 km.

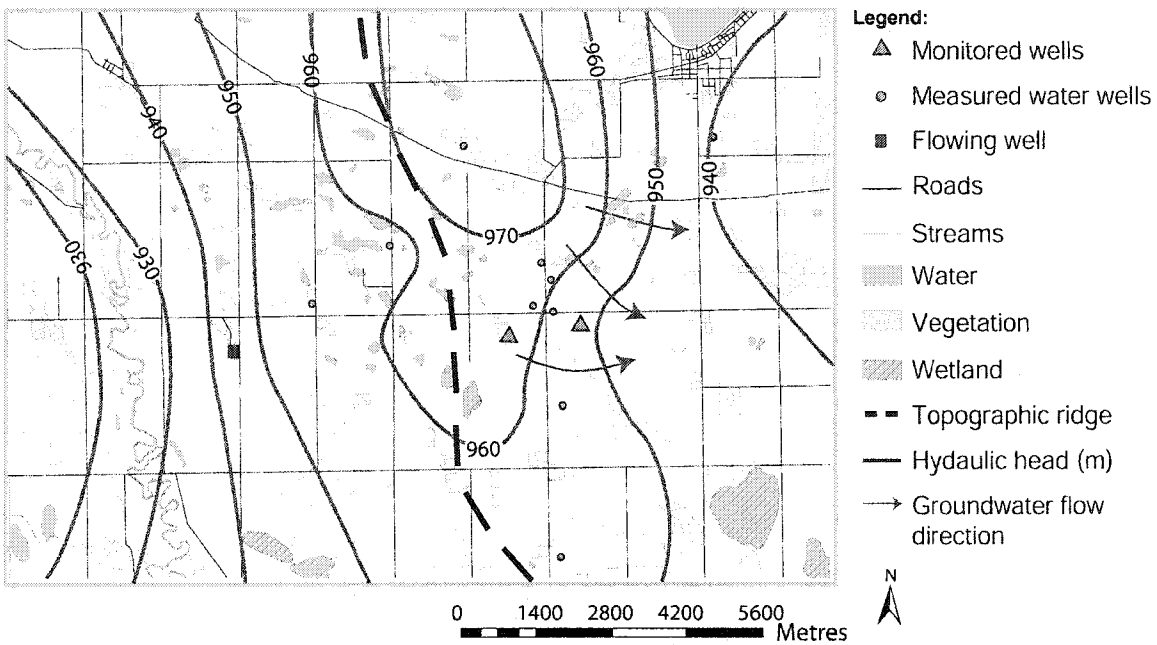

Figure 4.3: Hydraulic head distribution in the Paskapoo Formation, south of Sylvan Lake Alberta. Base map reproduced with the permission of Natural Resources Canada (2002a,b).

As Gabert (1975) described, the Staudinger well is located in a groundwater recharge area. Highest groundwater elevations are located in the north-central region of Figure 4.3. Groundwater flows away from the topographic ridge; some water flows northwest towards Sylvan Lake, and some flows southeast ultimately towards the Red Deer River. On the west side of the ridge, groundwater flows southwest towards the Medicine River. Several flowing wells were observed, and farmers indicated that other flowing wells exist on this side of the ridge. These wells exist because the loss in elevation towards the Medicine River is greater than the decrease in hydraulic head, leading water levels to rise above the ground surface.

Several breathing water wells are located southeast of the topographic ridge. These include the Staudinger well and the additional monitored breathing

well, the Ammeter well. These wells exist in a confined unsaturated zone (i.e., perched conditions) because the permeability of the shale aquitard is low enough so that the volume of water percolating through the shale is not sufficient to fully saturate the underlying Paskapoo sandstone unit.

The Staudinger well is drilled through a perched groundwater system. A perched aquifer is usually an unconfined aquifer that is separated from a deeper aquifer by a confining layer and an unsaturated zone (Bates and Jackson, 1987). The perched aquifer is located in the Quaternary deposits. Precipitation and snowmelt are the main source of recharge for this upper aquifer (Gabert, 1975). The main source of recharge for the deeper Paskapoo aquifer is water infiltrating from the perched aquifer through the shale unit. Recharge rates are highest in the spring. For example, the water level in the Staudinger well rose by over 0.5 m between March and May 2003, coinciding with surface snowmelt and ground thaw.

The Paskapoo formation is generally highly transmissive (Tokarsky, 1971). Results from aquifer tests indicate that a typical transmissivity of the aquifer is over 100 m^2/day, and typical hydraulic conductivities range between 10^{-7} and 10^{-4} m/s (Gabert, 1975). The natural hydraulic head gradient ($\Delta h/\Delta x$) near the Staudinger well is estimated to be 0.007 at 345°. Using Darcy's Law,

$$q = K\left|\frac{\Delta h}{\Delta x}\right| \qquad (4.1)$$

where q is groundwater flux [L/T], and K is hydraulic conductivity [m/s], the possible groundwater flux through the region ranges between 7×10^{-10} and 7×10^{-7} m/s.

4.2 Oxygen Concentrations and Barometric Pressure

Changes in oxygen concentrations (O_2) are directly correlated with changes in barometric pressure (Baro_P). The relationship between these two parameters was analyzed on a number of time scales: long (8 month), intermediate (2 week), and small (individual pressure cycle). The complete eight-month data set for all of the measured parameters (including barometric pressure, temperature, air velocity, and gas concentrations) is tabulated in Appendix A.

4.2.1 Eight Month Trends

The breathing behaviour of the Staudinger well is observable year round (Figure 4.4). During inhaling periods (rising barometric pressure), ambient air is drawn past the oxygen sensor and into the unsaturated zone of the aquifer. Concentrations in the pit were measured near atmospheric levels. Air circulation in the pit is limited, thus concentrations are lower than the expected atmospheric concentration (21%), at which the sensor was calibrated for the summer monitoring period.

During exhaling periods, oxygen-deficient subsurface air is blown out of the well. Minimum concentrations of 4.7% during the summer and 2.2% in the winter/spring were measured. Overall, the Staudinger well posed a potential health hazard, where exhaled air contained less than 16% oxygen, for over 40 days of the 8 months (i.e., 17% of the total monitored time). The magnitude of the individual pressure changes was greater during the winter/spring period having a maximum change of 4.0 kPa (between a trough and peak) compared to only 3.7 kPa during the summer period.

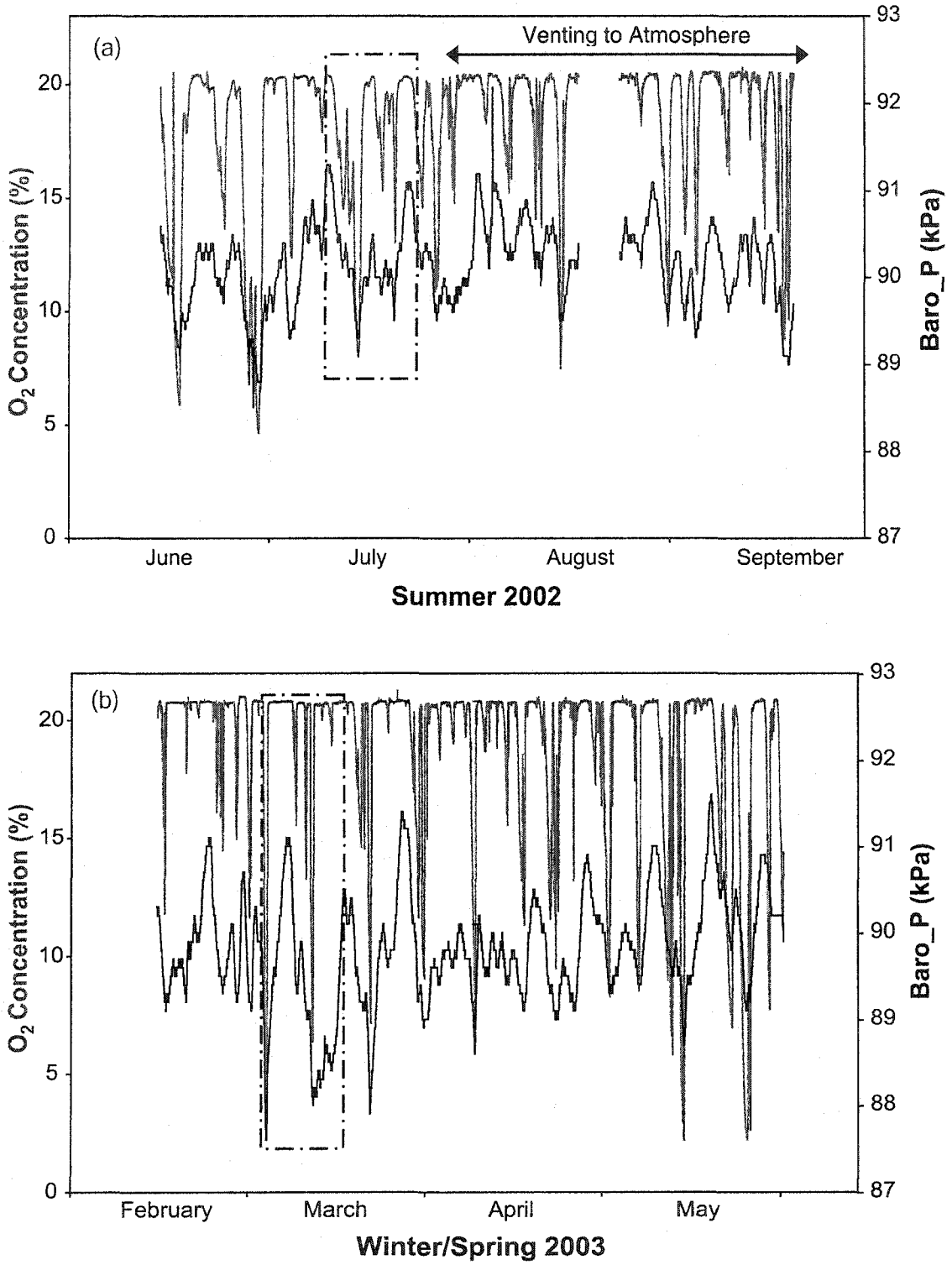

Figure 4.4: Distribution of oxygen concentrations emitted from the Staudinger well, and barometric pressure (Baro_P) during (a) the summer monitoring period, and (b) the winter/spring monitoring period. Dashed boxes outline the 2-week periods chosen for more detailed analysis (Figure 4.5).

The arrow spanning the top of Figure 4.4a indicates the two-month period in which the air moving through the Airmadillo vented directly to the atmosphere. For the remainder of the monitoring periods, the air vented into the pit. The oxygen concentration distribution during pit-venting periods is smoother compared to the atmosphere venting period. This is caused by the source of the incoming air. Air moving into the well during the atmosphere venting case is atmospheric air, whereas in the non-venting case, the source of air originates from within the well pit, where air circulation is poor. The oxygen gradient between the wellhead and the pit is smaller than the oxygen gradient between the wellhead and the atmosphere. Thus the small-scale oxygen fluctuations are minimized during pit-venting periods. The variations between these two conditions do not affect the overall relationship between oxygen concentrations and barometric pressure fluctuations.

4.2.2 Two Week Trends

The relationship between barometric pressure and oxygen concentrations are presented in more detail on a two-week time scale (Figure 4.5). Figure 4.5 shows observations for the periods extracted from the eight-month data in Figure 4.4. These particular two-week periods were chosen because they possess a number of barometric pressure cycles, varying in both magnitude and length.

The recovery of oxygen concentrations (i.e., returning to atmospheric conditions) appears to occur at a faster rate than that at which concentrations decrease. This is an artefact of the positioning of the sensor. The sensor is located at the surface; therefore, it detects atmospheric oxygen concentrations during inhaling periods earlier than it detects the oxygen-depleted gas being exhaled from the subsurface.

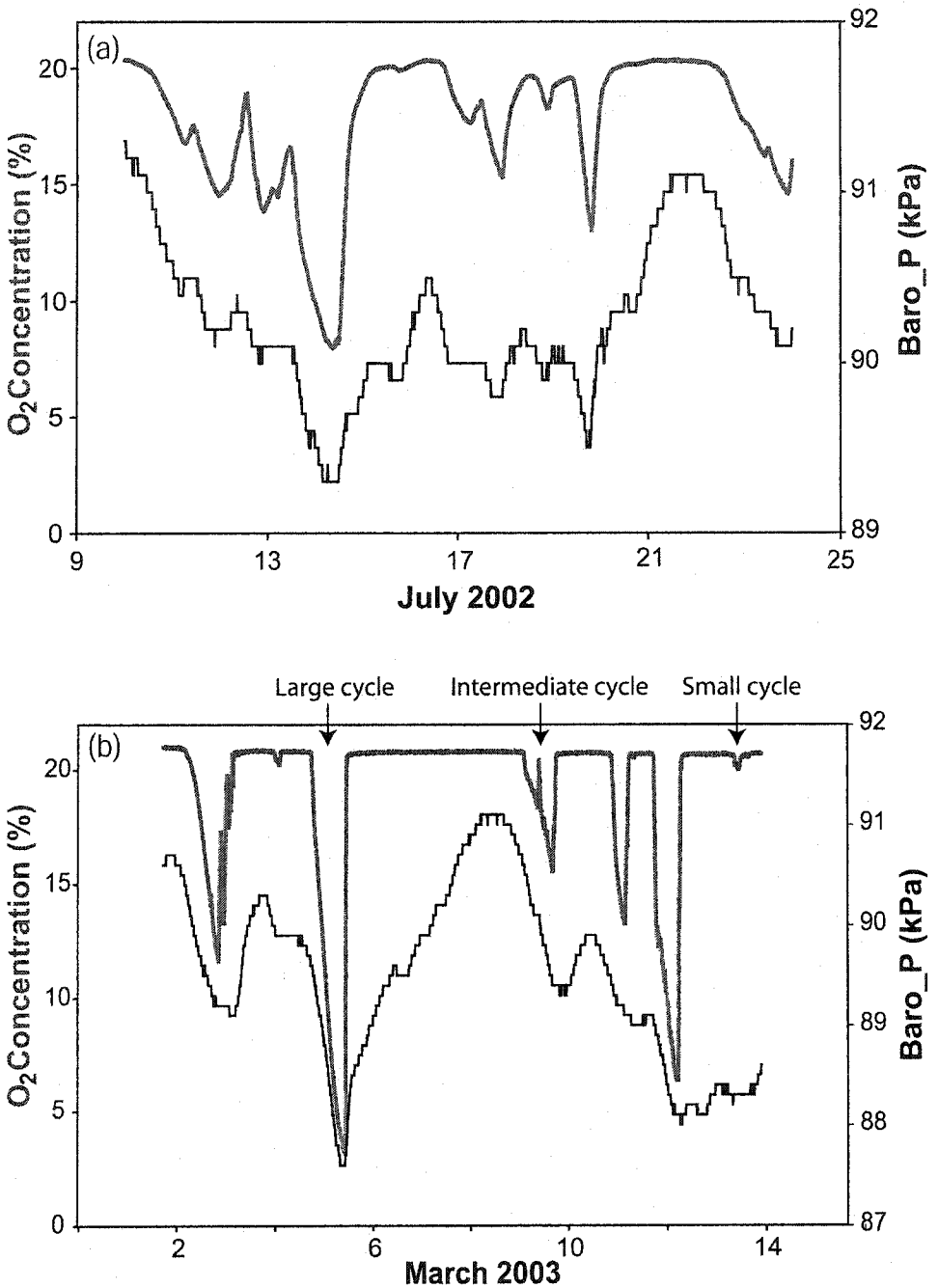

Figure 4.5: Distribution of oxygen and barometric pressure over 2 week periods in (a) the summer (July 2002) and (b) the winter/spring (March 2003). The individual cycles (Large, Intermediate, Small), analyzed in Section 4.2.3 (Figure 4.7), are identified in (b).

The rate of change in oxygen and barometric pressure were analyzed for each two-week period. For oxygen, these rates were calculated according to the following equation:

$$\Delta O_2 = \frac{O_{2t+\Delta t} - O_{2t}}{\Delta t} \tag{4.2}$$

where O_{2_t} is the recorded oxygen concentration at time t, and $O_{2_{t+\Delta t}}$ is the recorded oxygen concentrations at t+Δt. Analyses were performed for different time intervals (Δt). A Δt of 24 hours produced the highest correlation compared to other analyzed time intervals (i.e., 4, 12, 15, 20 and 30 hours). Corresponding calculations were completed for changes in barometric pressure (ΔBaro_P).

The correlation coefficient is a measure of the linear dependence between two variables (Deutsch, 2002). In general the correlation coefficient is:

$$\rho_{XY} = \frac{Cov(X,Y)}{\sqrt{Var(X)Var(Y)}} \tag{4.3}$$

where ρ_{XY} is the correlation coefficient between variable X and variable Y, Cov(X,Y) is the covariance between the two variables, and Var(X) or Var(Y) is the variance in either X or Y. A correlation of 1 implies that the two variables are perfectly correlated. A correlation of 0 implies the variables are perfectly uncorrelated. A negative correlation indicates that the variables are inversely correlated.

The correlation coefficient of changes in oxygen (ΔO_2) and changes in barometric pressure (ΔBaro_P) were determined. There is a definite positive linear relationship between the two parameters. Figure 4.6 displays the daily

(24 hour) rates of change in oxygen and barometric pressure over the two-week summer period, and the two-week winter/spring period. A decrease in oxygen over 24 hours (negative ΔO_2) corresponds to a decrease in barometric pressure (negative ΔBaro_P). The variance and scatter of the data can be explained by the incomplete mixing of air (i.e., poor air circulation in the well pit), and differences in the magnitude and duration of individual pressure cycles (see Section 4.2.3).

The total two-week correlation between the daily rates of change in oxygen and barometric pressure is 0.74 for the selected summer two-week period and 0.60 for the selected winter/spring period. The number of barometric pressure cycles, and their variance in magnitude, was greater during the winter/spring period. The variance between these cycles is greater, thus reducing the correlation between the overall oxygen and barometric pressure two-week changes. The correlation between these two parameters over the entire 4-month monitoring periods was 0.68 in the summer, and 0.22 in the winter.

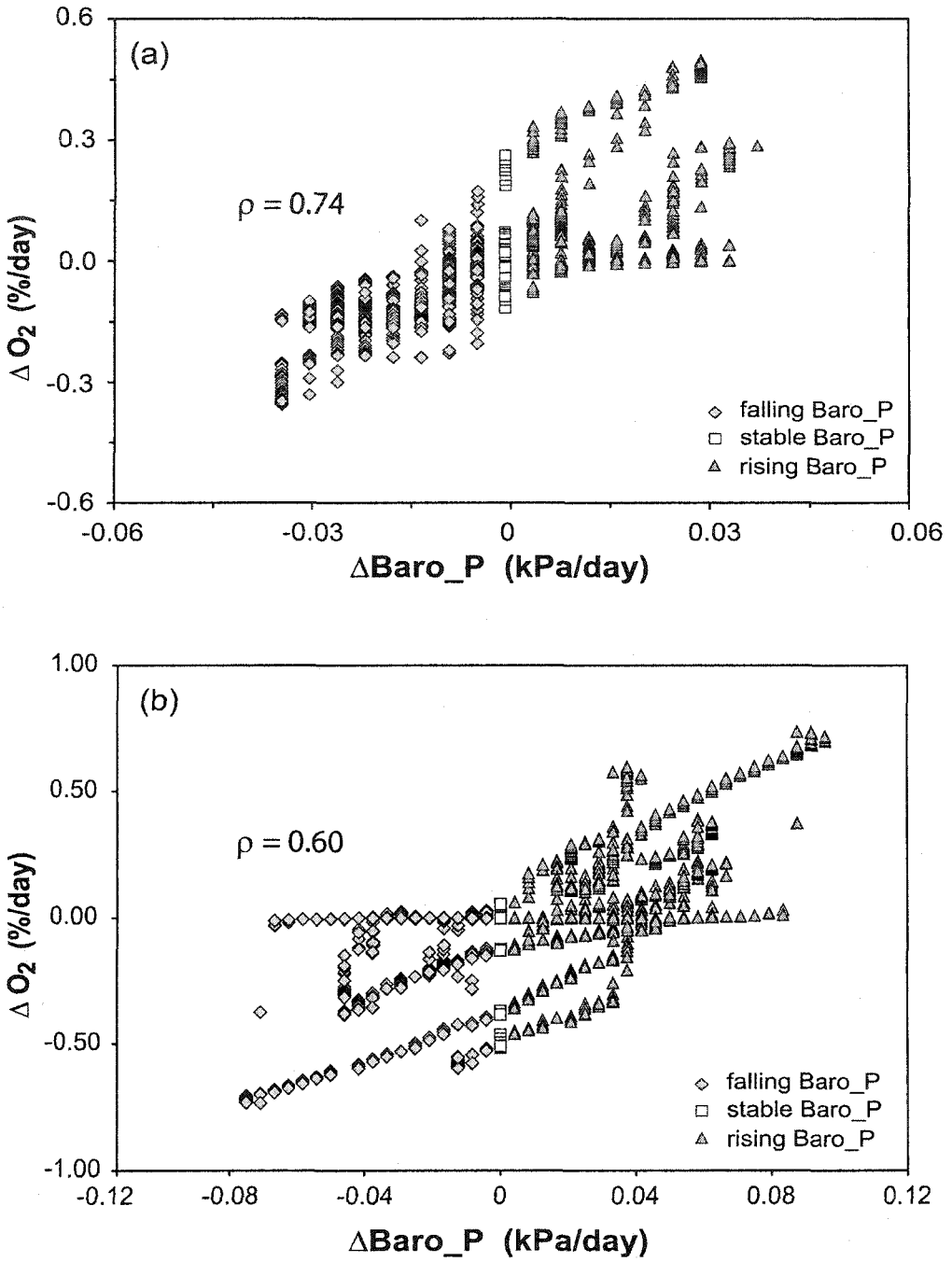

Figure 4.6: Daily rates of change in oxygen and barometric pressure for (a) two weeks during the summer monitoring period and (b) two weeks during the winter/spring monitoring period.

4.2.3 *Individual Trends*

Three individual cycles from the winter/spring monitoring period (identified in Figure 4.5b) were examined to determine the effects of the length and magnitude of a barometric cycle on oxygen concentrations. Each cycle was defined from the time at which oxygen concentrations first decreased to when concentrations recovered to atmospheric levels. The daily rates of change of the three cycles are shown in Figure 4.7.

The large cycle was 48 hours in length, with a maximum pressure decrease of 2.3 kPa. Oxygen concentrations fell to a minimum of 3.1%. The correlation between the daily rates of change in barometric pressure and O_2 is 0.94. The intermediate cycle was also 48 hours in length, but had a maximum pressure decrease of only 1.5 kPa. Barometric pressure stabilized mid-cycle for approximately 3 hours before continuing to decrease. Oxygen concentrations recovered over this 3 hour period, then decreased to a minimum of 15.6%. As a result, the cycle only demonstrated a correlation of 0.81.

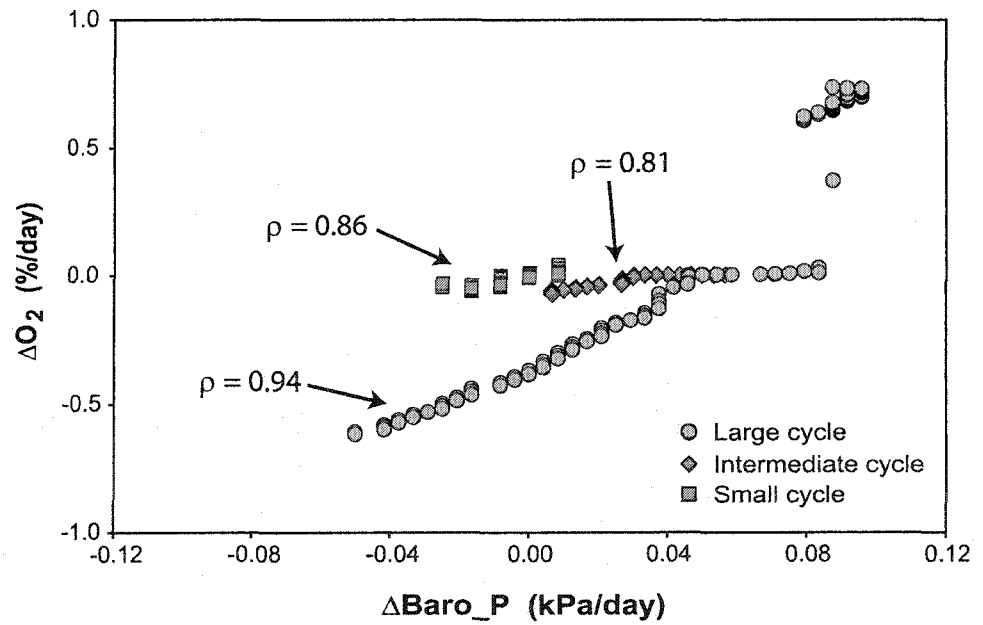

Figure 4.7: Daily rates of change in oxygen concentrations and barometric pressures for three individual cycles. These cycles were selected from the 2-week distribution during the winter/spring (*Figure 4.5b*).

Small weather patterns (smaller barometric pressure fluctuations) still affect subsurface concentrations; however, the effects are reduced. That is, the small cycle also showed a positive linear correlation of 0.86. The total length of the cycle was 12 hours, with a maximum pressure change of only 0.4 kPa. The shorter duration and magnitude of this cycle only allowed a total change of 1% in the oxygen concentrations.

A determining factor as to the extent of gas migration in the subsurface, due to atmospheric pressure changes, is the length and amplitude of the pressure fluctuation (Elberling et al., 1998). All three cycles demonstrate a high linear correlation between oxygen and barometric pressure fluctuations; however, because of their differences in length and strength, each cycle displays a unique result. This is observed in the scatter and variance observed in the overall rates of change for a selected period.

4.3 Carbon Dioxide and Methane

Carbon dioxide concentrations are inversely related to barometric pressure. Decreases in barometric pressure are followed by increases in carbon dioxide concentrations. The correlation coefficient between daily rates of change in CO_2 and barometric pressure, over the same chosen two-week summer period is –0.79, and –0.69 for the winter/spring period. Elevated concentrations of carbon dioxide, with respect to atmospheric, are exhaled from the well. The maximum CO_2 concentration emitted from the Staudinger well was 0.29% during the summer and 0.26% during the winter/spring. A two-week distribution of the measured CO_2 concentrations and barometric pressure (for the winter/spring monitoring period) is displayed in Figure 4.8a. The daily rates of change in the two parameters are depicted in Figure 4.8b. The plots for the summer period are available in digital form in Appendix A.

Methane gas was not emitted from the subsurface. Concentrations were below the instrument detection limit (<0.125%).

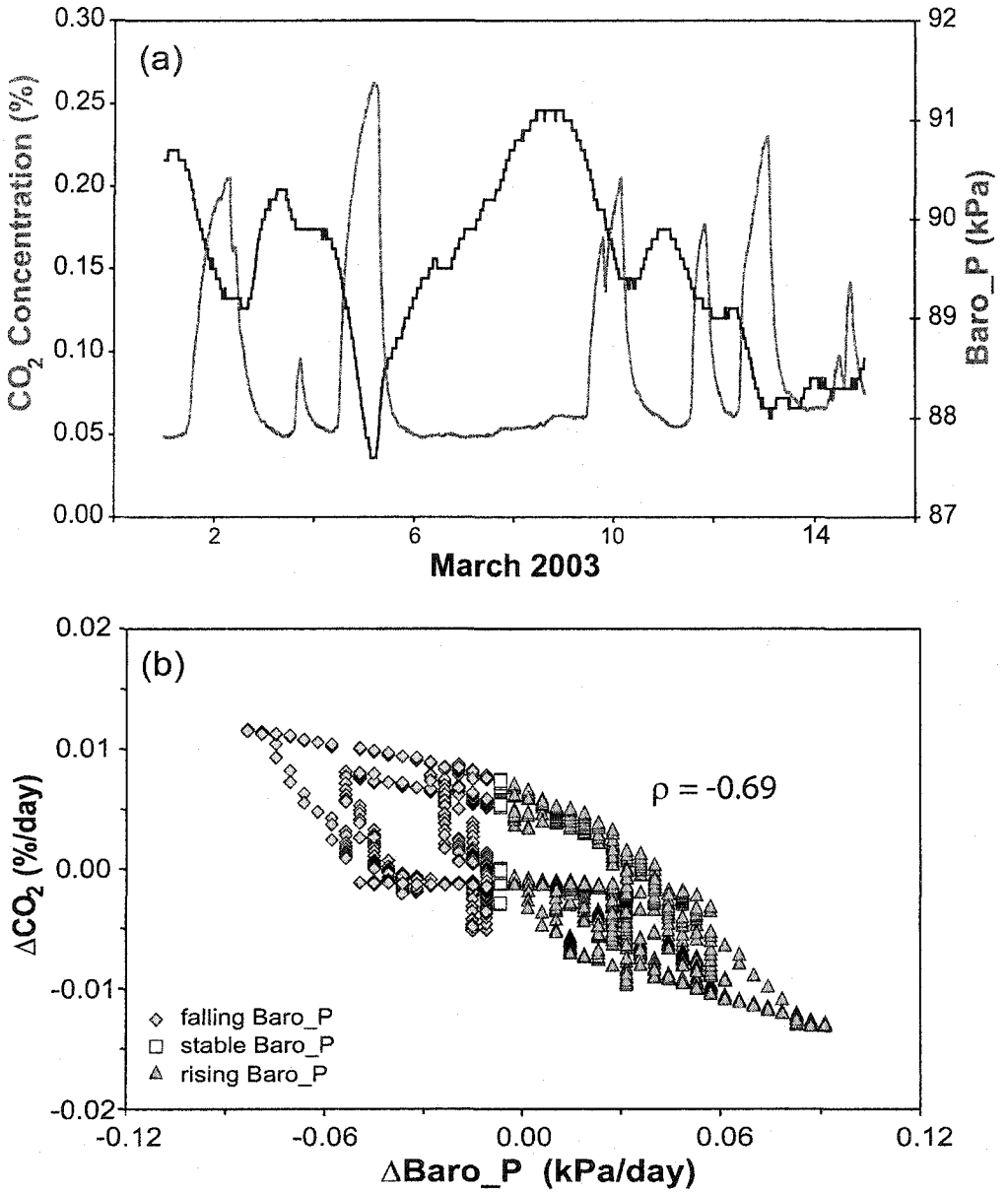

Figure 4.8: (a) Two week distribution of carbon dioxide concentrations and barometric pressure in March 2003. Rising concentrations coincide with dropping pressures (exhaling conditions). (b) Daily rates of change in carbon dioxide and barometric pressure over the same 2-week period.

4.4 Volumetric Flow Rate

Figure 4.9 displays the oxygen and volumetric air flow rate through the breathing well for two weeks in March 2003. To determine the flow direction, the volumetric flow rates were compared to oxygen peaks and troughs. Exhaling periods (negative flow rates) were defined when oxygen concentrations decreased over time. Inhaling periods (positive flow rates) were defined when oxygen concentrations either increased, or remained at atmospheric concentrations.

The well inhaled for 210 hours of the two-week period, and exhaled for only 78 hours. The well generally exhaled faster than it inhaled; the average inhaling flow rate was 1.2 x 10^{-4} m^3/s, compared to an average exhaling rate of 1.6 x 10^{-4} m^3/s. As discussed in Section 4.2.3, the length and magnitude

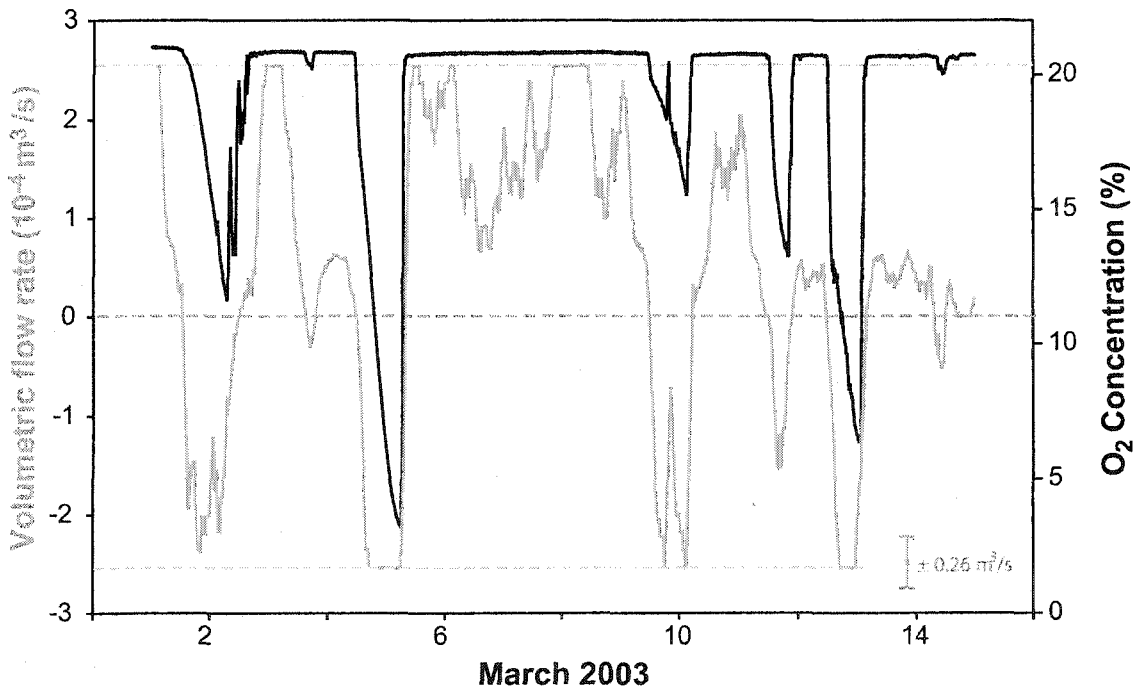

Figure 4.9: Volumetric flow rate (averaged over 24 hours to remove sampling noise) and oxygen concentration distribution in the Staudinger well (March 2003). Negative flow rates correspond to exhaling periods; positive flow rates correspond to inhaling periods.

of each individual cycle will determine the extent of gas migration within the subsurface. Stronger cycles emit stronger velocities and flow rates. Thus they influence a greater subsurface volume. The average flow rate of air during the large cycle was 2.2 x 10^{-4} m^3/s, compared to 0.5 x 10^{-4} m^3/s during the small cycle.

The correlation between O_2 concentrations and volumetric flow rates is 0.66. Unfortunately, the maximum detection limit of the sensor (0.5 m/s or 2.6 x 10^{-4} m^3/s) was often exceeded. Thus, the reported averages and correlation are skewed lower than if this instrument limitation did not exist.

4.5 Groundwater

The geochemical and bacteria results from the Staudinger and the shallow well groundwater are summarized in Table 4.1. All of the data is available in digital format in Appendix A. The stable isotope methods, results, and interpretation are described in Appendix B.

4.5.1 Shallow Water Chemistry

A shallow water well, completed in the perched surficial aquifer, was sampled to compare the expected source water to groundwater in the Paskapoo Formation. The shallow groundwater is relatively fresh, with a total dissolved solids (TDS) concentration just over 400 mg/L. The shallow well water is Mg-Ca-HCO_3^- dominant. Mg^{2+} and Ca^{2+} represent 47% and 46% of the total cations respectively, and HCO_3^- represents 82% of the total anions. This composition can be attributed to the dissolution of dolomite and calcite minerals dispersed within the Quaternary deposits. The measured pH of the water was 7.3, and the temperature was 6.5°C. The measured dissolved oxygen concentration in the shallow groundwater was 6.1 mg/L. The shallow

well water contained background concentrations of denitrifying bacteria, moderately aggressive populations of iron-related bacteria, and moderately aggressive populations of sulphate reducing bacteria.

Inorganic fertilizers and manure applied to crop land are the most common sources of nitrate in groundwater (Keeney, 1986; Hallberg, 1989; Rodvang and Simpkins, 2001). Nitrate (NO_3^-) concentrations in the shallow groundwater around Sylvan Lake range from 0 mg/L to over 15 mg/L (The Groundwater Centre, 2004). The drinking water guideline for nitrate is 44 mg/L of NO_3^-, or 10 mg/L NO_3-N (Health and Welfare Canada, 1996). The groundwater sampled from the shallow well contained just over 3 mg/L NO_3^- (0.7 mg/L NO_3-N), thus the quality of the shallow groundwater is still safe for drinking. It is suspected that the source of these nitrates is commercial fertilizers, and possibly manure.

4.5.2 Staudinger Well Water Quality

The measured field pH of the water sampled from the Staudinger well ranged from 7.4 to 7.8, which is within the normal range for natural groundwaters (Langmuir, 1997). The range of groundwater temperatures was 5.3 to 6.2°C; the highest temperatures occurred during spring recharge. The temperature profile, conducted in December 2002, showed a decrease from 5.7°C at the water table to 4.7°C at the pump (approximately 32 mbgs). The groundwater is extremely depleted in dissolved oxygen (DO) with respect to water in equilibrium with air (11.5 mg/L at 5°C). The average stabilized flow-through cell concentration was 0.5 mg/L. Dissolved oxygen concentrations measured in the DO profile decreased with depth, from 0.6 mg/L directly beneath the water table to 0.2 mg/L at the pump. Manual DO measurements are similar to the concentrations measured in the passive gas samplers (Section 4.6.2).

Table 4.1: Chemical composition of the groundwater sampled from the Staudinger well and the near-by shallow well.

	Parameter	Date							Avg.	Shallow
		24/7/02	31/7/02	9/8/02	16/8/02	9/9/02	17/9/02	31/5/03		12/7/03
Major cations and anions	Na^+ (mg/L)	127	143	149	145	123	163	186	148	8
	K^+ (mg/L)	1.58	1.67	1.66	1.6	1.48	1.96	1.84	1.68	2.17
	Ca^{2+} (mg/L)	15.5	16.1	16.2	9.8	9.2	12.7	9.6	12.7	50.5
	Mg^{2+} (mg/L)	4.2	4.7	4.6	4.4	4.2	5.4	4.3	4.5	31
	Cl^- (mg/L)	2.48	2.64	3.09	2.75	2.71	3.63	8.81	3.73	17.4
	SO_4^{2-} (mg/L)	14.3	15.2	16.6	18.8	15.3	19.9	28.6	18.4	22.5
	HCO_3^- (mg/L)	371	369	411	442	385	510	513	429	281
	CO_3^{2-} (mg/L)	< 0.01	< 0.01	< 0.01	< 0.01	< 0.01	< 0.01	< 0.01	< 0.01	< 0.01
Nitrogen content	TN (mg/L)	0.64	0.6	0.68	0.63	0.61	0.61	0.68	0.64	3.43
	NH_4^+ (mg/L)	0.45	0.46	0.48	0.48	0.42	0.47	0.32	0.44	0.01
	$NO_2^- + NO_3^-$ (mg/L)	0.04	0.02	0.06	0.05	0.06	0.05	0.11	0.06	3.04
	NO_3^--N (mg/L)	0.01	0	0.01	0.01	0.01	0.02	0.02	0.01	0.69
Lab parameters	DOC (mg/L)	3.16	2.67	2.5	2.73	2.85	2.36	2.62	2.7	2.8
	DIC (mg/L)	69.5	70.4	76.4	83.1	71.2	93.5	98.8	80.4	57.6
	Alkalinity (mg/L)	304	303	337	362	316	418	421	352	230
	pH	7.9	8	7.9	8	8	8	8.1	8	7.4
	TDS (mg/L)	536	553	603	625	541	717	752	618	415
	sum cations (meq/L)	6.7	7.5	7.7	7.2	6.2	8.2	9		5.5
	sum anions (meq/L)	6.4	6.5	7.2	7.7	6.7	8.9	9.3		5.6
	% error	1.8	7.2	3.6	3.4	4	3.9	1.7		1.2
Field parameters	Fe (mg/L)		0.2	0.3	0.3	0.3	0.4	0.1	0.2	0.3
	Total Fe (mg/L)		0.4	0.3	0.3	0.3	3	0.5	0.8	> 10
	Alkalinity (mg/L)				595	561	561	420	534	
	Conductivity (µS/cm)	788	850	974	856	874	886	881	873	764
	pH	7.8	7.6	7.4	7.7	7.7	7.7	7.6	7.6	7.3
	DO (mg/L)	2.5*	7.5*	0.3	0.3	0.6	0	1	0.5	6.1
	T (°C)	5.8	5.9	5.3	5.6	5.4	5.5	6.2	5.7	6.5
BARTs	Denitrifying		m.a	m.a	m.a	bck.		m.a		bck.
	Iron-related		n/a	a.	n/a	m.a		m.a		m.a
	Nitrifying		n/a	n/a	n/a					
	Sulphate Reducing							n/a		m.a

* Meter malfunction
m.a Moderately aggressive population
bck. Background population
a. Aggressive population
n/a No reaction

The groundwater is potable, with TDS ranging from 540 to 750 mg/L. The Paskapoo aquifer contains Na-HCO_3 type groundwater. Bicarbonate, HCO_3^- is the dominant anion, representing 94% of all anions. The Cl^- and SO_4^{2-}

anions are not abundant, making up only 1.3% and 5% of all the anions respectively. Sodium, at 85%, is the dominant cation, which is uncommon for recently infiltrated groundwater. Ca^{2+} and Mg^{2+} make up only 8.5% and 5% of the cations, respectively.

A likely contributor to the observed composition of the groundwater is the chemical weathering of plagioclase in the volcanic ash deposits within the Paskapoo Formation (Wallick, 1981). This breakdown would increase Na^{+}, Ca^{2+} and HCO_3^{-} concentrations; however, Ca^{2+} concentrations are low compared to Na^{+} and HCO_3^{-}. It is likely that the source of the excess sodium (or lack of calcium) is due to cation exchange within the shale aquitard. Sodium ions are more mobile than calcium ions; therefore, exchange will readily take place as the recharge waters move through the shale unit (Langmuir, 1997). The Ca^{2+} concentrations decrease as the ions are exchanged for Na^{+} ions on the cation-exchange sites of the shale. Every two moles of sorbed Na^{+} are replaced by one mole of Ca^{2+}, which increases the TDS, but does not change the pH or bicarbonate content of the groundwater (Freeze and Cherry, 1979). It is not known if the shale has a high initial sodium content; however, Wallick (1981) explains that even if the mass ratio of the ions in solution to the ions on the exchange complex is very small, significant exchange can take place without noticeably altering the composition of the shale.

The measured dissolved iron concentrations in the groundwater fluctuated between 0.1 and 0.4 mg/L. Iron precipitation was observed on the levelogger wire at 26.5 mbgs, or 1.5 m below the average water level in the well. Total iron concentrations ranged from 0.3 to 0.5 mg/L, except on September 17 2002 when the well had been unused for 2 days. On this day, total iron concentrations increased by an order of magnitude to 3.0 mg/L.

The total alkalinity, measured in the field, was 534 mg/L on average. For most natural systems, the total alkalinity is equivalent to the carbonate alkalinity. At a pH of 7.6, most of the alkalinity is attributed to bicarbonate (Drever, 1997), which is the dominant anion in this system.

DOC and DIC in the groundwater were detected at concentrations of 2.7 mg/L and 80.4 mg/L, respectively. Ammonium concentrations were measured at 0.44 mg/L on average. Average NO_2^-+NO_3^- concentrations were detected at 0.06 mg/L. NO_3-N concentrations were calculated to be 0.014 mg/L. Isotopic analyses on the nitrates (completed at the University of Calgary) found that their source is commercial fertilizers (Kendall and McDonnell, 1998; Ryan, 2004).

Moderately aggressive populations of denitrifying bacteria were detected in the Staudinger groundwater. Sulphate reducing bacteria were not detected; however, moderately aggressive populations of anaerobic bacteria were detected in the SRB BART. Moderately aggressive populations of iron related bacteria were also detected.

4.6 Down-hole Measurements

4.6.1 Total Dissolved Gas Pressure

Dalton's law states that that the pressure exerted by a mixture of gases is equal to the sum of the partial pressures of the gases in the mixture:

$$P_T = P_1 + P_2 + P_3 + ...P_n = \sum_{i=1}^{n} P_i \qquad (4.4)$$

where P_T is the total pressure, and P_i is the partial pressure of gas i, and n is the total number of gases. Total dissolved gas pressures (TDGP) were measured in the Staudinger well. The TDGP probe measures the total pressure (P_T), but does not distinguish between the individual gases dissolved in the groundwater.

Long-term TDGP measurements indicate that the Staudinger groundwater is consistently over saturated with gas relative to air. Between August 22 and September 5 2002, the TDGP of the water ranged between 101.9 and 103.4 kPa (Figure 4.10), which is equivalent to 112% and 115% gas saturation. Percent saturation is calculated by dividing the gas pressure exerted on the sensor by the air pressure. There is a positive correlation coefficient of 0.54 between the TDGP averaged over 6 hours (to remove sampling noise from output data) and barometric pressure.

The amount of a gas that is dissolved in solution depends on its concentration, pressure, temperature, and solubility (Langmuir, 1997). Gas solubility is described by Henry's law:

$$H_i = \frac{C_{w_i}}{P_i} \tag{4.5}$$

where H_i [mol/T^2/L^2/M] is the equilibrium constant (gas solubility) for constituent n, at a specific temperature, and C_{w_i} is the mass of gas dissolved in a given volume of water [M/L^3].

The more soluble the gas, the larger the equilibrium constant. The solubility of gas is proportional to the total pressure. Higher pressures (either barometric pressure, or P_i) will allow higher levels of gas to dissolve in the groundwater. Lower pressures result in lower gas solubility. Thus, the

change in a gas' solubility is dependent on the size of the barometric pressure change (Figure 4.10). A small pressure change of 0.8 kPa (September 3) coincided with a TDGP decrease of 0.3 kPa, whereas a larger pressure change of 1.4 kPa (August 28) coincided to a TDGP change of 1.2 kPa.

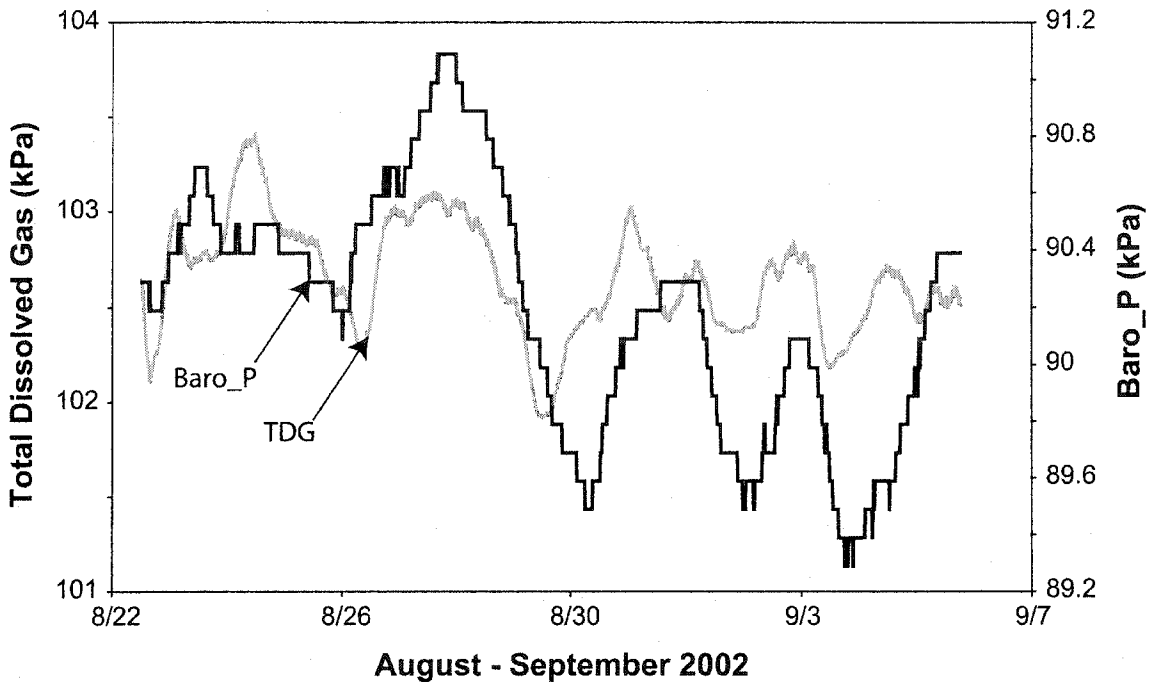

Figure 4.10: Total dissolved gas pressure and barometric pressure distribution over a two-week period. High barometric periods coincide with high TDGP periods in the groundwater.

4.6.2 Passive Gas Samplers

The passive gas samplers, installed below the water level in the Staudinger well, collected one-month averages of the dissolved nitrogen, oxygen, carbon dioxide and argon gas concentrations (Table 4.2). The concentrations in the table have been corrected for elevation, TDGP (115%), and water vapour pressure (0.8 kPa, assuming 100% humidity in the subsurface) (McLeish, in prep). R_{WEA} represents the ratio of the measured gas in the groundwater to the concentration of the gas in water in equilibrium with air (WEA) at 5°C.

R_{WEA} >1 indicates excess gas with respect to water in equilibrium with air; R_{WEA} <1 indicates gas depletion.

Table 4.2: Dissolved gas concentrations from the passive gas samplers. Data from McLeish (in prep.). R_{WEA} is the ratio of the measured gas in the groundwater to the concentration of the gas in water at equilibrium with air (WEA) at 5°C.

	N_2 conc.		O_2 conc.		CO_2 conc.		Ar conc.		N_2:Ar
Date	mg/L	R_{WEA}	mg/L	R_{WEA}	mg/L	R_{WEA}	mg/L	R_{WEA}	
Sep 2002	21.8	1.2	0.1	0.01	18.0	20.7	0.80	1.1	27.3
Oct 2002	20.5	1.2	0.0	0.00	16.6	19.1	0.71	1.0	28.9
Feb 2003	19.9	1.1	0.5	0.04	19.0	21.8	0.74	1.0	26.9
Mar 2003	20.1	1.1	0.1	0.01	16.5	19.0	0.74	1.0	27.2
WEA @ 5°C	18.1		11.5		0.9		0.74		23.9

Freshly infiltrated groundwater is expected to be in equilibrium with air because of its recent exposure to the atmosphere. Deviations are representative of the physical, chemical and biogeochemical processes that occur subsequent to recharge. There is excess nitrogen gas in the Staudinger groundwater (Table 4.2). Carbon dioxide is also elevated with respect to water in equilibrium with air. Dissolved oxygen is extremely depleted, signifying consumption along the groundwater flow path, possibly consumed in the soil or unsaturated zone. Because argon is an inert gas, it is expected that its dissolved concentration be similar to that in air (i.e., R_{WEA} ~ 1.0). The measured concentrations are similar to water in equilibrium with air (average R_{WEA} = 1.03), indicating that the recharge conditions of the groundwater were similar to the present day, and that recharge occurred at a similar temperature (Heaton, 1981). Because of the elevated amounts of nitrogen gas dissolved in water, the N_2:Ar ratios are also higher with respect to the ratio for water in equilibrium with air (Table 4.2). This suggests that the excess N_2 gas is generated subsequent to recharge (Blicher-Mathiesen et al., 1998).

4.7 Interpretation and Discussion

The following sections discuss how the water and gas chemistry results presented above explain the low oxygen breathing events observed in the Staudinger well. The first section characterizes the setting and environment around the Staudinger well, discussing the redox distribution from the surface, where water first infiltrates the ground, to the depth of the pump. The second section presents possible mechanisms that could contribute to the oxygen-deficient environment. The final section examines how one of these processes can be estimated, using a mass-balance model, to better understand how the changing gas compositions are produced in breathing water wells.

4.7.1 Geochemical Characterization

Redox conditions of groundwater are variable. They depend on the availability of electron donors and acceptors (McMahon, 2001), and consequently on geochemical conditions, the flowpath, and the distance travelled since recharge. Oxygenated (aerobic) water has a higher redox potential than oxygen-depleted (anaerobic) water. In general, the redox potential of groundwater decreases as the water moves along a flowpath. Direct measurement of redox potential is often difficult; therefore, a redox depth profile, from ground surface to the pump in the Staudinger well, was infered using the measured chemical and gas compositions of the groundwater and soil gas (Figure 4.11).

As rain and snowmelt enter a groundwater flow system, the water generally has a high redox potential due to its recent exposure to the atmosphere. Groundwater in the drift deposits is aerobic (Figure 4.11); the dissolved oxygen content is still high.

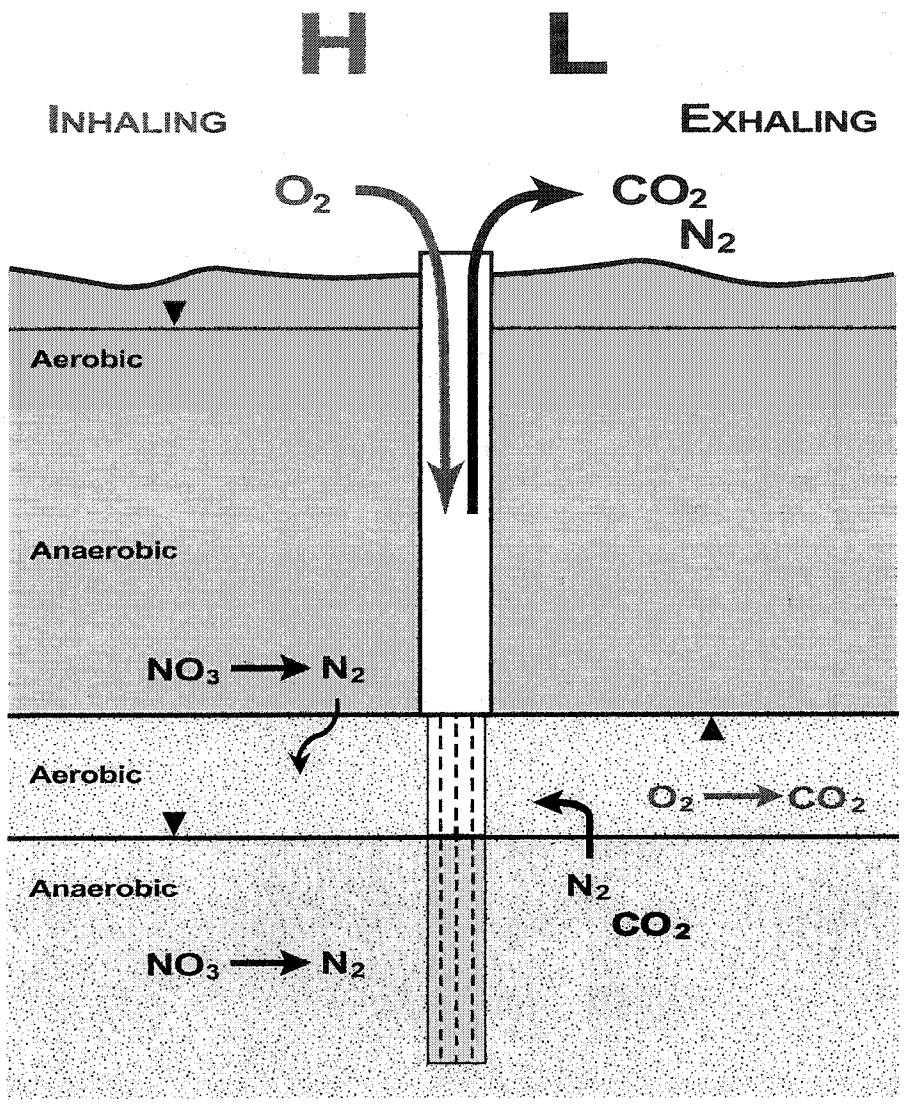

Figure 4.11: Proposed redox distribution between shallow groundwater and the partially saturated aquifer. Redox conditions alternate, spatially, between aerobic and anaerobic conditions depending on the availability of oxygen.

As groundwater percolates through the surficial aquifer and shale aquitard, its oxidation potential decreases as dissolved oxygen (DO) is consumed through aerobic biological processes. Once the DO is fully consumed, the system becomes anaerobic (Figure 4.11). Oxidation processes still occur in anaerobic settings, but nitrate and other elements or compounds become the terminal electron acceptors at dissolved oxygen concentrations below 0.5 mg/L (Kehew, 2001).

The unsaturated zone of the partially saturated Paskapoo aquifer is also predominantly aerobic because atmospheric oxygen is perodicially replenished during inhaling periods. Available organic matter within these zones should undergo oxidation, consuming some of the available oxygen to produce carbon dioxide gas.

The aerobic-anaerobic boundary in the partially saturated aquifer is near the water table (Figure 4.11). Some oxygen will diffuse below this boundary; however, diffusion of oxygen through water is a slow process and any DO is consumed rapidly. Rapid consumption with depth is evident in the DO profile performed on the Staudinger well, where concentrations below the water-air interface were higher than at the depth of the pump.

Below the water table, nitrate is assumed to be the preferred electron acceptor. Nitrate, followed by ferric iron and sulphate reduction would be expected under anaerobic conditions. Ferrous iron was measured at concentrations less than 0.3 mg/L, and elevated populations of SRB were not detected. Therefore, it is suspected that the groundwater has not achieved iron or sulphate reducing conditions. The absence of methane also suggests that denitrification is occurring, because the production of methane does not generally occur in the same area as denitrification (Blicher-Mathiesen et al., 1998).

4.7.2 Possible Mechanisms

There are a number of physical and geochemical processes that could contribute to the observed conditions in breathing water wells. These are presented in this section. The degree to which they occur within the Staudinger well is also examined.

4.7.2.1 Oxidation of Organic Matter

Oxidation of organic matter in aerobic zones of the subsurface likely contributes to the overall disappearance of oxygen in the air exhaled from a breathing water well. During this process, oxygen is consumed and carbon dioxide is produced. The respiratory coefficient (R) for this process,

$$R = \frac{CO_2 \text{ moles produced}}{O_2 \text{ moles consumed}} \tag{4.6}$$

typically varies between 0.7 and 0.9 (Langmuir, 1997). Assuming equilibrium, this coefficient should be applicable to both water and air.

The change in dissolved oxygen between the shallow and deep groundwater near the Staudinger well exceeds 5.5 mg/L. Using equation 4.6, 5.3 to 6.8 mg/L of dissolved carbon dioxide would be produced during infiltration if the entire change in dissolved oxygen were attributed to organic respiration.

In the air exhaled from the Staudinger well, the maximum detected carbon dioxide concentration was 0.29% v/v CO_2, indicating that there is 0.25% v/v of excess CO_2 with respect to the atmosphere. Using equation 4.6, this gas would only account for 0.28 to 0.36% v/v of consumed oxygen. Therefore, the oxidation of organic matter cannot be the sole contributor to the disappearance of oxygen within the subsurface, and is likely occurring in conjunction with other processes.

4.7.2.2 Dissolution of Calcite

Groundwater is rarely in equilibrium with the minerals that surround it (Fitts, 2002). Results from calculations performed with SOLMINEQ.88 (Kharaka et al., 1988) revealed that the Staudinger water samples were undersaturated with respect to most minerals. In particular, the samples were slightly

undersaturated with respect to calcite, indicating that calcite could be dissolving in the Staudinger groundwater.

The dissolution of calcite is described by:

$$CaCO_3(s) + CO_2 + H_2O \rightarrow Ca^{2+} + 2HCO_3^- \quad (4.7)$$

Carbon dioxide is utilized in the dissolution of calcite. When coupled with the oxidation of organic matter, some of the carbon dioxide produced through oxidation could replace the dissolved CO_2 that is consumed during the dissolution of calcite. If so, the oxidation of organic matter could play a larger role in the depletion of oxygen in breathing water wells than previously stated.

4.7.2.3 Iron/Sulfide Oxidation

Thorstenson and Pollock (1989) state that in aerobic environments additional processes may lead to the consumption of oxygen, other than the oxidation of organic matter. These processes may include the oxidation of iron and/or sulfide minerals (Madigan et al., 2003). For example:

$$Fe^{2+} + 1/4O_2 + H^+ \rightarrow Fe^{3+} + 1/2H_2O \quad (4.8)$$

$$FeS_2(s) + 7/2O_2 + H_2O \rightarrow Fe^{2+} + 2SO_4^{2-} + 2H^+ \quad (4.9)$$

Beaucaire et al. (1998) state that the redox buffering capacity in sedimentary systems is often controlled by the iron bearing minerals (as stated in Sacchi et al., 2001). It is not suspected that the disappearance of oxygen in the Staudinger well is dominated by to oxidation of iron bearing minerals because high concentrations of the typical products (Fe^{3+} or SO_4^{2-}) are not present in the groundwater samples.

4.7.2.4 Denitrification

Nitrate reduction (denitrification) ultimately returns nitrogenous compounds to nitrogen gas (Wilson et al., 1990), in one or more of the following steps:

$$NO^-_{3(aq)} \rightarrow NO^-_{2(aq)} \rightarrow NO_{(g)} \rightarrow N_2O_{(g)} \rightarrow N_{2(g)} \quad (4.10)$$

These steps are governed by bacterial resistance (Cullimore, 1999). Denitrification is most likely occurring in the shale aquitard and the saturated zone of the partially saturated aquifer (Figure 4.11). McMahon et al. (1999) determined that nitrate in an oxygenated aquifer was completely reduced to N_2 in an adjacent shale. Because the organic content of the shale is likely high, the probable denitrification reactions involve carbon as the electron donor (Madigan et al., 2003):

$$5C_{organic} + 4NO^-_{3(aq)} + 4H^+ \rightarrow 2N_{2(g)} + 5CO_{2(g)} + 2H_2O \quad (4.11)$$

The source of the nitrates in the Staudinger well is thought to be commercial fertilizers, which are often applied to the ground surface to enhance crop growth. Excess nitrate would infiltrate with recharging groundwater. The change in the nitrate concentration between the groundwater sampled from the shallow aquifer and the Staudinger well was 0.67 mg/L of NO_3-N. If this change is entirely attributed to denitrification of organic matter in the shale aquitard, this would produce 0.7 mg/L of dissolved N_2 and 2.6 mg/L of dissolved CO_2 (calculations in Appendix D). For a 5 metre radius around the well, dissolved nitrogen could percolate into the partially saturated aquifer, from the overlying shale, at rate of 1.5 mg/day (Appendix D).

Both N_2 and CO_2 gas are produced in Equation 4.11. The passive gas samplers installed in the Staudinger well detected elevated concentrations of both of these gases in the groundwater. If disequilibrium was created

between the unsaturated and saturated zones, because of gas production below the water table, gas would be forced into the unsaturated zone. If CO_2 were predominantly consumed by calcite dissolution, the majority of the exsolved gas would be nitrogen.

To determine the equivalent partial pressure of gas (P_i) that should exist in the unsaturated zone, in order for equilibrium to exist between the two reservoirs, the following calculation is required:

$$P_i\,(\%) = \left(\frac{m_i}{H_i \left(P_T - P_{H_2O}\right) MW} \times 1000 \right) \times 100\% \qquad (4.12)$$

where m_i is the dissolved concentration of the gas (mg/L, Table 4.2), H_i (mol/L/kPa) is Henry's equilibrium constant, P_T is the total pressure (kPa), P_{H_2O} is the water vapour pressure (kPa), and MW is the molecular weight (g/mol).

Assuming a barometric pressure equal to 90 kPa (the monthly average pressure), a temperature of 5°C, and a water vapour pressure equal to 0.8 kPa (Byers, 1974), an equivalent of 86 to 94% v/v N_2 gas and 0.66 to 0.76% v/v CO_2 gas (Table 4.3) would need to exist above the water table in order to achieve equilibrium with the saturated zone of the aquifer.

Table 4.3: Equivalent aqueous (from Table 4.2) and gas concentrations of nitrogen and carbon dioxide in the Staudinger well. Calculated using Equation 4.12.

	N_2 conc.		CO_2 conc.	
MW (mol/L)	28		44	
H (mol/L/kPa)*	9.31E-06		6.35E-04	
Date	mg/L	%	mg/L	%
Sep 2002	21.8	94	18.0	0.72
Oct 2002	20.5	88	16.6	0.67
Feb 2003	19.9	86	19.0	0.76
Mar 2003	20.1	88	16.5	0.66
WEA @ 5°C	18.1	78	0.9	0.04

* from Langmuir (1997) at 5°C

4.7.2.5 Pop Bottle Effect

Most natural groundwater has dissolved gas concentrations elevated above that expected for water in equilibrium with air (Heaton and Vogel, 1981; Dahlgren et al. 1997; Holocher et al., 2002; Manning et al., 2003). Dissolved gases can originate from a number of processes including exposure to the atmosphere, contact with soil gases during infiltration through the unsaturated zone, or by gas production below the water table due to chemical or biochemical reactions (Freeze and Cherry, 1979), including denitrification as previously discussed. Dissolved gases can also originate from the incorporation of excess air (Vogel et al., 1981; Heaton and Vogel, 1981).

The TDGP observations in the Staudinger well indicate there is indeed excess gas in the groundwater. Saturations in excess of 100% and elevated N_2:Ar ratios indicate that gas production had occurred subsequent to groundwater recharge (Heaton and Vogel, 1981).

Henry's Law (Equation 4.5) shows that the solubility of a gas is a function of pressure (and temperature). An increase in atmospheric or partial pressure will increase the solubility of the gas, resulting in a state of disequilibrium. Therefore, a change in atmospheric pressure forces the exchange of gas

across an air-water interface in an attempt to restore equilibrium. For example, if the pressure above the water table is decreased, an imbalance is created between the saturated and unsaturated zones: gas will exsolve from solution in an attempt to re-establish equilibrium due to the overlying decrease in pressure. During high or rising barometric pressure periods, the resulting increase in solubility will force gas to dissolve, or allow any gases produced below the water table to remain in solution.

The observed TDGP behaviour (Figure 4.10) can be compared to the behaviour of CO_2 in a bottle of pop. The pop is bottled under high pressure, resulting in relatively high gas solubility, thus increasing the concentration of dissolved gas in solution. When the bottle is opened, its pressure is reduced to the pressure of the surrounding atmosphere; gas solubility is greatly reduced, and the gas comes out of solution, often observed as bubbles.

Much like pop in a bottle, groundwater is able to contain higher concentrations of dissolved gas during high-pressure periods. Most of the excess gas is N_2 (Section 4.6.2) produced by denitrification processes. During rising or high barometric pressure periods, the resulting increase in solubility allows the excess gas produced below the water table to remain in solution. Because N_2 is non-reactive, it accumulates in groundwater during these high-pressure periods. Decreases in atmospheric pressure allow the dissolved gases to exsolve, releasing the excess gas from solution into the unsaturated zone. This corresponds to a decrease in the TDGP of the groundwater (Figure 4.10). When the gases released from below the water table mix with pre-existing gases in the unsaturated zone, the elevated levels of nitrogen gas dilute the oxygen in the unsaturated zone. Consequently, the air exhaled from the well becomes depleted in oxygen relative to atmospheric air.

These gas exchange processes across the water table, and the production of excess nitrogen gas subsequent to recharge (Section 4.7.2.5) are believed to be major contributors to the depletion of oxygen in the air exhaled from the Staudinger well. The effects and magnitude of this dilution are discussed in the following section.

4.7.3 Mass-Balance Model

A simple mass-balance model was used to simulate the changing gas compositions emitted from the Staudinger well during falling barometric pressure events. This model was used to establish whether the observed compositions (i.e., disappearance of O_2) could be explained by the dilution of gases in the unsaturated zone due to degassing of nitrogen (and carbon dioxide) from the groundwater during exhaling events. The model was applied only to exhaling (decreasing barometric pressure) periods. The model was not applied to the inhaling events because the observed concentrations in the field do not represent air existing within the well, but air existing at the surface.

4.7.3.1 Conceptual Model Definition

The model represents a cylindrical portion of the partially saturated aquifer, centred about the well and extending across the unsaturated zone, from the base of the confining layer to the water table of the partially saturated aquifer (Figure 4.12). The model calculates the gas concentrations within this cylindrical volume. To estimate the concentrations, the following parameters must be specified.

The total volume (V_T) of the cylinder is represented by:

$$V_T = \pi r^2 b \qquad (4.13)$$

where b is the thickness of the unsaturated zone [L] and r is the radius of influence [L].

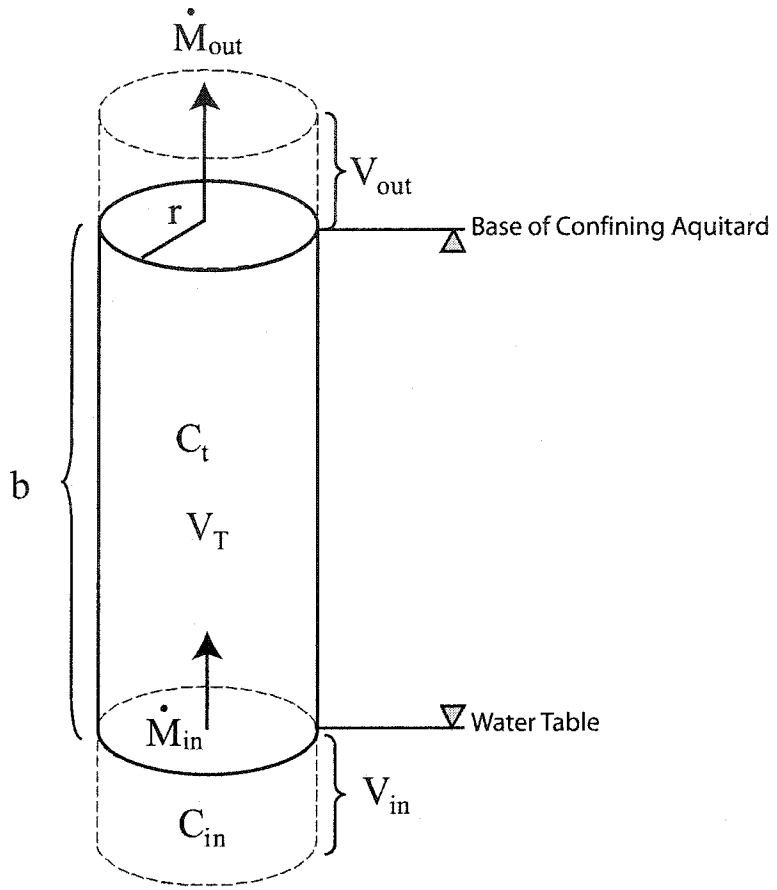

Figure 4.12: Conceptual design of the mass balance model. A volume of gas (V_{in}) originating in groundwater is released into a volume of the unsaturated zone. The same volume of gas (V_{out}), is removed via the well at the base of the overlying aquitard.

The volume of air (V_{air}) within V_T [L^3], in which the gases are contained, is a function of the air-filled porosity (n_{air}) of the aquifer:

$$V_{air} = V_T n_{air} \tag{4.14}$$

The effect of gas compressibility on density is assumed to be negligible in the mass-balance model. This is justified because barometric pressure changes by less than 4kPa.

At a given point in time, the total mass of a particular gas within this volume is:

$$M = CV_T n_{air} \tag{4.16}$$

where C [M/L^3] is the concentration of the gas of concern (e.g., oxygen, carbon dioxide or nitrogen).

The water table, which represents the bottom boundary of V_T, is defined as a mass flux boundary. Any mass of gas input to V_T is assumed to originate below the water table. The upper boundary of V_T, the base of the confining shale unit, is also defined as a mass flux boundary, with gas exiting through the well.

The volume of gas contributed to V_T from below the water table (V_{in}) is equal to the volume of gas removed (V_{out}) from the well over a defined time interval:

$$V_{in} = V_{out} = Q\Delta t \tag{4.15}$$

where Δt is the time interval [T], and Q is the volumetric flow rate of air through the well [L^3/T].

The rate at which mass is input to ($\dot{M}_{in}$) or output from ($\dot{M}_{in}$) V_T over a specified time interval can be represented by:

$$\dot{M}_{in} = \frac{C_{in} V_{in}}{\Delta t} \tag{4.17}$$

$$\dot{M}_{out} = \frac{C_{t-1} V_{out}}{\Delta t} \tag{4.18}$$

where C_{in} and C_{t-1} represent the concentrations of the gas input from below the water table, and output (i.e., exhaled) from the unsaturated zone of the aquifer, respectively.

The change of mass within V_T over Δt is represented by:

$$\dot{M}_{in} - \dot{M}_{out} = \frac{M_t - M_{t-1}}{\Delta t} \tag{4.19}$$

where M_{t-1} is the mass of gas in V_T at the beginning of the time interval, and M_t is the mass of gas in V_T at the end of the time interval.

Finally, equation 4.19 can be rearranged to determine the resulting concentration (C_t) of the gas in the volume of interest:

$$C_t = C_{t-1} + \frac{C_{in}V_{in} - C_{t-1}V_{out}}{V_T n_{air}} \tag{4.20}$$

This mass-balance model assumes that the transport of gas into and out of V_T is controlled by advection alone, ignoring any effects of diffusion. However, the model assumes that gases within V_T fully mix within a time interval, Δt. The depletion of oxygen is considered to be solely controlled by dilution of gas contributed from below the water table. Biodegradation processes are not included in the model.

The radius of influence and the air-filled porosity of the aquifer are the fitting parameters of the model. They are used to first optimize the model's fit to the observed oxygen data. Then these same fit parameters are used to predict changes in CO_2 and N_2 concentrations for the same scenario.

4.7.3.2 Application

The mass-balance model was used to calculate concentrations of oxygen, carbon dioxide, and nitrogen in the subsurface. The distribution of these gases was calculated for the three individual pressure cycles, which vary in length and magnitude (Section 4.2.3). The decreasing period of the large-scale pressure cycle is 20¼ hours long, the intermediate-scale pressure cycle is 17 hours long, and the small-scale pressure cycle is 6¼ hours long. An electronic version of the model is available in Appendix A.

Table 4.4 lists the assigned parameters in the model. Volumetric gas concentrations [%] were used instead of mass concentrations. The initial concentrations (i.e., C_{t-1} at t = 0) of oxygen and carbon dioxide were those values measured by the Airmadillo sensors at the beginning of each cycle. Because nitrogen gas concentrations were not measured in the field, the initial concentration of N_2 was assigned the expected atmospheric value of 78%.

The input concentrations (C_{in}) of the three gases were assigned the March 2003 values calculated from the passive gas samplers (Section 4.7.2.4). Ideally, the input concentrations should equal the dissolved gas concentrations in the groundwater measured at the time of the barometric pressure cycle; however, these exact concentrations are not available, so one-month averages are used. They are assumed to not deplete over the timeframe of a pressure cycle.

The volumetric flow rates used in the model are from the field data. During periods in which the maximum detection limit (MDL) of the air velocity sensor was exceeded, the MDL of 0.5 m/s, or 3×10^{-4} m^3/s, was assigned. The influence of this equipment limitation is explored in a sensitivity analysis later.

Table 4.4: Mass balance model input parameters

Parameter		Large-scale	Intermediate-scale	Small-scale
Δt (min)		15	15	15
Number of time intervals		81	68	25
n_{air} (-)		0.1	0.1	0.1
b (m)		8.7	8.7	8.7
C_{in}	O_2 (%)	0.01	0.01	0.01
	N_2 (%)	88	88	88
	CO_2 (%)	0.6	0.6	0.6
$C_{t=0}$	O_2 (%)	20.8	20.8	20.7
	N_2 (%)	78	78	78
	CO_2 (%)	0.054	0.061	0.066

The large-scale pressure cycle displayed steady and consistent deceases in pressure, as did the oxygen concentrations (Figure 4.13). The best-fit radius was established to be 2.5 m, allowing the calculated oxygen concentrations to recreate the observed concentrations (R^2 = 0.99). The minimum modelled O_2 concentration was 3.15%, compared to an observed minimum concentration of 3.14%. .

The modelled carbon dioxide concentrations increased from an initial 0.054% to 0.52% (Figure 4.14). The model reproduces the general behaviour of the carbon dioxide changes (R^2 =0.96), but significantly over-estimates the final output concentrations because C_{in} exceeds the final observed CO_2 concentrations. The modelled nitrogen concentrations increased from 78% to 86.5%. Using the calculated concentrations, and measured flow rates, the mass of excess nitrogen gas (i.e., above atmospheric) exhaled from the well during the large-scale pressure cycle was calculated to be 21 mg, exhaled at a mass rate of 25 mg/day.

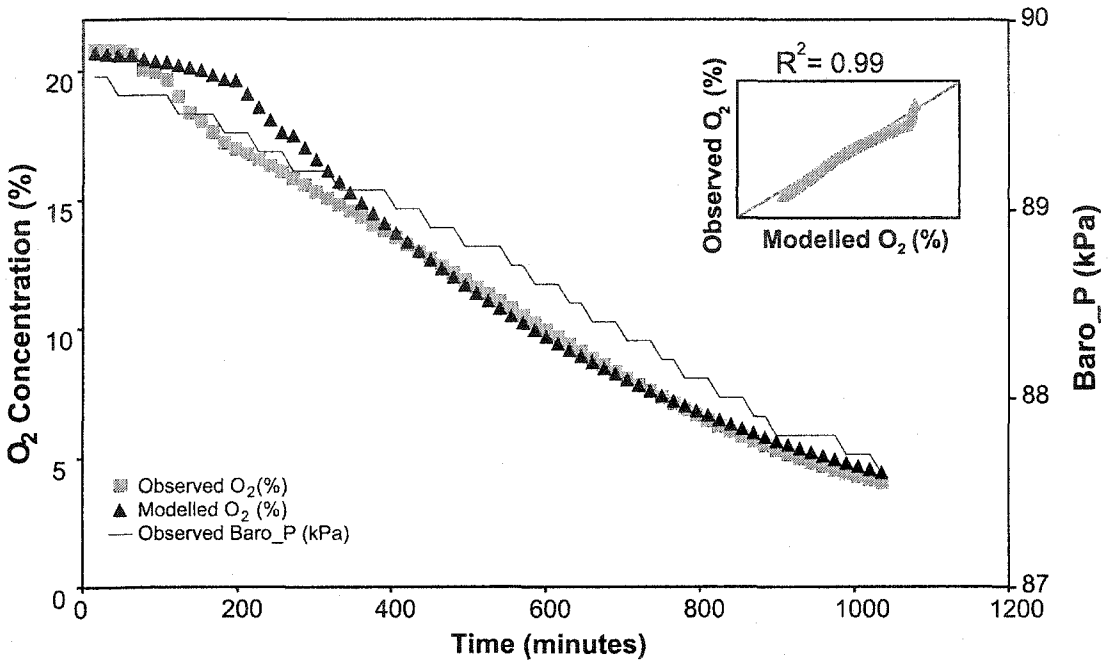

Figure 4.13: Modelled and observed oxygen concentrations and barometric pressure, over the large-scale pressure cycle. Inset figure displays 1:1 ratio line.

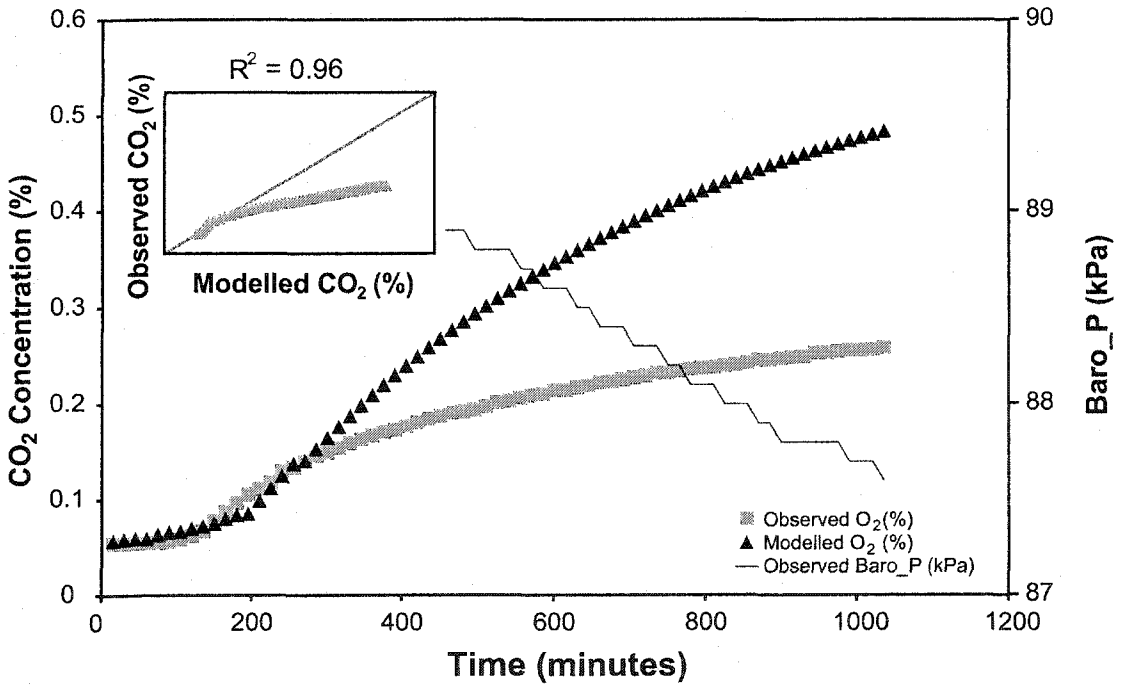

Figure 4.14: Modelled and observed carbon dioxide concentrations over the large-scale pressure cycle. Inset figure displays 1:1 ratio line.

In the above simulation, if the observed air velocity transducer data exceeded the maximum detection limit (MDL) of the sensor, the volumetric flow rate was arbitrarily assigned the MDL of 3×10^{-4} m^3/s. These output flow rates were varied to establish the model's sensitivity to this parameter. Flow rates over time were linearly extrapolated to two and three times the MDL of the sensor. The resulting radii were 2.75 m at two times the MDL and 3.25 m at three times the MDL. The fit of the model, using these increased flow rates, was not as good as the original simulation but still achieved high R^2 values of 0.97 and 0.95 respectively. The calculated mass of excess nitrogen gas exhaled from the well for these simulations was 25 mg and 35 mg respectively.

A radius of 5.2 m produced the best fit for the calculated oxygen concentrations for the intermediate-scale pressure cycle. The minimum-modelled O_2 concentration was 15.53%, compared to an observed concentration of 15.50% (R^2 = 0.88, Figure 4.15a). The final modelled carbon dioxide concentration was 0.20% compared to an observed concentration of 0.20% (R^2 = 0.90). The modelled N_2 concentrations increased to a maximum of 80.5%. The calculated mass of excess nitrogen released from the well was 3 mg, exhaled at a rate of 5 mg/day.

During the intermediate-scale pressure cycle, barometric pressure stabilized long enough for the observed oxygen concentrations to recover to atmospheric levels before decreasing again. The model does not represent the observed O_2 concentrations appropriately over this stable period because the modelled and observed concentrations are representative of two different volumes. During the stable period, the well is inactive (neither inhaling nor exhaling). The observed oxygen concentrations shift back to atmospheric levels as atmospheric air diffuses past the Airmadillo sensor. However, gas is neither removed nor added to V_T during the stable period; therefore, the

model concentrations maintain the same concentrations as the previous time interval ($C_t = C_{t-1}$) until flow is re-established (Figure 4.15a).

A radius of 4.95 m was used to recreate the oxygen distribution emitted from the Staudinger well during the small-scale pressure cycle ($R^2 = 0.75$). The minimum-modelled O_2 concentration was 19.97%, with an observed concentration of 20.02% (Figure 4.15b). The modelled CO_2 concentrations corresponded to the observed concentration of 0.09% ($R^2 = 0.86$). The maximum-modelled N_2 concentration was only 78.4%. The calculated mass of excess nitrogen was only 0.06 mg, exhaled at a rate of 0.23 mg/day.

4.7.3.3 Discussion

The mass-balance model calculated oxygen concentrations of the individual pressure cycles, assuming that the depletion of oxygen is caused, solely, by the release of gas from below the water table. Thorstenson and Pollock (1989) demonstrate that when a gas component is added to a volume of interest, the concentrations of the other gases will decrease in response. This behaviour is observed in both the field and model concentrations. Excess nitrogen (and some CO_2) gas is added to the unsaturated zone during exhaling periods. The new mixture of gas is elevated in nitrogen, and the contribution to the total mass by oxygen is, thus, reduced.

The radius used to recreate the oxygen concentration distribution for the large-scale pressure cycle was smaller than expected. This is due to the limitations of the air velocity transducer, which exceeded its maximum detection limit for much of each cycle. Volumetric flow rates were varied to determine their effects on the outcome of the model. Larger flow rates allow larger volumes of air to be emitted from the well over a particular length of time, thus increasing V_T and the radius of influence.

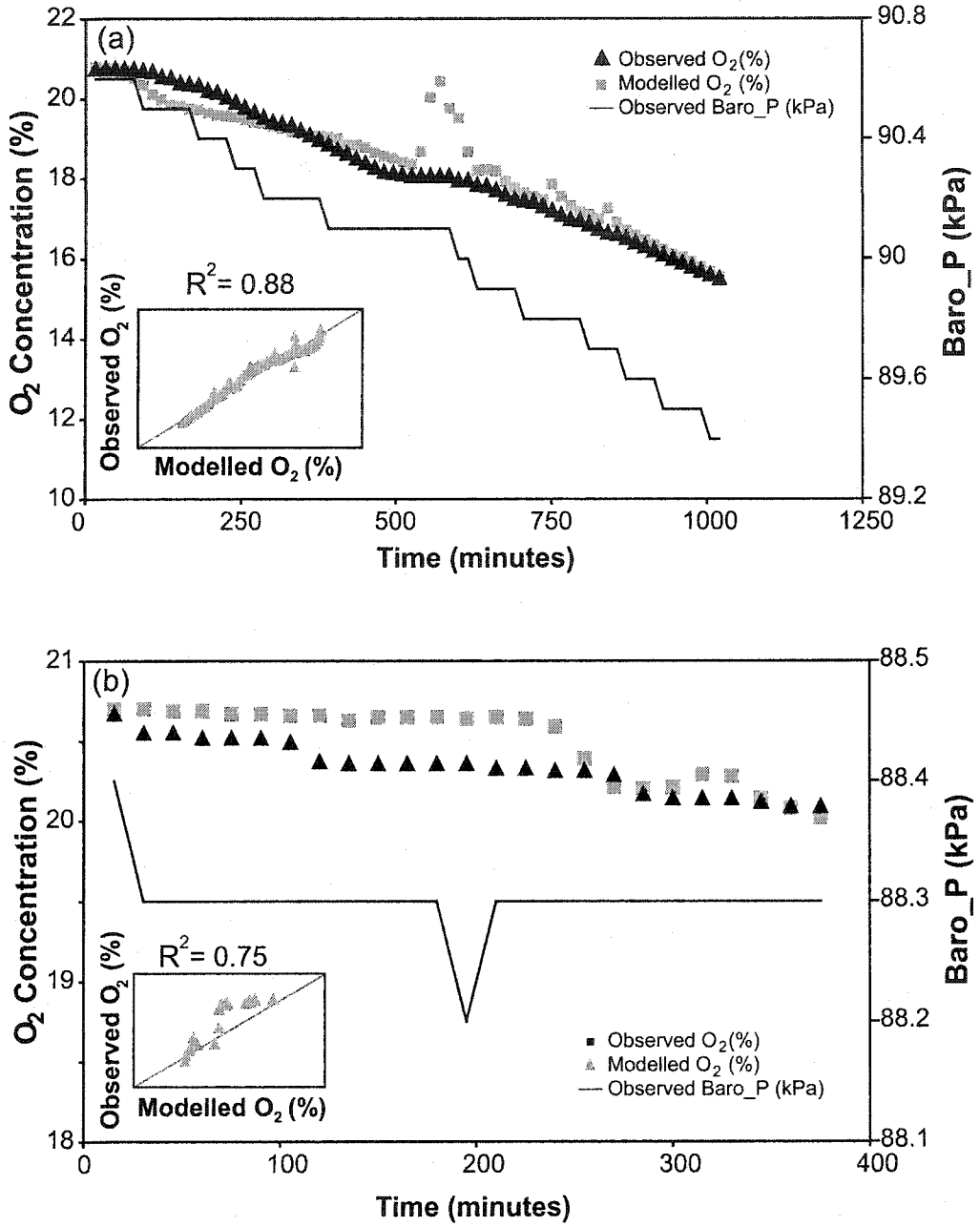

Figure 4.15: Modelled results of the distribution of oxygen over the (a) intermediate-scale pressure cycle, and the (b) small-scale pressure cycle. Inset figure displays 1:1 line.

To represent the intermediate and small-scale pressure cycles, radii larger than those used to fit to the large-scale pressure cycle were required. This is opposite to what one would expect, as the larger cycle should influence a larger subsurface volume due to its extended length and increased flow

rates. The reason for this is that the input concentrations (C_{in}) used in the model are likely not representative of the true input concentrations during the smaller magnitude cycles. The model assumes that the entire volume of gas input to V_T originates below the water table of the partially saturated aquifer; however, smaller pressure decreases draw out smaller amounts of dissolved gas (Section 4.6.1). A larger radius is needed to slow the dilution effect on oxygen. Secondary processes, such as the oxidation of organic matter or pyrite oxidation, likely control the depletion of oxygen during these smaller pressure cycles.

An alternative source of nitrogen gas originates in water seeping from the overlying shale, entering at a rate of 1.5 mg/day (Section 4.7.2.4). This input rate is greater than the mass flow rate of nitrogen gas emitted from the well during the small-scale pressure cycle, also indicating that the degassing of nitrogen from the saturated zones is not the controlling process in the depletion of oxygen during these smaller cycles.

It is not certain how much of the dissolved CO_2 is actually released during exhaling periods. To achieve equilibrium with the groundwater, an equivalent of 0.6% CO_2 would need to exist above the water table; however, because observed concentrations never exceeded 0.29%, it is likely the release of CO_2 is limited by its solubility, and carbonate dissolution processes.

The mass-balance model assumes equilibrium conditions; however, breathing well environments are dynamic. Despite the mentioned limitations, the model was effectively able to simulate the gas distributions from three exhaling events observed at the Staudinger well, showing that dilution of oxygen from the degassing of excess N_2 from below the water table is plausible in the Staudinger well, and likely occurring in combination with the other possible mechanisms mentioned in Section 4.7.2.

4.8 Summary

The following is a summary of the results presented and discussed in this chapter:

- The Staudinger well is situated in an intensively cultivated region of Alberta. The well is completed in the Paskapoo Formation, which comprises the uppermost bedrock deposits of the region and is situated in a perched groundwater system. The breathing well is located in a groundwater recharge area. Recharge occurs through a confining shale aquitard and an overlying perched aquifer. The dominant source of the recharge water for the shallow aquifer is precipitation and snowmelt during the spring.

- There is a clear relationship between barometric pressure fluctuations and changes in the distribution of subsurface gas. During exhaling periods, or falling barometric pressure periods, the air emitted from the well becomes progressively depleted in oxygen, and enriched in carbon dioxide. The minimum concentration of oxygen was measured at 2.2%, and the maximum CO_2 concentration was 0.29%. The length and magnitude of each individual pressure cycles is unique. Stronger, larger cycles cause the well to emit larger volumes of gas and lower concentrations of oxygen

- Shallow groundwater in the perched aquifer is oxygenated due to its recent exposure to the atmosphere. During infiltration through the shale aquitard, the dissolved oxygen content of the groundwater is reduced. Denitrification processes follow the depletion of oxygen. The nitrates involved in these reactions originate as excess commercial fertilizers applied at the surface. Below the shale aquitard, oxygen is replenished

in the unsaturated zone of the Paskapoo aquifer during inhaling, or high barometric pressure, periods. An aerobic/anaerobic boundary exists at the water table of this partially saturated aquifer. Denitrification can again proceed below the water table, resulting in elevated concentrations of dissolved nitrogen and carbon dioxide gas. N_2:Ar ratios confirm that the nitrogen gas is produced subsequent to recharge.

- Transfer of dissolved gas from beneath the water table and into the unsaturated zone of the aquifer will occur during exhaling periods. Excess gas produced in the groundwater is released during low barometric pressure periods. This gas, predominantly nitrogen from denitrification reactions, is released into the unsaturated zone, contributing to the dilution of oxygen in the unsaturated zone. Thus, air exhaled to the surface is relatively depleted in oxygen, and elevated in nitrogen gas.

- A mass-balance model shows that a plausible mechanism causing the disappearance of oxygen in the Staudinger well is the release of gas from below the water table. Simulations of three individual pressure cycles, of varying magnitude and duration, indicate that the distribution of gas emitted from breathing well are partially a result of the dilution of oxygen by the exsolution of N_2.

CHAPTER 5: COMPARISON and DISCUSSION of OTHER BREATHING WELLS

Three additional breathing water wells were monitored to confirm whether the observations at the Staudinger well were unique, or shared by other breathing wells. The three necessary conditions for breathing wells, outlined in Chapter 1, are met by all three wells, although the specifics vary for each. Similar relationships between the composition of the air moving through a breathing well and barometric pressure fluctuations were observed at all of the monitored locations.

This chapter presents a brief site description and the significant observations from each of the three wells. A brief discussion of whether these observations can be explained by the same processes occurring at the Staudinger well is also presented.

5.1 Site Description

5.1.1 Ammeter well

The Ammeter well was monitored for four weeks, from June 26 to July 25 2003. The well is located at 11 N 0695584 E and 5793640 N, in the northwest corner of Section 7, Township 38, Range 1, West of the 5th Meridian. It is located approximately 1600 m east of the Staudinger well. The elevation of the Ammeter well is 989 masl. The geographical, geological and hydrogeological features of the Ammeter well are similar to that described for the Staudinger well (Chapter 4).

The well is completed to a depth of 33.5 mbgs (Figure 5.1), situated in a 2.75 m deep well pit. The pit opens directly to the atmosphere, but is covered by a piece of sheet metal to prevent objects from falling in. The non-pumping

water level in the well was measured at 29.2 mbgs, leaving an unsaturated thickness, open to the well bore, of 8.8 m in the Paskapoo sandstone unit. The shale aquitard is 10.3 m thick at this location.

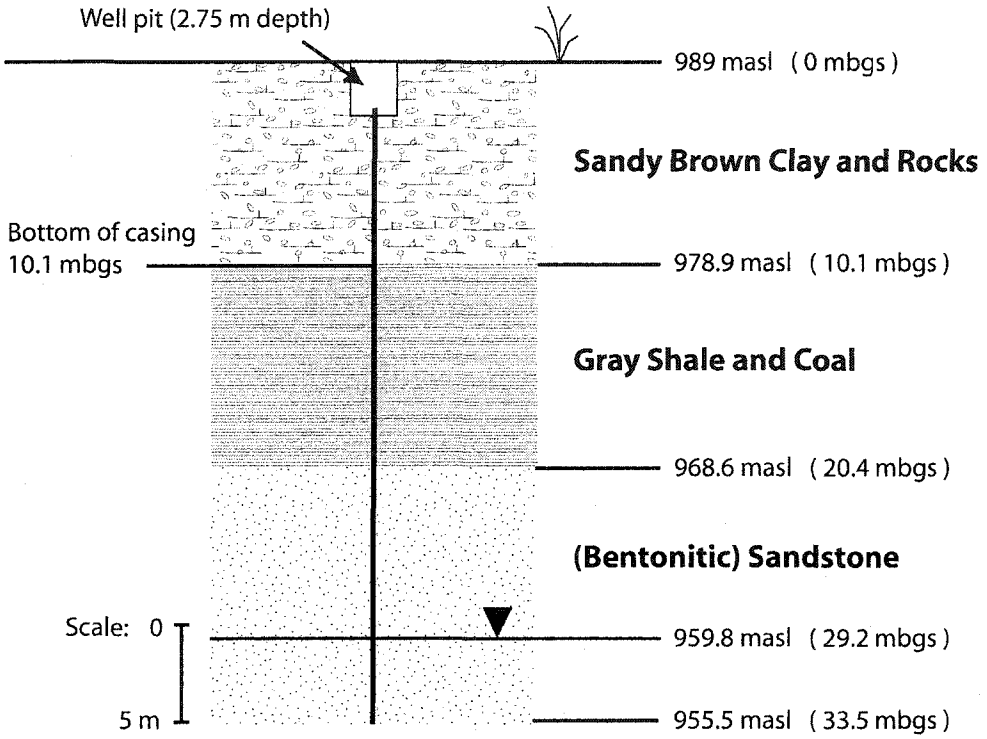

Figure 5.1: Completion details of the Ammeter well (generalized from the driller's log)

5.1.2 Onoway well

The Onoway well was instrumented from September 19 to October 23 2002. The well is located at UTM 11N 0694374 E and 5949903 N, in the southeast corner (legal subdivision 1) of Section 18, Township 54, Range 1, west of the 5th Meridian. The elevation of the well is 748 masl.

The well is completed to 693.1 masl, or 54.9 mbgs (Figure 5.2), with the well casing extending to a depth of 30.5 mbgs. The well is situated within a small well shack. A one-inch polyvinyl tube is attached to the surface casing and fed through one of the walls of the shack, to allow the well to vent to the atmosphere.

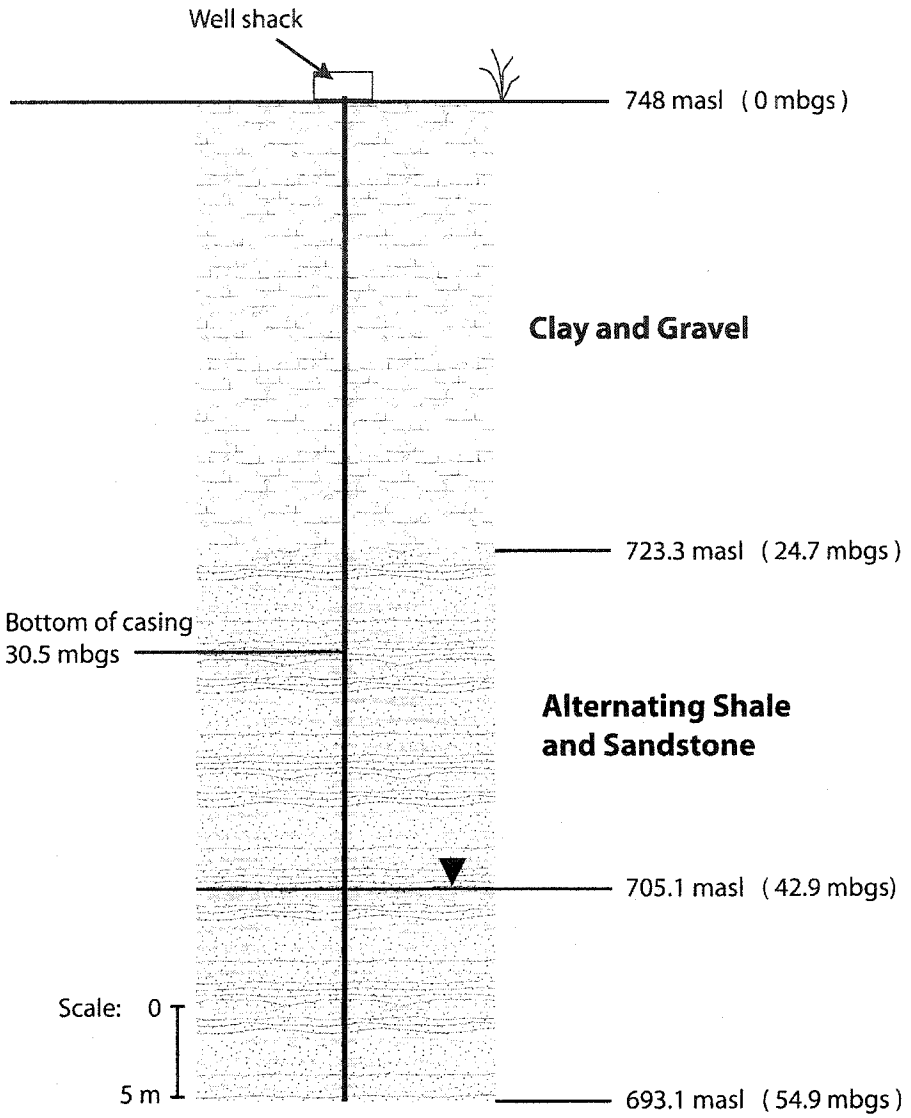

Figure 5.2: Completion details of the Onoway well (generalized from the driller's log)

Much like Sylvan Lake, Onoway is in the midst of a rich agricultural area. Sand and gravel are an abundant resource for the area. The landscape is varied, consisting of hill ranges, rolling landscapes, and hummocky moraines (Ozoray, 1972). The breathing water well is located on a local topographic high, with a small stream located to the west of the well (elevation of 720 m). The annual precipitation in the area is approximately 500 mm, which is exceeded by the annual potential evapotranspiration of 665 mm (Environment Canada, 2000).

The Onoway well is completed in the Upper Cretaceous Edmonton Group; this group represents the uppermost bedrock deposit of the area, consisting of green and grey shale with interbedded bentonitic sandstones (Carrigy, 1970). Quaternary glacial deposits overlie the Edmonton Group. These deposits are part of a buried valley composed of mainly gravel and sand, and clays (Ozoray, 1972). These deposits are 24.7 m thick, and serve as a confining unit to the system.

Unlike the Staudinger well, the Onoway well does not penetrate a perched groundwater system. The average non-pumping water level in the well is 42.9 mbgs. The thickness of the unsaturated zone in the Edmonton group, from the bottom of the unconsolidated surficial deposits to the water level, is 18.2 m; however, because the unit is composed of alternating shale and sandstones, only a portion of the unsaturated zone is able to easily transport air and gas. The driller's log indicates that approximately 6.7 m of the 18.2 m consist of sandstone. It is suspected that these layers comprise the material capable of transmitting air and gas.

5.1.3 Delburne well

The Delburne well was monitored from May 31 to June 26 2003. The well is located at UTM 12 N 0335604 E and 5787597 N, in legal subdivision 4 of Section 32, Township 37, Range 24, west of the 4th Meridian. The well is at an elevation of 864 masl.

The Delburne well is cased to the surface, with no covering structures. Like the Staudinger and Ammeter wells, the Delburne well is completed in the upper sandstone unit of the Paskapoo Formation, to a depth of 42.7 mbgs (Figure 5.3). The overlying surficial deposits are 29.6 m thick, comprised of brown or grey till, and lacustrine clay. The bottom of the well casing extends 2.1 m below the bottom of these deposits. The water level was measured at

a depth of 32.8 mbgs, leaving an unsaturated thickness of 3.2 m between the bottom of the unconsolidated deposits and the water level.

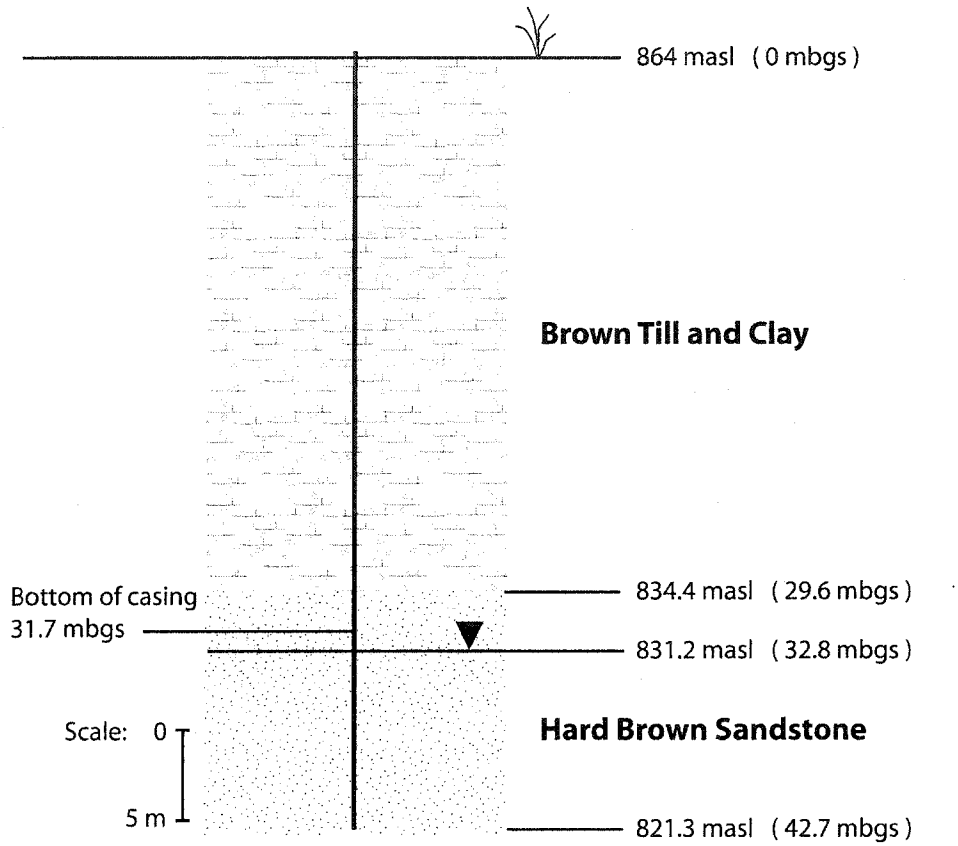

Figure 5.3: Completion details of the Delburne well (generalized from the driller's log)

A number of breathing wells are reported in the region, also known as the Rosebud region. It is a rich agricultural area; mixed farming, livestock and dairying are prominent (Gabert, 1975). The area is predominately open country, with northwest trending ridges having local relief of 30 to 90 m (Allan and Sanderson, 1945). The Red Deer River flows through the region, 2½ km north of the monitored well. Annual precipitation is approximately 460 mm (Environment Canada, 2000), which is exceeded by potential evapotranspiration of approximately 685 mm per year (Environment Canada, 2000). The climate is similar to the Sylvan Lake area, being humid continental.

Similar to the Staudinger well, the Delburne well penetrates a perched groundwater system. The shallow water table is located in the surficial deposits at 6 to 7 mbgs. The perched water insufficiently recharges the lower bedrock aquifer, thus the Paskapoo Formation is not fully saturated in this region.

5.2 Gas and Meteorological Sensor Observations

Positive correlations between oxygen and barometric pressure fluctuations were observed at the three additional monitored well locations. Because of the differences in well completions, geology, and weather conditions, the magnitude of correlation differs for each site. Two-week distributions of oxygen and barometric pressure for the three wells are presented in Figure 5.4. The periods presented in the figure exhibit representative barometric pressure cycles within a similar time frame as was analyzed for the Staudinger well. Digital versions of the figures and the data collected for the three wells are available in Appendix A. A comparison of the maximum and minimum values of the measured oxygen, carbon dioxide concentrations and barometric pressure is presented in Table 5.1.

Table 5.1: Maximum and minimum observations of barometric pressure, O_2 and CO_2 concentrations at the four breathing water well locations over the course of their monitored periods.

Breathing Well	Oxygen (%)		Carbon Dioxide (%)		Baro_P (kPa)	
	max	min	max	min	max	min
Ammeter	21.7	12.3	0.11	0.02	90.8	89.3
Onoway	21.6	3.7	0.10	0.03	93.6	91.5
Delburne	21.7	10.7	0.28	0.02	92.4	90.0
Staudinger (summer)	20.8	4.7	0.29	0.06	92.2	88.5
Staudinger (winter/spring)	21.3	2.2	0.26	0.04	91.6	87.6

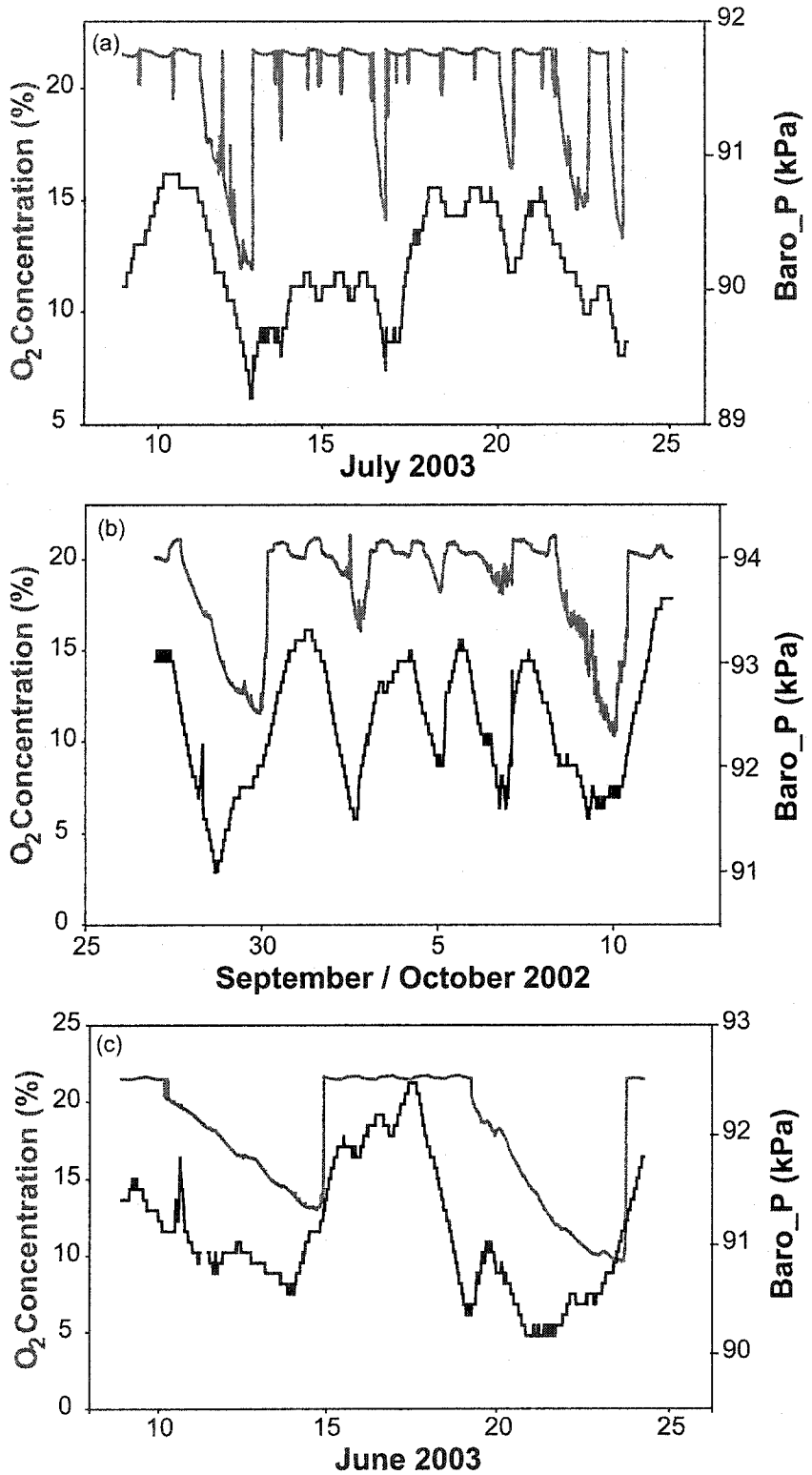

Figure 5.4: Two-week distributions of oxygen and barometric pressure for the (a) Ammeter, (b) Onoway, and (c) Delburne wells. Diurnal fluctuations of oxygen from the raw data have been removed (see Appendix C)

The correlation coefficients between the daily rates of change in oxygen and barometric pressure are presented Table 5.2. All wells displayed positive correlations between the two parameters; periods of decreasing oxygen concentrations are correlated with periods of barometric pressure decreases.

Table 5.2: *Comparison of the correlation coefficients for daily rates of change in oxygen and* barometric pressure over a chosen two week period, and the correlation coefficients for the daily rates of change in carbon dioxide and barometric pressure over the same two week period.

Breathing Well	O_2 and Baro_P	CO_2 and Baro_P
Ammeter	0.51	-0.62
Onoway	0.69	-0.85
Delburne	0.52	-0.66
Staudinger (summer)	0.74	-0.79
Staudinger (winter/spring)	0.60	-0.69

An inverse relationship, of increasing CO_2 concentrations emitted from the well during falling barometric pressure periods, was observed in all four of the monitored wells (Table 5.2). CO_2 concentrations exceed 0.1% during exhaling periods at all locations (Table 5.1). Due to poor air circulation in the Staudinger well pit, CO_2 concentrations rarely reached the recorded minimum of 0.04% (i.e., atmospheric), whereas the carbon dioxide sensor regularly recorded atmospheric concentrations at the additional well locations. A significant amount of methane gas was not observed at any of the monitored breathing well locations, measuring below the detection limit of the sensor. H_2S (manually measured with the Defender) was not detected at any of the locations.

The air velocity transducer was in operation at all of the monitored locations; unfortunately, the Ammeter well was the only additional well location that provided useful data. The similar physical settings of the Ammeter and the Staudinger wells, led to similar behaviour (Figure 5.5). As with the Staudinger well, the Ammeter well inhaled for a longer period of time (328 hours) than it exhaled (193 hours). Large negative volumetric flow rate periods are

correlated with low oxygen concentration periods. The correlation between oxygen concentrations and volumetric airflow rate is 0.68. The average flow rate at the Ammeter well was lower than at the Staudinger well, likely from atmospheric interference because the sensor was located at the surface. The average exhaling flow rate was 5.8 x 10^{-5} m^3/s, which is comparable to the average inhaling flow rate of 5.7 x 10^{-5} m^3/s.

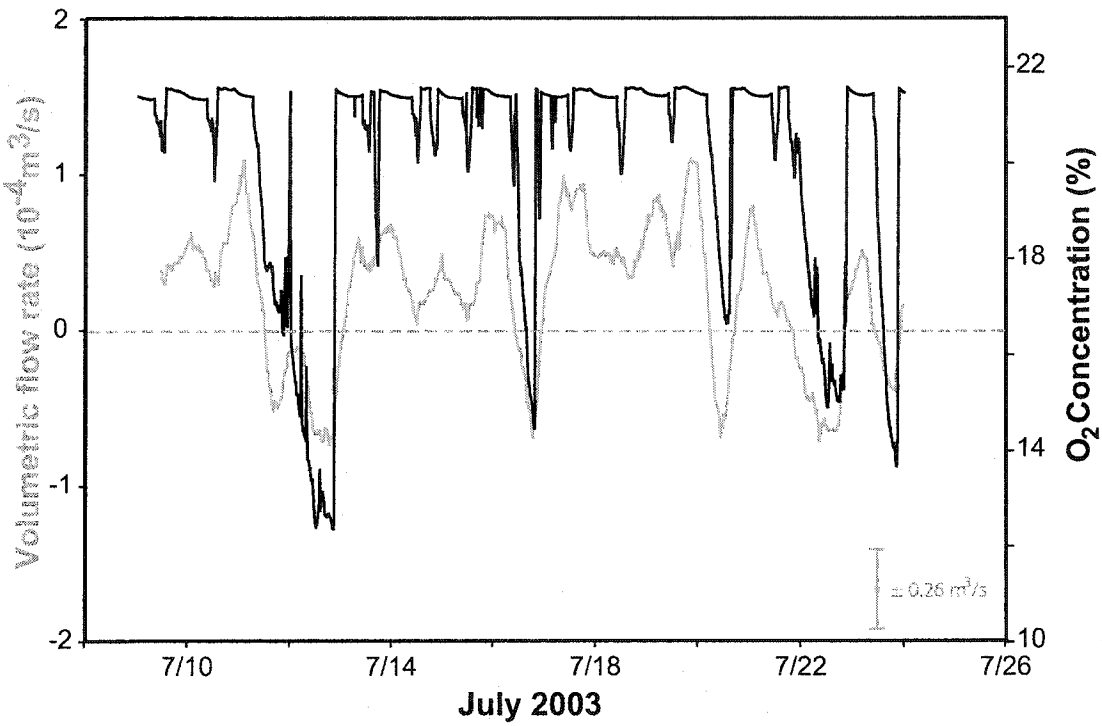

Figure 5.5: Volumetric flow rate (averaged over 24 hours) and oxygen concentration distribution through the Ammeter well, July 2003. Negative flow rates correspond to exhaling periods; positive flow rates correspond to inhaling periods.

The Delburne well is a very active well. The air velocity transducer data is not presented (but is available in Appendix A) because the maximum limit of the sensor was exceeded for most of the monitoring period. The well continuously exhibits strong, observable breathing characteristics, such as loud blowing and sucking noises, and the release of strong currents of air. The Onoway well also displays observable breathing behaviours, emitting noticeable currents of air. Unfortunately, because of the positioning of the transducer at Onoway, the volumetric flow rates cannot be used for analyses.

5.3 Groundwater

The geochemical and bacterial data of the three additional wells are summarized in Table 5.3. The distribution of major cations and anions, for all of the wells sampled in this study, is depicted in Figure 5.6.

The groundwater in the Ammeter well is similar to that in the Staudinger well. The water is Na-HCO_3 dominant, with a pH of 7.8 at a temperature of 6.5°C. Sulphate concentrations are elevated relative to the Staudinger well, suggesting that this well is completed down gradient of the point of recharge. The dissolved oxygen probe was, unfortunately, not working on the day of sampling. The total and dissolved iron content of the groundwater are both essentially below the detection limit (<0.1 mg/L).

The Onoway groundwater is Ca-HCO_3 dominant. Ca^{2+} represents 60% of the total cations, and HCO_3^- represents 87% of the total anions. The groundwater is fresh; the TDS content of the water is 456 mg/L. Presumably, groundwater recharge occurs through the surficial deposits quickly, and very little material is dissolved during infiltration. The pH of the water was measured at 7.3, and the temperature was 7.5°C, on average. The dissolved oxygen content of the water was below detection (<0.01 mg/L). Dissolved iron concentrations range between 2.5 and 4 mg/L, and the total iron concentrations range between 5 and 7 mg/L.

The Delburne groundwater is Na-SO_4-HCO_3 dominant. Na^+ represent 70% of the total cations. HCO_3^- and SO_4^{2-} together represent nearly 100% of the total anions. The measured TDS concentration at Delburne was the highest of any of the monitored breathing wells, at 1400 mg/L. The high SO_4^{2-} and high TDS concentrations suggest that this well is not located in a groundwater recharge area. The water is still alkaline, with a pH of 7.4, at a temperature of 8.7°C. The measured dissolved oxygen content was 0.9 mg/L, and the

dissolved iron and total iron concentrations were 0.15 and 1.0 mg/L, respectively.

The nitrate concentration in the groundwater sampled from the Delburne well was 0.001 mg/L NO_3-N, and the Onoway well had 0.003 mg/L of NO_3-N. The Ammeter groundwater sample yielded over 0.094 mg/L of nitrate, higher than that detected in the Staudinger well.

The dissolved nitrate in the Staudinger groundwater had an isotopic signature indicative of commercial fertilizers. The $\delta^{15}N$ and $\delta^{18}O$ content of the dissolved nitrate samples from the other locations were not analyzed. However, because all of the monitored wells are located in agricultural intensive regions, all of the monitored wells have the potential for nitrate contamination due to agricultural practices.

Moderately aggressive populations of denitrifying bacteria were detected in the Ammeter groundwater. Although the DO probe was not working properly when the well was sampled, the presence of denitrifying bacteria suggests that the dissolved oxygen is likely depleted, as in the other wells. Moderately aggressive populations of denitrifying bacteria were detected at the Onoway well, and background populations were detected in the Delburne well. Aggressive populations of iron related bacteria (IRB) were detected in all three additional wells. Sulphate reducing bacteria were not detected in either the Ammeter or Delburne wells, and were not tested for in the Onoway well.

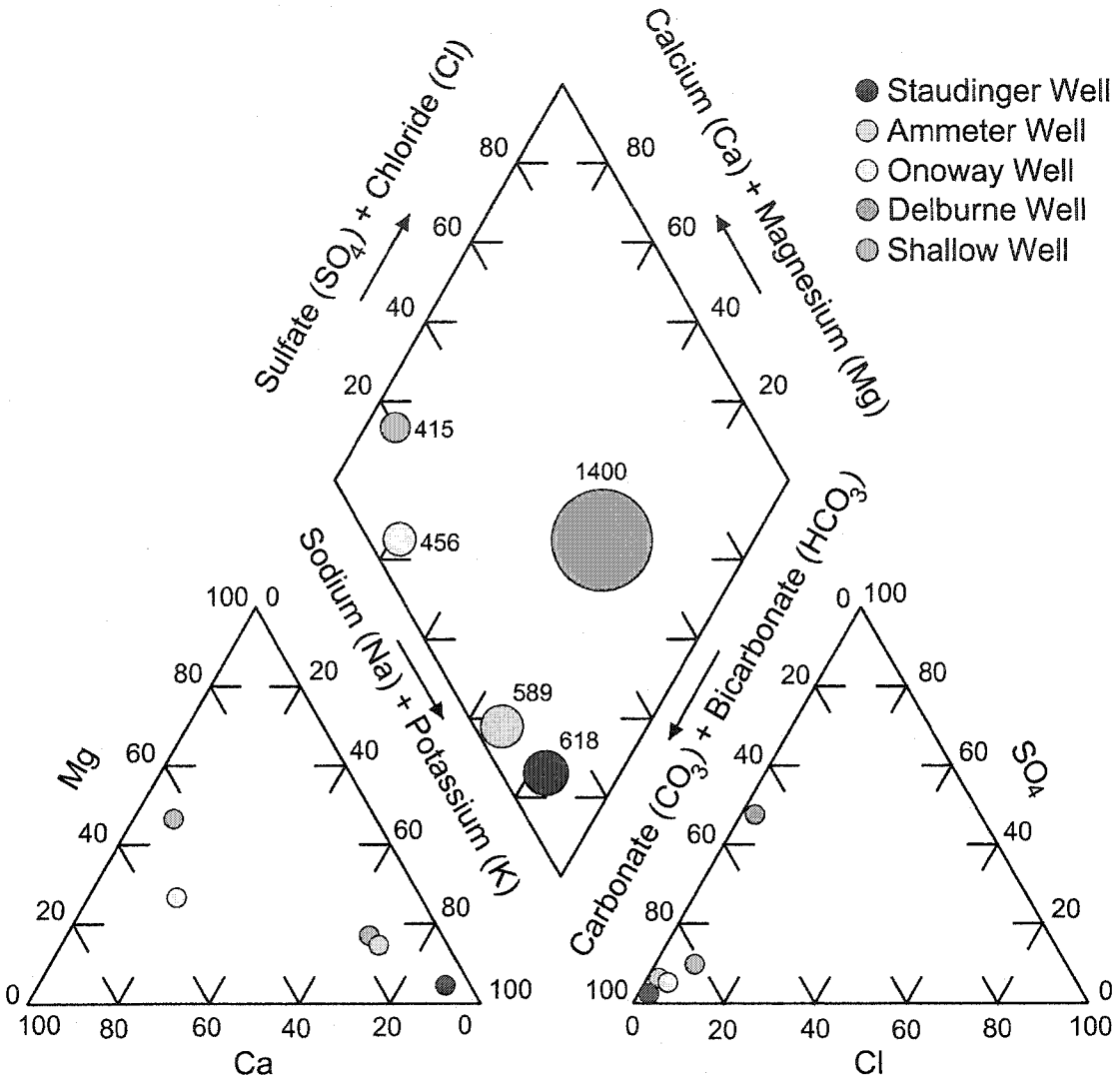

Figure 5.6: Piper diagram representing the major cations and anions of the four monitored breathing water wells. The shallow well is also included. The size of the complete composition circle represents TDS on a linear scale. The TDS (mg/L) value is indicated beside each composition circle.

Table 5.3: Chemical composition of the groundwater sampled from the three additional breathing wells, and the average chemical composition of the groundwater in the Staudinger well.

	Parameter	Onoway 2/10/2002	Onoway 12/10/2002	Delburne 12/7/2003	Ammeter 12/7/2003	Staudinger Avg.
Major cations and anions	Na^+ (mg/L)	27	25	267	112	148
	K^+ (mg/L)	1.67	1.62	3.23	1.75	1.68
	Ca^{2+} (mg/L)	83.3	60.2	43.8	20.2	12.7
	Mg^{2+} (mg/L)	18.3	17.6	24.9	13.4	4.5
	Cl^- (mg/L)	0.20	0.23	4.68	5.22	3.73
	SO_4^{2-} (mg/L)	28.0	27.2	455	29.8	18.4
	HCO_3^- (mg/L)	312	311	600	406	429
	CO_3^{2-} (mg/L)	< 0.01	< 0.01	< 0.01	< 0.01	< 0.01
Nitrogen content	TN (mg/L)	0.42	0.51	0.49	0.68	0.64
	NH_4^+ (mg/L)	0.35	0.37	0.15	< 0.01	0.44
	$NO_2^- + NO_3^-$ (mg/L)	< 0.01	< 0.01	0.003	0.42	0.06
	NO_3^--N (mg/L)	0.001	0.001	0.005	0.094	0.014
Lab parameters	DOC (mg/L)	2.7	3.1	6.04	2.3	2.7
	DIC (mg/L)	56.0	56.6	114.6	77.9	80.4
	Alkalinity (mg/L as $CaCO_3$)	256	255	492	333	352
	pH	7.3	7.3	7.9	7.9	8.0
	TDS (mg/L)	470	443	1400	589	618
	sum cations (meq/L)	6.9	5.6	14.3	7.0	
	sum anions (meq/L)	5.7	5.7	19.4	7.4	
	% error	9.4	0.7	9.9	2.7	
Field parameters	Fe (mg/L)	4.0	2.5	0.6	0.0	0.2
	Total Fe (mg/L)	6.5	5.0	1.0	0.1	0.8
	Alkalinity (mg/L as $CaCO_3$)	442	408	629		534
	Conductivity (µS/cm)	336	317	833	379	873
	pH	6.9	7.3	7.4	7.8	7.6
	DO (mg/L)	< 0.01	< 0.01	0.9	5.0	0.5
	T (°C)	7.5	7.4	8.7	6.5	5.7
BART's	Denitrifying bacteria	m.a	m.a	bck.	m.a	
	Iron-related bacteria	a.	a.	a.	a.	
	Nitrifying bacteria	n/a	n/a			
	Sulphate reducing bacteria			n/a	n/a	

bck. Background population
m.a Moderately aggressive population
n/a No reaction
a. Aggressive population

5.4 Comparison to the Staudinger Well

The question that must still be answered is "are the same processes, which produce the gas distributions observed at the Staudinger well, also responsible for the gas distributions observed at all monitored breathing well locations?" Similar characteristics were observed in all of the wells; hence, similar conclusions can be extrapolated to all four monitored well locations.

The same physical characteristics (i.e., the gas composition fluctuations within the breathing water wells) are consistent at all of the monitored well locations. All of the wells display positive correlations between oxygen concentration and barometric pressure fluctuations; similarly, changes in carbon dioxide concentrations are negatively correlated with barometric pressure changes.

The same redox sequence used to describe the changing conditions with depth at the Staudinger well (Figure 4.14) can be applied to explain the conditions at the additional well locations. All of the sampled groundwaters are depleted in dissolved oxygen with respect to expected recharge concentrations (i.e., water in equilibrium with air). Most of the dissolved oxygen is suspected to be consumed by biological processes during infiltration through the overlying aquitard, producing elevated carbon dioxide concentrations. Oxygen in the unsaturated zone can also be partially depleted by iron and/or sulfide reactions.

As was stated earlier, most natural groundwaters have dissolved gas concentrations elevated above that expected for water in equilibrium with air. The amount of excess gas is site specific, depending on location and physical conditions. Excess gas can be produced below the water table by biogeochemical processes (such as denitrification), or by contact with soil gases during infiltration through an unsaturated zone (Heaton and Vogel,

1981). The amount of excess gas is dependent on the physical setting of the unsaturated zone and recharge conditions.

The production of nitrogen gas by denitrification and its release during exhaling periods is a plausible contributor to the depletion of oxygen within these wells. Even without dissolved gas measurements collected from passive gas samplers, the dissolved N_2 gas concentrations are suspected to be high in the additional wells. Dissolved oxygen is depleted in all of the sampled groundwater. All of the wells are located in agricultural intensive regions. It is suspected that nitrate, applied at the surface with commercial fertilizers, or from intensive livestock operations (manure), percolates with recharging groundwater. These nitrates are utilized in denitrification reactions through the confining aquitards and in the aquifer, producing excess nitrogen gas.

The aquitards can provide the underlying aquifer protection from nitrate contamination, hence low nitrate concentrations are observed. High levels of nitrates are not detected in the aquifers because the overlying aquitards act as a permeable reactive barrier (Simpkins and Parkin, 1993; Robertson et al., 1996). The water is denitrified as it is carried through the subsurface. The relatively higher nitrate concentrations detected in the wells near Sylvan Lake suggests that the overlying shale aquitard is, possibly, not able to withhold nitrates to the same degree as the aquitards above the Onoway and Delburne wells, or that application rates are more intense in this region. The nitrate that is able to proceed through the aquitard is denitrified in the lower aquifer.

The mass balance model used to recreate the changes in the gas compositions observed in the Staudinger well did show that the dilution of oxygen by nitrogen is a plausible process. The magnitude of this effect is dependant on well completion, geology, and barometric pressure fluctuations. Since dissolved gas concentrations were not measured in three additional

wells, the mass-balance model cannot be applied; however, the same physical and geochemical requirements for dilution are plausible at all of the monitored locations.

5.5 Summary

- Although the specifics of each well completion and geology varied, the three required criteria for breathing wells were met at the four monitored locations. The physical setting of the Ammeter well is very similar to the Staudinger well, due to their close proximity. Both the Onoway and Delburne wells display strong observable breathing characteristics, attributed to the thin unsaturated zone thickness of the aquifers in which the wells are completed.

- Observations at the Staudinger well reveal that changes in oxygen concentration at the wellhead are positively correlated with changes in barometric pressure fluctuations, whereas changes in carbon dioxide are inversely correlated to barometric pressure. The additional wells also displayed these characteristics, although each displayed a difference in magnitude, because of their physical variations.

- It is suspected that excess nitrogen gas is produced in the subsurface by denitrification, either in the overlying confining unit or in the saturated pores of the completion aquifer. This gas is released into the unsaturated zone during exhaling periods because of the decrease in the surrounding pressure (barometric pressure). Oxygen in the unsaturated zone is diluted during the release of this gas from water. The source of the original nitrate was confirmed as agricultural fertilizers in the Staudinger well, and is the assumed source of the nitrates in the additional monitored breathing wells.

- The cause of the oxygen deficient environments observed in these wells can be assumed, in part, as dilution by the production of excess gas below the water table. The degree to which this process plays a role is still unclear at each site. Each well is site specific, and a combination of processes could be responsible for the oxygen deficient environment observed in these wells. Nevertheless, the related trends observed in all of these wells can be extrapolated to other known breathing wells.

CHAPTER 6: CONCLUSIONS

The tragic accident on the Staudinger farm in July 1999 generated interest and concern in the physical and geochemical behaviours of breathing wells. Prior to this investigation, there was a general understanding about these wells, but their full distribution and influence was not recognized. The purpose of this project was to increase the awareness and knowledge of the physical characteristics of such wells.

Breathing wells are often identified by the observable noises, or currents of air they emit; however, not all breathing wells will show observable signs. Breathing wells can be located in a variety of regions and completion settings, but all require the three following conditions:

1. They must be completed in a partially saturated aquifer
2. An overlying confining aquitard must be present
3. An open zone of the well must be in contact with the unsaturated zone of the aquifer

Breathing wells were reported across the continent, in areas of the United States and Canada. The probability that the distribution of breathing wells is greater than that reported is high because results depended on volunteer contributions. The results do, however, confirm that breathing wells are more widespread than first believed, and bear the potential to be located worldwide.

Oxygen, carbon dioxide, and barometric pressure measurements at four breathing water wells in central Alberta confirmed that transient gas compositions exist within the unsaturated zone of the partially saturated aquifers penetrated by the breathing wells. During inhaling periods, the unsaturated zone is inundated with atmospheric air. The air released from

the subsurface during exhaling periods becomes progressively depleted in oxygen, correlated with the decrease in barometric pressure over the same time period. Carbon dioxide concentrations exhibit the inverse relationship, with concentrations progressively increasing over an exhaling period. The magnitude of these changes is dependent on the amplitude and length of the barometric pressure cycle and the physical properties of the material in which the gas is transported.

At the Staudinger well, atmospheric air is drawn into the subsurface during inhaling periods. This oxygen is consumed and diluted in the subsurface. Some of the oxygen is utilized by the oxidation of organic matter, or by the oxidation of iron sulfides that exist in the matrix. Excess gas (N_2 and CO_2) is produced in the groundwater by denitrification, and is exsolved into the unsaturated zone when the surrounding pressures decrease. The air in the unsaturated zone is then depleted in oxygen with respect to atmospheric air, and elevated in both nitrogen and carbon dioxide.

A simple mass-balance model was used to replicate the observed gas compositions from the Staudinger well. The model considered advection to be the dominant transport process, with advective fluxes initiated by barometric pressure changes. The model reasonably reproduced the gas compositions of the air within the subsurface for three individual pressure cycles of different intensity and length. In the model, the only source of air/gas originated below the water table. This model could be applied to additional breathing well locations if dissolved gas concentrations are measured.

The possibility of warmer and drier winters on the prairies, and increased extraction of groundwater, have added a further concern as to the creation of more breathing wells. Reduced precipitation and high summertime water demands affect surface and shallow groundwater supplies, reducing

groundwater recharge to underlying aquifers. If conditions persist, hydraulic head potentials will decrease, lowering the water levels across the prairies. Existing wells, which do not breathe today, have the potential to begin breathing if water levels drop below the open zone in the well.

Breathing wells possess the greatest risks when located in confined spaces, such as well pits or well shacks. Awareness of these hazards is essential, in addition to taking necessary precautions (i.e., ensuring proper ventilation, or the use of portable gas monitors). The initial construction of breathing wells is, for the most part, preventable. Locating the water level in a well prior to completion, and insuring that the well casing extends considerably below this elevation, is one preventative method.

This study has not only identified the possible mechanisms behind the oxygen-deficient environment observed in breathing wells, but has also enhanced the knowledge and understanding of them. These conclusions and findings draw on many aspects of science, including geology, biology, chemistry and social science, and will hopefully be applied and brought to the attention of those who are exposed to the potential hazards associated with breathing wells.

REFERENCES

Allan, J.A. and Sanderson, J.O.G. (1945) *Geology of the Red Deer and Rosebud Sheets, Alberta*. Report No. 13. Research Council of Alberta.

Auer, L.J., Rosenberg, N.D., Birdsell, K.H. and Whitney, E.M. (1996) The effects of barometric pumping on contaminant transport. *Journal of Contaminant Hydrology*. 24 (2), p. 145-166.

Bates, R.L. and Jackson, J. (1987) *Glossary of Geology*. 3rd ed. American Geological Institute, Alexandria, VA.

Beaucaire, C., Pitsch, H. and Boursat, C. (1998) Modelling of redox conditions and control of trace elements in clayey groundwater. *In: Arehart, G.B. (ed) and Huston, J.R. (ed) Proc Water-Rock Interaction WRI 9, Taupo, New Zealand, 30 March – 3 April 1998*. Balkema, Rotterdam, p. 141-144.

Blicher-Mathiesen, G., McCarty, G.W. and Nielsen, L.P. (1998) Denitrification and degassing in groundwater estimated from dissolved dinitrogen and argon. *Journal of Hydrology*. 208 (1-2), p. 16-24.

Burgess, P.M. (2002) A guide to limnology laboratory safety practices and routine operations and analyses. Limnology Service Laboratories. Department of Biological Sciences, University of Alberta.

Byers, H.R. (1974) *General Meteorology*. 4th ed. McGraw-Hill, New York, NY.

BW Technologies Ltd. (2002) *BW Defender Multi-Gas Detector – Operator's Manual*. BW Technologies Ltd. Calgary, AB.

Carrigy, M.A. (1970) Proposed revision of the boundaries of the Paskapoo Formation in the Alberta Plains. *Bulletin of Canadian Petroleum Geology*. 18 (2), p. 156-165.

CHEMetrics, Inc. (n.d.) *Iron CHEMets®* CHEMetrics Inc. Calverton, VA.

Clesceri, L.S. (ed.), Am Public Health ASN, Greenberg, A.E., Eaton, A.D. (1998) *Standard Methods for the Examination of Water and Wastewater.* 20th ed. American Public Health Association. Washington, D.C.

Creelman, M.E. (1967) *Schools of the parkland; N.W.T., 1886-Alberta.* Red Deer District, Alberta Teacher's Association. No. 24 Centennial Project.

Cooper, M. (1999) Teens' July deaths blamed on cellar's high nitrogen levels. *The Edmonton Journal,* 16 August 1999, p. A5.

Cullimore, R. (1999) *Microbiology of Well Biofouling.* Lewis Publishers, Boca Raton, FL.

Dahlgren, R.A., Percival H.J. and Parfitt, R.L. (1997) Carbon-dioxide degassing effects on soil solutions collected by centrifugation. *Soil Science.* 162 (9), p. 648-655.

Deutsch, C. V. (2002) *Geostatistical Reservoir Modeling.* Oxford University Press, New York, NY.

Drever, J.I. (1997) *The Geochemistry of Natural Waters: Surface and Groundwater Environments.* 3rd ed. Prentice Hall, Inc., Upper Saddle River, NJ.

Elberling, B., Larsen, F., Christensen, S. and Postma, D. (1998) Gas transport in a confined unsaturated zone during atmospheric pressure cycles. *Water Resources Research.* 34 (11), p. 2855-2862.

Environment Canada. (2000) Canadian Monthly Climate Data and 1961-1990 Normals [CD-ROM]. Environment Canada, Atmospheric Environment Service, Downsview, Ontario.

ESRI Software Inc. (2001) *Arcmap 8.1.* Environmental Systems Research Institute, Inc. Redlands, CA.

Fitts, C. (2002) *Groundwater Science.* Academic Press, London.

Freeze, R.A. and Cherry, J.A. (1979) *Groundwater.* Prentice-Hall, Inc., Englewood Cliffs, NJ.

Gabert, G.M. (1975) *Hydrogeology of Red Deer and Vicinity, Alberta.* Bulletin 31. Research Council of Alberta.

Golden Software Inc. (1999) *Surfer 7 User's Guide.* Golden Software Inc., Golden, CO.

Hach Company. (1997) *Alkalinity Test Kit Model AL-AP.* Hach Company. Loveland, CO.

Hallberg, G.R. (1989) Pesticide pollution of groundwater in the humid United States. *Agriculture Ecosystems and Environment.* 26, p. 299-367.

Health and Welfare Canada. (1996) *Guidelines for Canadian Drinking Water Quality.* 6th ed. Supply and Services Canada. ISBN 0-660-16295-4, Ottawa, ONT

Heaton, T.H.E. (1981) Dissolved gases: Some applications to groundwater research. *Transaction of the Geological Society of South Africa.* 84, p. 91-97.

Heaton, T.H.E., and Vogel, J.C. (1981) "Excess air" in groundwater. *Journal of Hydrology.* 50, p. 201-216.

Holocher, J., Peeters, F., Aeschbach-Hertig, W., Hofer, M., Brennwald, M., Kinzelback, W. and Kipfer, R. (2002) Experimental investigations on the formation of excess air in quasi-saturated porous media. *Geochimica et Cosmochimica Acta.* 66 (23), p. 4103-4117.

Hydrogeological Consultants Ltd. (2000) *Water wells that breathe: Proposal for funding through Alberta Environment.* Hydrogeological Consultants Ltd., Edmonton, AB.

Keeney, D.R. (1986) Sources of nitrate to ground water. *CRC Critical Reviews of Environmental Control.* 16 (3), p. 257-304.

Kendall, C. and McDonnell, J.J. (eds.) (1998) *Isotope Tracers in Catchment Hydrology.* Elsevier Science B.V., Amsterdam, NL.

Kehew, A. E., 2001. *Applied Chemical Hydrogeology.* Prentice-Hall Inc., Upper Saddle River, NJ.

Kharaka, Y.K., Gunter, W.D., Aggarwal, P.K., Perkins, E.H. and DeBrall, H.D. (1988) *SOLMINEQ.88: a computer program for geochemical modeling of water-rock interactions.* U.S. Geological Survey, Water Resources Investigations. Report 88-4227.

Langmuir, D. (1997) *Aqueous Environmental Geochemistry.* Prentice-Hall Inc., Upper Saddle River, NJ.

Le Breton, E.G. (1971) *Hydrogeology of the Red Deer Area, Alberta.* 71-1. Research Council of Alberta.

Lewis, M. (1999) Tragedy in Canada: The dangers of wells that "breathe". *Water Well Journal.* November, p. 70-72.

Manning, A.H., Solomon D.K. and Sheldon, A.L. (2003) Applications of a total dissolved gas pressure probe in ground water studies. *Ground Water.* 41 (4), p. 440-448.

Massmann, J. and Farrier, D.F. (1992) Effects of atmospheric pressures on gas transport in the vadose zone. *Water Resources Research.* 28 (3), p. 777-791.

Madigan, M.T., Martinko, J. and Parker, J. (2003) *Brock Biology of Microorganisms.* 10th ed. Prentice-Hall Inc., Upper Saddle River, NJ.

McLeish, K., (in prep.) PhD Thesis. University of Calgary, Department of Civil Engineering, Calgary, AB.

McMahon, P.B., Böhlke, J.K. and Bruce, B.W. (1999) Denitrification in marine shales in northeastern Colorado. *Water Resources Research.* 35 (5), p. 1629-1642

McMahon, P.B. (2001) Aquifer/aquitard interfaces: mixing zones that enhance biogeochemical reactions. *Hydrogeology Journal.* 9 (1), p. 34-43.

Natural Resources Canada. (2002a) National Topographic Data Base, 83B01 version 3.2. [electronic resource]. Natural Resources Canada, Geomatics Canada.

Natural Resources Canada. (2002b) National Topographic Data Base, 83B08 version 3.2. [electronic resource]. Natural Resources Canada, Geomatics Canada.

Oakton Instruments. (2002a) *pH 300 and 310 Portable Waterproof pH/mV/°C Meter - Operating Instructions.* Oakton Instruments. Vernon Hills, IL.

Oakton Instruments. (2002b) *Portable Waterproof Dissolved Oxygen Meter - Operating Instructions.* Oakton Instruments. Vernon Hills, IL.

OMEGA Engineering Inc. (2000) *FMA-900 Series Air Velocity Transducers: User's guide.* Omega Engineering Inc. Stamford, CT.

OxyGuard. (n.d.) *OxyGuard D.O Profie – Dissolved Oxygen Probe for Profiling Measurements in the Environment.* OxyGuard International. Birkerød, DK.

Ozoray, G.F. (1972) *Hydrogeology of the Wabamun Lake Area, Alberta.* 72-8. Research Council of Alberta.

Powell, R.M. and Puls, R.W. (1993) Passive sampling of ground water monitoring wells without purging: Multilevel well chemistry and tracer disappearance. *Journal of Contaminant Hydrology.* 12, p. 51-77.

Province of Alberta (1993) *Alberta Protection and Enhancement Act.* Queen's Printer for Alberta, Edmonton, AB.

Quatrosense Environmental Ltd., (2002a) *Installation, operation, and maintenance manual. Model QTS-1300 Oxygen (O_2) analog transmitter/sensor.* Quatrosense Environmental Ltd., Ottawa, ON.

Quatrosense Environmental Ltd., (2002b) *Installation, operation, and maintenance manual. Model QTS-1710 series combustible gas transmitter/sensor.* Quatrosense Environmental Ltd., Ottawa, ON.

Quatrosense Environmental Ltd., (2002c) *Installation, operation, and maintenance manual. Models CTS M-20 Operating Manual.* Quatrosense Environmental Ltd., Ottawa, ON.

Robertson, W.D., Russel, B.M. and Cherry, J.A. (1996) Attenuation of nitrate in aquitard sediments of southern Ontario. *Journal of Hydrology.* 180 (1-4), p. 267-281.

Rodvang, S.J. and Simpkins, W.W. (2001) Agricultural contaminants in Quaternary aquitards: A review of occurrence and fate in North America. *Hydrogeology Journal.* 9 (1), p. 44-59.

Rossabi, J. and Falta, R.W. (2002) Analytical solution for subsurface gas flow to a well induced by surface pressure fluctuations. *Groundwater.* 40 (1), p. 67-75.

Ryan, C. (2004) Personal Communication. March 8, 2004. Associate Professor, University of Calgary, Department of Geology and Geophysics, Calgary, AB.

Sacchi, E., Michelot, J.L., Pitsch, H., Lalieux, P. and Aranyossy, J.F. (2001) Extraction of water and solutes from argillaceous rocks for geochemical characterisation: Methods, processes, and current understanding. *Hydrogeology Journal.* 9 (1), p. 17-33.

Simpkins, W.W. and Parkin, T.B. (1993) Hydrogeology and redox geochemistry of CH_4 in a Late Wisconsinan till and loess sequence in central Iowa. *Water Resources Research.* 29 (11), p. 3643-3657.

Staudinger, H. (2002) Personal Communication. April 15, 2002.

The Groundwater Centre. (2004) Enhanced, live database, updated and maintained by MOW-Tech Ltd. www.tgwc.ca.

Thorstenson, D.C. and Pollock, D.W. (1989) Gas transport in unsaturated zones: Multicomponent systems and the adequacy of Fick's law. *Water Resources Research.* 25 (3), p. 477-507.

Trewartha, G.T. (1980) *An Introduction to Climate.* 5th ed. McGraw-Hill Book Co., New York, NY.

Tokarsky, O. (1971) *Hydrogeology of the Rocky Mountain House Area, Alberta.* 71-3. Research Council of Alberta.

Tóth, J. (1966) *Groundwater geology, movement, chemistry, and resources near Olds, Alberta.* Bulletin 17. Research Council of Alberta.

Vogel, J.C., Talma, A.S. and Heaton, T.H.E. (1981) Gaseous nitrogen as evidence for denitrification in groundwater. *Journal of Hydrology.* 50, p. 191-200.

Wallick, E.I. (1981) Chemical evolution of groundwater in a drainage basin of Holocene age, east-central Alberta, Canada. *Journal of Hydrology.* 54 (1-3), p. 245-283.

Wilson, G.B., Andrews, J.N. and Bath, A.H. (1990) Dissolved gas evidence for denitrification in the Lincolnshire Limestone groundwaters, Eastern England. *Journal of Hydrology.* 113 (1-4), p. 51-60.

APPENDIX A: COLLECTED DATA FILES

Appendix A consists of a CD with the field and laboratory data collected from the four monitored breathing water wells. The README.txt file on the CD explains the directory structure of the Appendix along with descriptions of the contents.

The folders included in the Appendix are:

- Corrected Oxygen
- Datalogger
- Downloaded Data
- Geochemistry
- Isotopes
- Monitored Wells
    - Staudinger Data
    - Ammeter Data
    - Delburne Data
    - Onoway Data
- Questionnaire

Data can also be obtained by contacting the author's supervisor:

- Dr. Carl Mendoza: carl.mendoza@ualberta.ca

APPENDIX B: ISOTOPES

The oxygen and hydrogen isotope composition of groundwater is routinely included in hydrogeological investigations. In each stage of the hydrogeologic cycle, the isotopic composition of water will change because of external interactions and phase changes. Groundwater in recharge areas will display an isotopic signature similar to rainwater and surface water. As it flows, either on a local, intermediate or regional scale, it is subjected to different fractionation processes (thermodynamic, kinetic, or diffusive), which may alter its isotopic ratio.

Stable isotope analyses were completed on groundwater samples obtained from the Staudinger well to determine the isotopic processes that occur subsequent to recharge, and within the vicinity of the water well itself. Analysis was also completed on the water sampled from the three additional breathing wells.

B.1 Methods

B.1.1 Sampling

The sampling procedure for stable groundwater isotopes is less complex than the water quality sampling procedure. Chemical and biological processes affect neither deuterium nor oxygen-18; evaporation is the biggest concern in the sampling procedure (Clark and Fritz, 1997). To prevent evaporation, a sampling bottle must be filled so that there is no head (air) space. A vacutainer, often used in medical applications, was used to collect water from the breathing wells for isotope analyses. The vacuum within the vacutainer draws water into the sample chamber through a two-way needle preventing

any contact or exchange with ambient air. Samples were stored at room temperature, in a dry location until analyses.

B.1.2 Laboratory Analysis

Laboratory analyses were performed in the stable isotope laboratory at the University of Alberta. The procedures for both deuterium and oxygen-18 anaysis are described below.

To determine the deuterium composition of a water sample, the water must be converted to hydrogen gas prior to mass spectrometric analysis. This is done by reacting 10μg of water with 160 mg of zinc (± 20 mg) at 500°C ± 20°C (Coleman et al., 1982). During this procedure, the zinc is oxidized and the water is reduced to hydrogen-deuterium gas. Once cooled, the gas can then be analyzed on a mass spectrometer without any need for further purification.

The oxygen isotope composition of water is measured by equilibrating the water sample with carbon dioxide gas of a known ^{16}O content:

$$H_2{}^{18}O + C^{16}O_2 \leftrightarrow H_2{}^{16}O + C^{16}O^{18}O \qquad (A.1)$$

After equilibration, usually performed in a thermostated bath at 25°C for three days (Epstein and Mayeda, 1953), the CO_2 is isolated from the equilibration tube and purified (frozen) with liquid nitrogen. The samples are analyzed on a mass spectrometer for isotopic ratio measurements.

Both $\delta^{18}O$ and δD ratios are expressed in per mil relative to Vienna Standard Mean Ocean Water (V-SMOW) (Craig, 1961; Gonfiantini, 1978) calculated using standard regression lines. Analytical reproducibility is ±0.3 ‰ for $\delta^{18}O$, and ±3 ‰ for δD.

B.1.3 Vacuum Extraction

A vacuum extraction test was conducted September 9 2002, on the Staudinger well. The hose of an industrial vacuum cleaner was attached to the 2-inch diameter opening on the top of the well seal. The rest of the well seal was made air tight, using silicone, to prevent air leakage during the extraction. The vacuum was run for 2 hours, pumping air from within the subsurface at a rate of 3.5 m^3/min. Water pooled in the tubing during the test indicating high humidity of the subsurface air. Following the air extraction test, geochemical, bacteria and isotope sampling were performed.

B.2 Oxygen and Hydrogen Isotope Compositions

B.2.1 Staudinger Well Results

The isotopic data from all of the investigated groundwaters are summarized in Table B.1. The $\delta^{18}O$ and δD values from the Staudinger and shallow well are plotted in Figure B.1. The purpose of this plot is to provide some indication as to the origin of groundwater and processes affecting it after infiltration. Craig's global meteoric water line (1961) and the Edmonton meteoric water line (Maulé et al, 1994) are also plotted. The meteoric water lines (MWL) define the relation between hydrogen and oxygen isotopes in precipitation water.

$\delta^{18}O$ and δD values of the groundwater in the Staudinger well vary from -18.1‰ to -18.8‰ for oxygen and from -147‰ to -151‰ for hydrogen. The general composition of the groundwater falls below the MWL, indicating an isotopic enrichment subsequent to precipitation. The data from the Staudinger well vary along an evaporation line with a slope of 4.52, with and interception point of -21.2‰. The measured isotopic composition from the shallow well groundwater is also plotted in Figure B.1, falling in the vicinity of the MWL.

Table B.1: Isotopic composition of the four sampled breathing water well groundwaters and the shallow water well (near Sylvan Lake).

Sampled Well	Sampling Date	δD (‰) vSMOW	δ18O (‰) vSMOW
		±3 ‰	±0.3 ‰
Staudinger	12/7/2002	-149	-18.6
	24/7/2002	-151	-18.5
	31/7/2002	-150	-18.7
	9/8/2002	-147	-18.4
	16/8/2002	-150	-18.8
	9/9/2002	-148	-18.4
	17/9/2002	-145	-18.0
	11/4/2003	-149	-18.3
	31/5/2003	-151	-18.5
Onoway	12/10/2002	-141	-18.5
Delburne	31/5/2003	-154	-18.4
Ammeter	12/7/2003	-151	-18.9
Shallow	12/7/2003	-141	-19.1

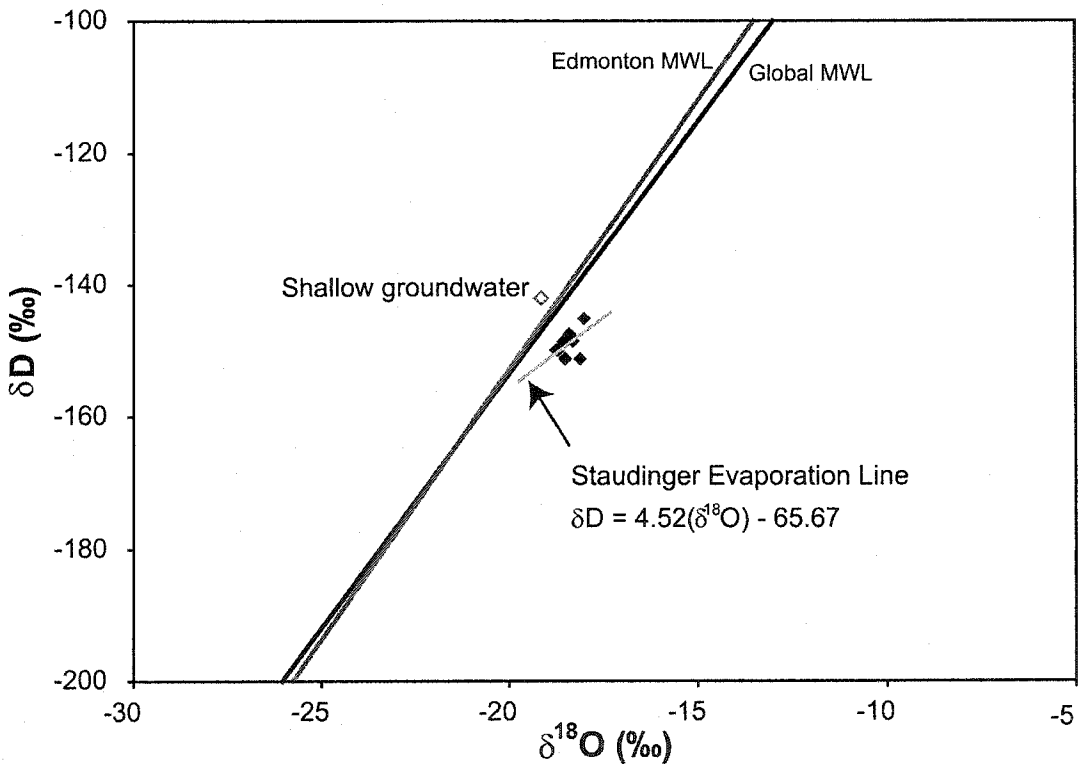

Figure B.1: $\delta^{18}O$-δD plot for Staudinger and shallow well groundwater. Edmonton MWL equation is represented by $\delta D = 7.32(\delta^{18}O) - 6.35$. The Global MWL is represented by the equation $\delta D = 8.17(\delta^{18}O) - 10.56$. Calgary MWL is similar to Global MWL on this scale.

B.2.2 Staudinger Well: Interpretation and Discussion

Figure B.1 suggests that the general isotopic signature of the Staudinger groundwater is a result of evaporation processes. Physical processes possibly occurring in the Sylvan Lake region (an arid to semi-arid area) include evaporation from surface water bodies, secondary evaporation or snow melt processes.

Water that has been evaporated from a lake or other such water body will be isotopically enriched relative to precipitation. This process usually follows an evaporation line with a slope ranging between 1 and 5 (Domenico and Schwartz, 1990). The interception point with the GMWL is the point of unaltered precipitation. Secondary evaporation (partial evaporation during rainfall, or after condensation) will also enrich the water in ^{18}O and D. This will occur when the humidity of the air in which the water falls is less than 100%.

Snowmelt can also produce an isotopic enrichment of the water prior to groundwater recharge. The stable isotope distribution of snow is modified by sublimation and vapour exchange processes that occur at the surface subsequent to deposition, or exchange processes that occur between the snow and melt waters during snow melt (Clark and Fritz, 1997). The bulk of the recharging water in the Sylvan Lake area originates as snow. After deposition, snow becomes isotopically enriched with respect to precipitation because of sublimation, and snowmelt processes. Final melt waters late in the spring are isotopically enriched with respect to early melt waters, plotting further along the evaporation line.

A more detailed analysis of the δD-$\delta^{18}O$ cross-plot (Figure B.2) suggests that small-scale deviations in the isotopic signatures of the Staudinger groundwater are results of secondary fractionation processes, occurring subsequent to infiltration.

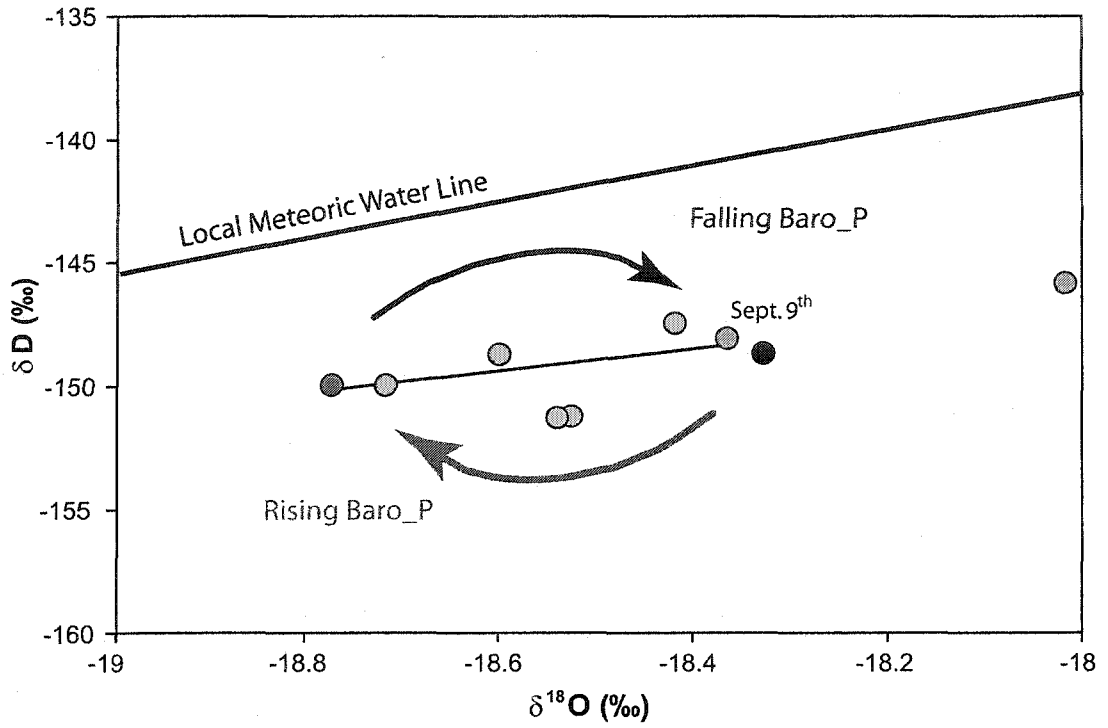

Figure B.2: Barometric pressure influence on the isotopic composition of groundwater sampled from the Staudinger well.

Analysis of the barometric pressure fluctuations twelve hours prior to each sampling event (representing an average length of time for individual inhaling or exhaling events) indicate that the groundwater does become enriched in oxygen-18 (and deuterium) during falling periods (Figure B.2). Samples collected during exhaling periods plot farther along the evaporation line. During a recovery period, or inhaling event, the water-vapour equilibrium re-adjusts itself; the composition of the groundwater represents the average isotopic composition of the aquifer.

These small-scale deviations can be attributed to evaporation occurring across the water table in the partially saturated aquifer. Craig and Gordon (1965) first proposed the theory for non-equilibrium evaporation processes, which can be applied to evaporation occurring in breathing water wells (Figure B.3).

Above the fully saturated layer, there is a semi-saturated sublayer of water vapour, which can also be considered as the capillary fringe (Figure B.3). At equilibrium, diffusive processes lead to the exchange of water vapours. Light isotopes diffuse preferentially from the saturated zone into the sublayer because their diffusivity in air is greater than heavier isotopes (Clark and Fritz, 1997). The saturated layer is thus enriched in with isotopes. Water vapour is also exchanged between the overlying reservoir (the unsaturated zone) and the sublayer.

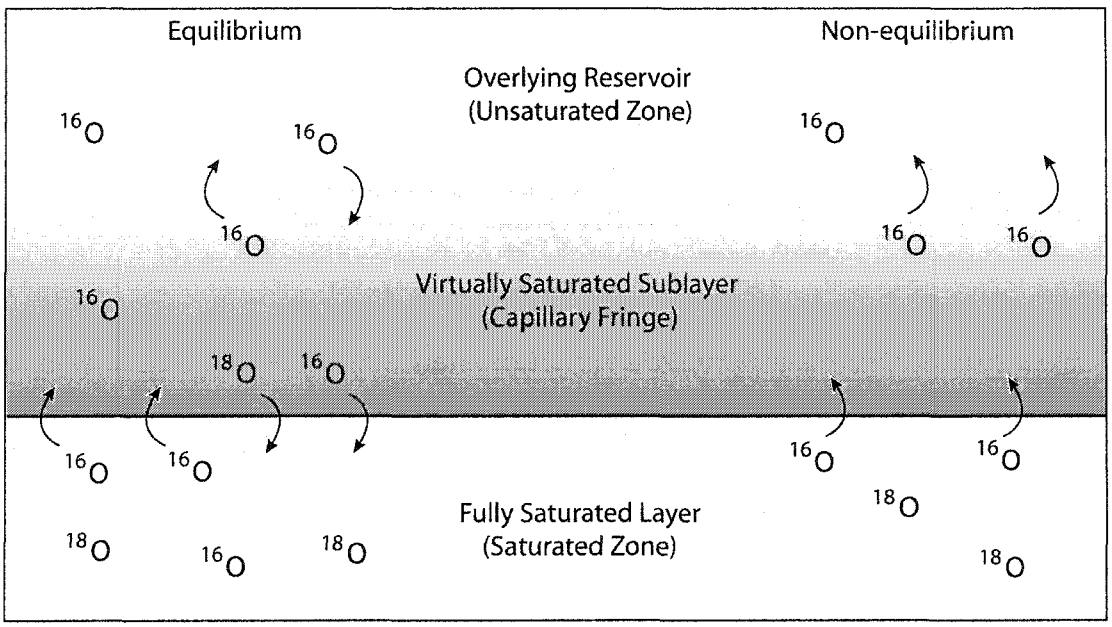

Figure B.3: Model for non-equilibrium evaporation processes across the water table in the partially saturated aquifer. The arrows indicate relative fluxes of oxygen in the water between the three layers. Differences in the rate of diffusion of ^{18}O to ^{16}O (and D to ^{1}H, not shown) produce a kinetic isotope enrichment in the saturated zone during non-equilibrium periods (adapted from Clark and Fritz, 1997).

When equilibrium is disrupted (i.e., during an exhaling event in a breathing well when air is removed from the unsaturated zone), these exchange process are enhanced in an attempt to re-establish equilibrium. The drop in the water vapour pressure in the overlying unsaturated zone (because of vapour removal through the well) elevates the rate of exchange between the sublayer and the overlying reservoir. Exchange between the sublayer and the saturated zone is thus amplified. The saturated zone effectively becomes

enriched in heavy isotopes as the light isotopes are evaporated into the sublayer to re-supply water vapour.

Barometric pressure activity, prior to sampling on September 9 was stable. The $\delta^{18}O$ value obtained from this sampling day conflict with the trends previously stated. The believed cause for this inconsistency is from the air extraction test that was conducted for 2 hours before water sampling. During the extraction test, gas and water vapour were continuously removed from the subsurface. Water condensation was observed in the vacuum tubes. The vacuum extraction test increased the rate of evaporation from the saturated and sublayers; thus, enriching the groundwater with the heavier oxygen-18 and deuterium isotopes. Large amounts of oxygen-16 were removed from the system, mimicking an isotopic signature representative of a falling barometric pressure event.

It must be stated that these are discrete data, and do not represent the isotopic composition changes over a complete pressure cycle. More analyses are required to confirm the theory presented. Sampling of a complete pressure cycle is required to verify whether an atmospheric influence on the changing isotopic trends within the groundwater does indeed exist.

B.3 Additional Wells

Groundwater was sampled from the three additional wells for isotopic analyses to distinguish the overall stable isotope composition of the groundwater in these wells (Figure B.4). The evaporation theory, used to explain the events in the Staudinger well cannot be extrapolated to these other wells because of data quantity. Only individual samples were taken for each location; thus, one can only determine an average isotopic composition at these locations.

The composition of the Ammeter groundwater is very similar to the composition of the Staudinger well, falling along the same evaporation line. The groundwater moving through these two wells likely infiltrated in the same recharge area, traveled along a similar flow path, and has undergone similar geochemical/physical processes.

The Onoway groundwater is very fresh. Its isotopic composition is representative of precipitation, falling on the Edmonton MWL. This indicates that few, if any, fractionation processes occur subsequent to initial infiltration. The Delburne sample falls below the MWL. The relatively high $\delta^{18}O$ values of the Delburne water is attributed to the increased length of time the water has remained in the subsurface, undergoing an increased number of water-rock interactions, or evaporation processes subsequent to precipitation.

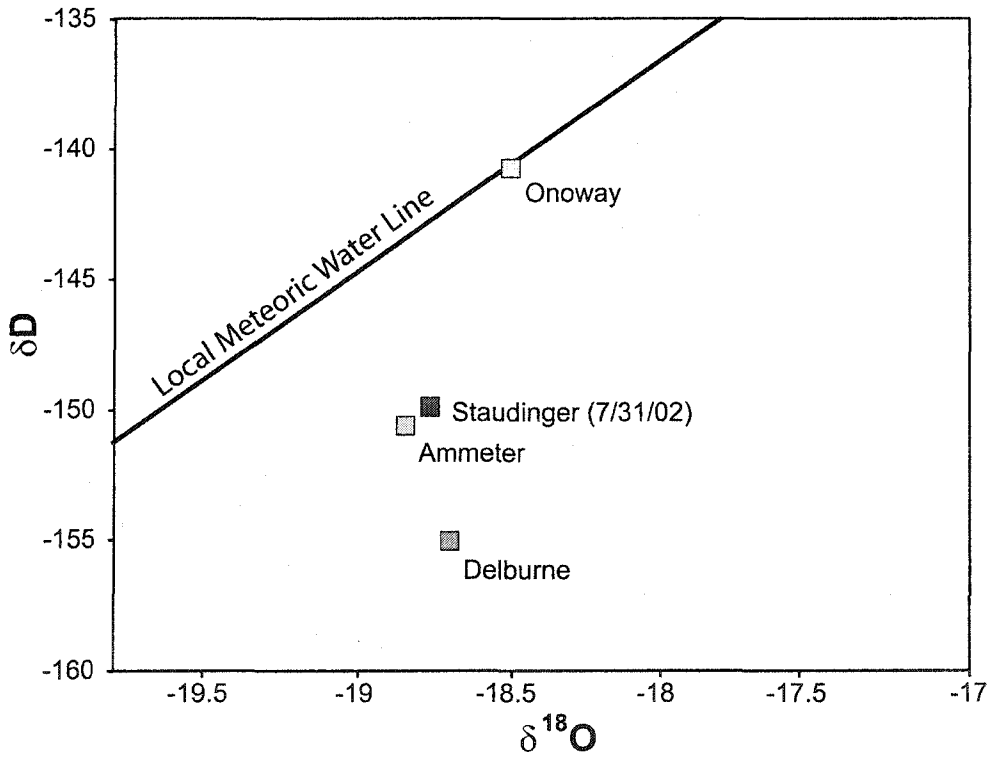

Figure B.4: The stable isotopic composition of the four monitored breathing wells. Edmonton local MWL is also shown.

B.4 Conclusions

The breathing characteristics of the Staudinger water well do not only affect the distribution of gas species (discussed in Chapter 4), but also affect the isotopic composition of the groundwater. Graphical representation of the δD and $\delta^{18}O$ values of the groundwater illustrate that evaporation processes, undergone prior to or during initial infiltration, control the general isotopic composition of the groundwater. Further analysis suggests that the inhaling and exhaling behaviour of the well also affects the isotopic composition of the water, but on a smaller scale. Isotopic enrichment of the water is caused by the removal and evaporation of water vapour (and other gases) from the aquifer during exhaling periods. Contrary to this, the groundwater is isotopically light during inhaling periods, representing the average stable isotopic composition of the water in the aquifer.

B.5 References

Coleman, M.L., Shepherd, T.J., Durham, J.J., Rouse, J.E. and Moore, G.R. (1982) Reduction of water with zinc for hydrogen isotope analysis. *Analytical Chemistry. 54* (6), p. 993-995.

Clark, I.D. and Fritz, P. (1997) *Environmental Isotopes in Hydrogeology.* Lewis Publishers, New York, NY.

Craig, H. (1961) Isotopic variations in meteoric waters. *Science.* 133, p.1702-1703.

Craig, H. and Gordon, L.I. (1965) Deuterium and oxygen-18 variations in the ocean and marine atmosphere. *In: Tongiorgi E. (ed.), Stable Isotopes in Oceanographic Studies and Paleotemperatures.* Spoleto. p.9-130.

Epstein, S. and Mayeda, T.K. (1953) Variation of ^{18}O content of water from natural sources. *Geochimica et Cosmochimica Acta.* 4 (5), p. 213-224.

Gonfiantini, R. (1978) Standards for stable isotope measurements in natural compounds. *Nature.* 271, p. 534-536.

Maulé, C.P., Chanasyk, D.S. and Muehlenbachs, K. (1994) Isotopic determination of show-water contribution to soil water and groundwater. *Journal of Hydrology.* 155, p. 73-91.

Domenico, P.A. and Schwartz, F.W. (1990) *Physical and Chemical Hydrogeology.* John Wiley and Sons, New York, NY.

APPENDIX C: TEMPERATURE DEPENDENCE of OXYGEN SENSOR

Temperature variations of the oxygen sensor were found to strongly influence its resistive responses; therefore, it was necessary to investigate the influence of temperature on the sensor's data output.

While monitoring the Staudinger well, the gas sensors were protected from diurnal temperature fluctuations and diurnal heat radiation because they were located in the well pit. The oxygen sensor did not exhibit a dependence on temperature when it was located in such an environment (maximum diurnal temperature change of 1.6°C). At the additional monitored well locations, the Airmadillo sat on the ground surface, exposed to extreme diurnal temperature variations and direct solar radiation. After analyzing the data collected from Onoway, it became evident that the raw oxygen measurements contained influences of temperature. Higher temperatures increase the resistance of the sensor, resulting in artificially high oxygen concentrations. These responses were isolated by performing temperature corrections to the raw data.

Tests were conducted in a controlled oxygen environment in the University of Alberta Hydrogeology laboratory. The oxygen sensor was placed next to a window to expose it to large diurnal temperature fluctuations. A temperature probe was inserted directly within the sensor housing to record the actual temperature of the sensor. An approximate linear relationship of the form $O_2 = 0.0386(T) + 20.65$ was established (Figure C.1). The correlation coefficient between the two parameters is 0.97. This equation was applied to the raw data collected from the Onoway well (Figure C.2), but only to inhaling and stable periods as the equation requires a reference concentration of 20.65%

and would over-correct the depleted concentrations emitted during exhaling periods.

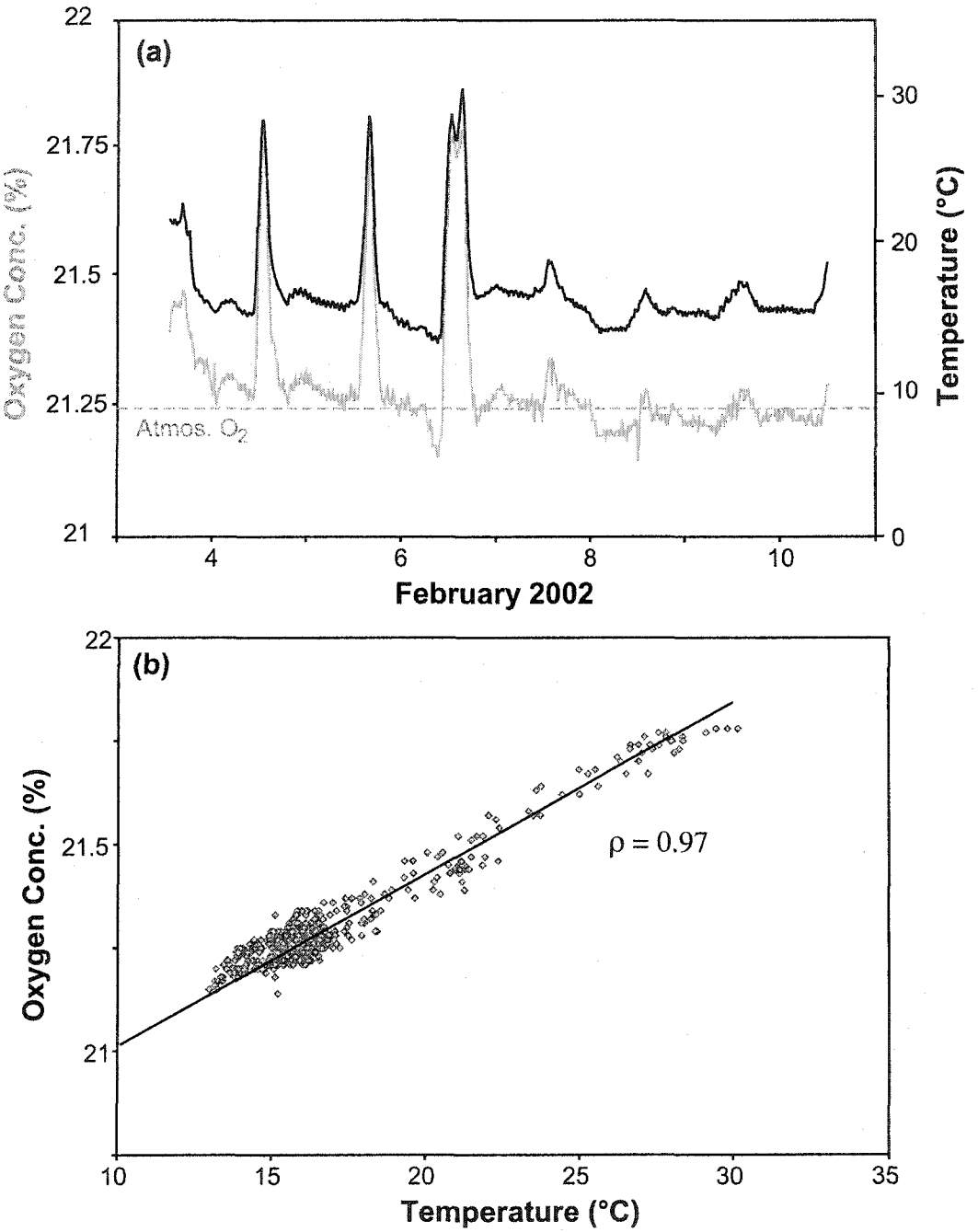

Figure C.1: (a) Distribution of oxygen and temperature during laboratory testing. (b) linear relationship between the two parameters in a controlled setting.

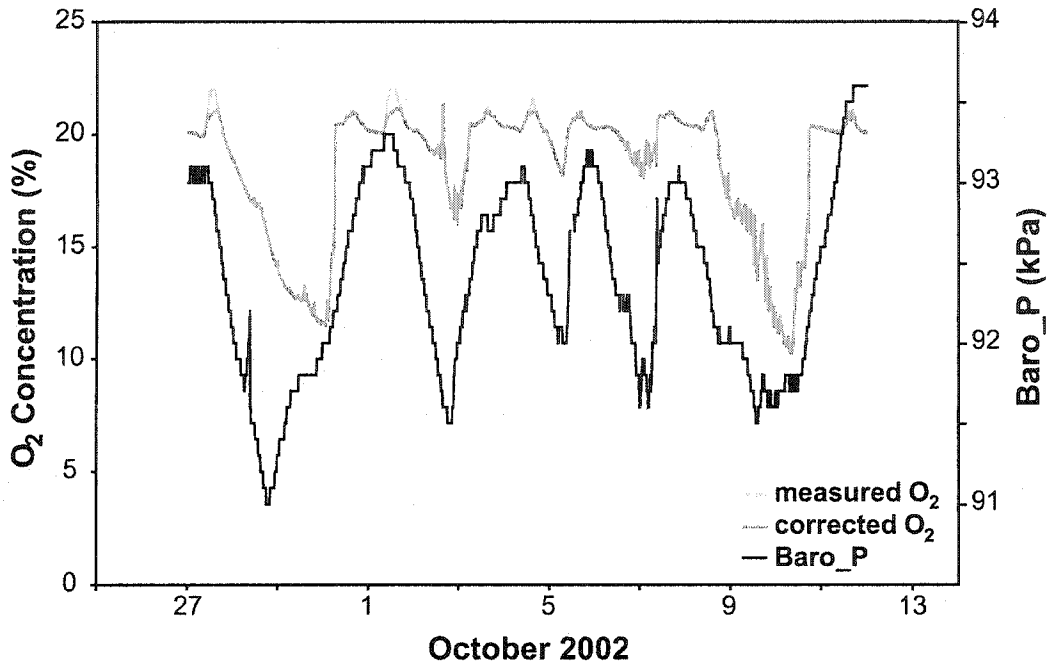

Figure C.2: Distribution of barometric pressure and oxygen concentration at Onoway. Light grey line represents raw output data, dark grey line represents the corrected data using the relationship obtained in the laboratory tests.

The O_2 sensor's dependency on temperature was particularly evident in the raw data collected from the Ammeter and Delburne wells. These wells were monitored in the months of June and July when the solar radiation and ambient temperatures are greatest. The oxygen sensor experienced great fluctuations of temperature during these periods. On some days, recorded oxygen concentrations exceeded 23%. The O_2 sensor displayed relatively smaller temperature dependence at Onoway than at the Ammeter and Delburne wells because it was monitored during the fall when solar radiation and the temperature range are subdued.

While monitoring the Ammeter and Delburne wells, the temperature probe was placed directly in the oxygen sensor housing to obtain a more accurate temperature of the sensor itself. The observed linear relationships between temperature and oxygen were $O_2 = 0.017(T)+21.3$ at the Ammeter well, and $O_2 = 0.0087(T)+21.4$ at the Delburne well. Corrections were made to the raw data using these obtained relationships (Figure C.3).

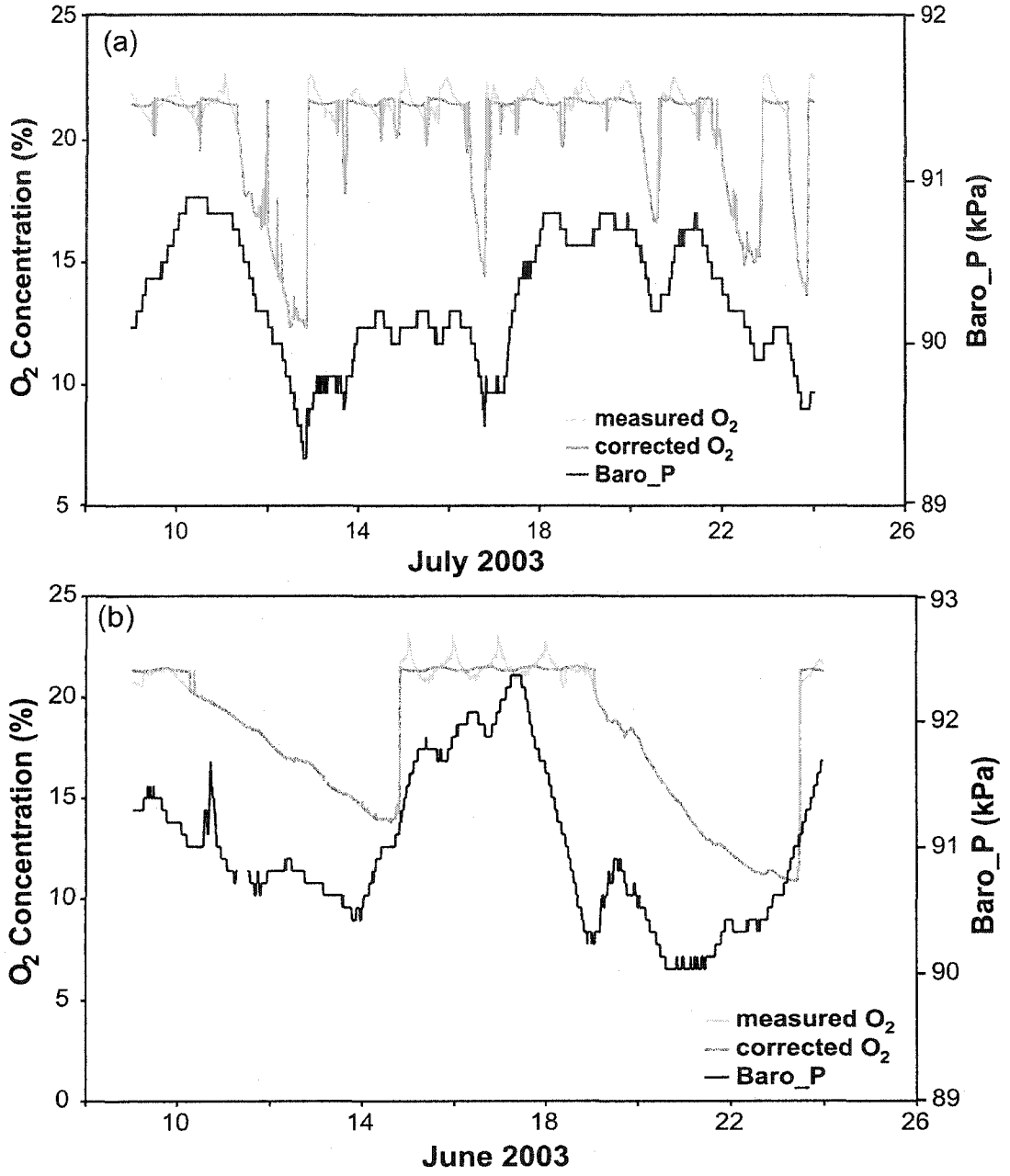

Figure C.3: Corrected and raw oxygen concentration distribution at the Ammeter and Delburne wells, with barometric pressure.

As mentioned, a drawback to these corrections is the accuracy of the recorded temperatures. The only available temperatures at the Onoway well were ambient temperatures and not the actual temperatures experienced inside the sensor. The second limitation is that these corrections can only be

applied to periods were oxygen concentrations are assumed to be atmospheric. The oxygen deficient periods cannot be corrected using these same relationships, and would require controlled laboratory experiments where both oxygen and temperatures are varied.

APPENDIX D: GAS PRODUCTION by DENITRIFICATION

Section 4.7.2.4 discusses the possibility that denitrification reactions are occurring in the shale aquitard. The organic carbon content of the shale is suspected to be quite high, thus denitrification of organic matter is the expected biogeochemical reaction producing elevated levels of dissolved CO_2 and N_2 gas (Madigan et al., 2003):

$$5C_{organic} + 4NO^-_{3(aq)} + 4H^+ \rightarrow 2N_{2(g)} + 5CO_{2(g)} + 2H_2O \qquad (D.1)$$

The suspected quantity of gas that would be produced through denitrification of organic matter in the shale aquitard is calculated below.

The groundwater sampled from the shallow perched aquifer contains 0.686 mg/L of NO_3-N. The underlying Paskapoo aquifer contains only 0.014 mg/L on average. If the total loss of nitrate between these two aquifers can be attributed to the denitrification of organic matter, a total of 0.672 mg/L of nitrate are utilized in the process.

Using the mol ratios from Equation D.1, the concentration of nitrogen gas produced by denitrification can be calculated:

$$\frac{0.672\ mg\ NO_3^-N}{L} \times \frac{1\ mol\ NO_3^-N}{14\ g\ NO_3^-N} \times \frac{2\ mol\ N_2}{4\ mol\ NO_3^-N} \times \frac{28\ g\ N_2}{1\ mol\ N_2}$$

$= 0.672\ mg/L\ N_2$

Therefore, the amount of produced nitrogen gas would be 0.67 mg/L. The concentration of NO_3-N detected in the shallow aquifer in the Sylvan Lake area range from 0.0 mg/L to over 3.3 mg/L (0.0 to 15 mg/L NO_3 (The

Groundwater Centre, 2004)). If an average of 2.7 mg/L of NO_3-N (10 mg/L of NO_3) exists in the shallow aquifer, a suspected nitrate concentration of 2.2 mg/L would be consumed during infiltration through the shale aquitard, producing 2.2 mg/L of nitrogen gas.

The same method can be used to determine the concentration of carbon dioxide that would be produced:

$$\frac{0.672 \text{ mg } NO_3^-N}{L} \times \frac{1 \text{ mol } NO_3^-N}{14 \text{ mg } NO_3^-N} \times \frac{5 \text{ mol } CO_2}{4 \text{ mol } NO_3^-N} \times \frac{44 \text{ mg } CO_2}{1 \text{ mol } CO_2}$$

$= 2.6$ mg/L CO_2

Therefore, 2.6 mg/L of CO_2 would be produced if 0.67 mg/L of NO_3-N were consumed. Additionally, if 2.2 mg/L of NO_3-N were consumed, 8.8 mg/L of carbon dioxide gas would be produced.

To calculate the mass rate (J_{N_2}) at which dissolved nitrogen gas is delivered to the unsaturated zone of the partially saturated aquifer from the confining aquitard, the following equation can be used:

$$J_{N_2} = C_{N_2} \pi r^2 q \qquad \text{(D.2)}$$

where C_{N_2} is the concentration of the dissolved nitrogen (calculated above), r is the radius of the area of the confining aquitard through which the gas is delivered, and q is the flux of the groundwater into the aquifer.

A number of assumptions must be made in order to apply equation D.2. First, one must assume that the confining aquitard is fully saturated (i.e., hydraulic head is equal to one); therefore, q is equal to the hydraulic conductivity of the shale; approximately 10^{-10} m/s. One must also assume a radius of influence,

r, in which the groundwater seeps into the partially saturated aquifer. The box model, applied in Section 4.7.3, simulated that the radius of influence can range between 3 and 5 m for the Staudinger well. Table D.1 displays the calculated minimum and maximum mass fluxes of nitrogen gas entering the unsaturated zone from the overlying shale aquitard. J_{N_2} can range between 0.16 and 1.5 mg per day.

Table D.1: Maximum and minimum mass flux of nitrogen gas moving from the shale aquitard into the underlying unsaturated zone.

	units	min.	max.
C_{N_2}	mg/L	0.672	2.24
r	m	3	5
q	m/s	10^{-10}	10^{-10}
J_{N_2}	mg/day	0.16	1.5